Inverse Transients to Define Deficiencies in Pipelines

Report to the

Water Research Commission

by

Fanie van Vuuren
University of Pretoria

WRC Report No. 1721/1/12
ISBN 978-1-4312-0331-4

September 2012

Obtainable from

Water Research Commission
Private Bag X03
Gezina, 0031

orders@wrc.org.za or download from www.wrc.org.za

Seven appendices are listed in the Table of Contents. These appear on the enclosed CD.

Inverse transients to determine deficiencies in pipelines

Executive Summary

Introduction and objectives of this research project

A major operational and management problem associated with the optimal use of water infrastructure is the identification and quantification of deficiencies which developed in the system. Two major deficiencies which are difficult to identify in bulk water pipelines is the presence of localised trapped air bubbles and leaks.

The objective of this research was to use inverse transients to detect these deficiencies. The procedure of inverse transients is based on the notion that the propagating pressure wave will be influenced by the deficiencies (trapped air pockets and leaks) and by analysing the recorded pressures at different locations on the system, the location of the deficiency can be determined.

The value of the implementation and development of this technique of Inverse Transients is that it offers a non-destructive, non-intrusive and un-intermittent procedure for the status assessment of water distribution systems.

The approach is related to the pressure wave propagation in closed conduit systems and the scientific behaviour of wave propagation and reflection at positions where the conduit characteristics change. These positions of the change in the characteristics to propagate the pressure wave could amongst others either be the presence of trapped air or leaks or the change in the elasticity of the conduit.

Methodology

In the research a number of pipelines from different organisations, which were suitable for the investigation was investigated. For the selected pipelines, which were reviewed, a theoretical assessment of the hydraulic performance were conducted and compared with the recorded hydraulic capacity. Furthermore the pipelines were assessed for dynamic instability from which the wave propagation characteristics were defined and the pressure fluctuations at positions along the pipeline were modelled.

The methodology to investigate the presence of deficiencies in pipelines by inverse transient required the installation of pressure transducers and data recorders to capture the propagation of induced pressure waves. The frequency of the pressure recordings directly influences the accuracy to locate a deficiency in a pipeline.

The recorded data of the Arendsnes pipeline (Tshwane Metropolitan Municipality) as well as the field tests conducted on the B16 pipeline (Rand Water) and the Kuthala to Kendal Pipeline (DWA) are discussed in the report.

The objective to locate the deficiency as accurate as possible necessitated the implementation of the following step-by-step procedure:

- Determine average expected wave celerity of the system (say 800 m/s);

- Define the accuracy required to identify the deficiency (say 10 m);

- Calculate the minimum frequency at which the data need to be recorded (10/800 = 0,0125 s which require a recording rate of 80 Hz; and

- Select the data recording equipment applicable to store long data sets in such a format that it can be viewed and abstracted to a spread sheet environment that does not exceed the capacity of the spread sheet programme due to limited capacity (number of lines or rows).

During the fieldwork, a pressure wave was introduced in the pipeline by either the start or stoppage of a pump or through the variation of the flow rate in the pipeline either by closing or opening a scour valve. During these field tests the pressures were recorded at a number of nodes along the pipeline at a high frequency (> 10 Hz but preferably > 100 Hz). The wave propagation characteristics and changes in the magnitude of the wave were used to verify the presence of leakages and/or air pockets which were introduced to the pipeline.

Experience and time improve the capacity for interpretation of the pressure graphs to pinpoint the deficiencies.

Conclusions

The results obtained from the field tests and theoretical evaluation, reflected that the use of inverse transients as a non-destructive, non-intrusive and un-intermittent technique could be used to detect the presence and location air pockets and leaks.

The research further highlighted how the pressure time relationships should be evaluated and indicates the importance to identify and assess the influence of the reflection wave from the discrepancies, since all loss elements in any water distribution system will generate reflection waves, influencing the recorded pressure-time relationship at the pressure recording positions.

The interpretation of the results should consider the influence on the pressure wave from all loss components (valves, cross connections, bends, pumps, diameter changes, off takes and locations where the wave celerity changes). This requires a systematic review of the wave patterns and calculation of the possible origin of the reflection wave.

The precise location and size of the leaks are more challenging to identify when employing inverse transients than to identify the location and size of trapped air in the pipeline, mainly due to the specific characteristics of the reflection waves from air bubbles.

In the case of an air pocket the reflection wave will result in:

- An increase in the pressures in the direction the reflection wave is travelling (**Figure 3-8);**

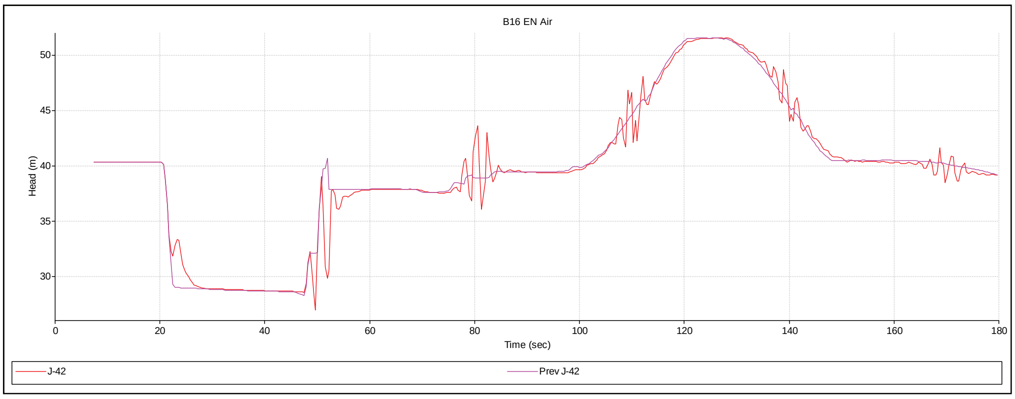

Figure i: Pressure head comparison at a node (J-42) between an air bubble and the position where the transient was created. The Prev J-42 graph represents a system without an air bubble and the J-42 graph reflects the situation with and air bubble of 2,1 nm^3 at Node J-17

- The discharge at the point where the transient is created will increase for a short period of time (**Figure** 3-11); and

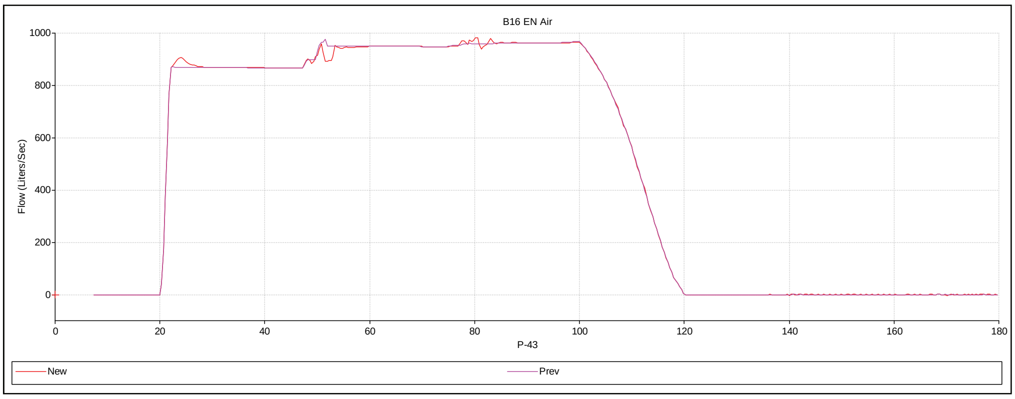

Figure ii: Flow rate-time comparison at the node (J-43) where the transient was created. The Prev graph represents the flow without an air bubble and the New graph reflects the situation with and air bubble of 2,1 nm^3 at Node J-17

- Beyond the location of the air pocket (moving away from the position where the transient was created) the propagating pressures will decrease and the variation in the pressure fluctuation will be dampened (**Figure** 3-7 **iii**).

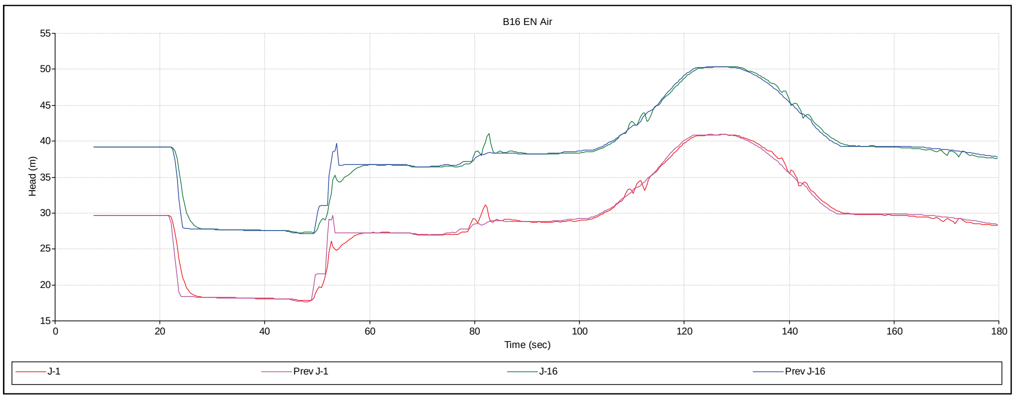

Figure iii: Pressure head comparison at nodes (J-1 and J-2) beyond the location of the air bubble and further away from where the transient was created. The graphs Prev J-1 and Prev J-16 reflects the pressure variation without an air bubble while graphs J-1 and J-16 reflects the pressure fluctuation when an air bubble of 2,1 nm^3 has been captured nearer to the node in comparison to the positions of nodes J-1 and J-16, where the transient was generated.

The following steps are recommended for the implementation of inverse transient procedure to evaluate existing systems:

- Obtain and verify all the data required to compile a theoretical assessment of the system;
- Determine how much detail must be included for accurate computation;
- Identify the practical difficulties of the implementation and possible success of this methodology for the system to be reviewed;
- Theoretically analyse the system as the base case to obtain details of the wave dynamics from which the favourable position where the pressure recordings should be undertaken could be identified;
- Select the appropriate pressure and flow recording equipment and the apparatus required to induce a transient in the system;
- Define an outline of a set of rules to define the sampling rate, the sample size and the location of the measurements sites;
- Install and verify the operation of all the recording equipment;
- Initiate a safe (non-destructive) transient event;
- Measure the transient pressures at the measurement sites;
- Assess the recorded data and determine if the inverse transients which were introduced provided sufficient pressure variance in the system (If not the field recordings might have to be repeated);
- Reproduce an accurate model of the variable input used in the physical setup;
- Identify the possible locations of the deficiencies in the system by comparing the simulated and field recordings;
- Introduce these deficiencies in the theoretical model and compare the results with the recorded results;
- Compile a report on the possible location, nature and extent of the discrepancies; and
- Conduct a physical field inspection to verify deficiencies.

Based on the findings of this research it is recommended that:

- Further field investigations and modelling of different pipe systems be undertaken to provide more results and understanding of the interpretation of the recorded pressure records;
- Typical pressure graphs should be produced based on further field work, reflecting the wave propagation and pressure variance resulting from leaks and trapped air pockets. These typical "interpretation graphs" could be used by operational staff to verify the integrity of the infrastructure.

ACKNOWLEDGEMENTS

The research findings presented in this report emanated from a study funded by the Water Research Commission (WRC), whose support is acknowledged with gratitude.

The Reference Group made an important contribution in steering and guiding this study to obtain the format and results reflected in this report. The support of the Chairman and Manager of this study, Mr Jay Bhagwan, as well as the staff of WRC, is greatly appreciated.

The Reference Group and Project Team responsible for this study consisted of the following persons:

Mr Jay Bhagwan	Water Research Commission – Chairman
Mr Paul le Roux	GMKS
Prof Geff Pegram	University of KwaZulu-Natal
Prof Johannes Haarhoff	University of Johannesburg
Mr Nic Trebicki	Rand Water
Mr Andre Dyer	Amatola Water
Dr Mike Shand	Aurecon
Mr Stephan Burke	Umgeni Water
Mr Edwin Varkevisser	Rand Water
Mr Roelf le Roux	Magalies Water
Mr Walther van der Westhuizen	DWA
Prof Fanie van Vuuren (Project leader)	University of Pretoria
Mr Marco van Dijk	University of Pretoria
Mr Anton de Klerk	University of Pretoria

This study was made possible with the co-operation of many individuals and institutions. The authors therefore wish to record their sincere thanks to the following: Mr A Kurtz and Mr D du Preez from Tshwane Metropolitan Municipality for allowing the use of their pipelines and for all the arrangements they made.

The Water and Sanitation Division of the Tshwane Metropolitan Municipality for all the excavations and preparations they made on the pipelines that were tested.

Mr Nic Trebicki from Rand Water was instrumental in arranging the field setup on the B16 pipeline. His positive support of the development and implementation of new techniques to assess water infrastructure is appreciated

The project team's willingness to explore new ground and in the process to try some unsuccessful options, was greatly appreciated. The work by a number of students from the University of Pretoria who undertook some of the experimental work and assisted in the field work is appreciated.

They were:

William Archer
Ross Mahaffey
Kako Agyare-Manu
Ulrich Drotsky
Louis Coetzee

Table of Contents

List of Figures

List of Tables

Inverse transients to determine deficiencies in pipelines

1 Introduction

1.1 Background

A major shortcoming in the optimal utilisation of water distribution systems is the uncertainty about the physical status and the identification of operational deficiencies. In a WRC study (Report 1177/1/04) the influence of localized air pockets on the hydraulic capacity of pipelines was identified.

Another major problem that negates the optimal distribution of water is the presence of unidentified leaks in the systems.

It was hypothesized that inverse transients could be used to determine the location and magnitude of leaks and air pockets. The technique has already been tested in laboratory conditions (Chapter 3), indicating the advantage of this technique. The procedure could be applied without isolating the section of pipe to be investigated (no interruption of the service). The objective was to test and develop this technique further and provide assistance in the implementation of this procedure for the situation assessment of infrastructure for asset management.

The value of the development of this technique is that a non-destructive, non-intrusive and un-intermittent procedure would be available to investigate the status of water distribution systems.

1.2 Methodology

The researchers identified a number of pipelines of various organisations that would be suitable for the investigation. The theoretical assessment of the hydraulic performance was evaluated to obtain an indication of the expected pressures at different locations along the pipeline.

Equipment was then installed at scour valves (or air valves) for the creation of a fast flow variation (release) that would result in a drop in pressure (negative pressure wave). Instrumentation was positioned along the pipeline to capture the wave movement at a high frequency (> 10 Hz but preferably > 100 Hz). The wave propagation characteristics and changes in the magnitude of the wave were used to detect the presence of leakages and/or air pockets in the pipeline.

Wave plan theory was used to calculate the expected propagation of the pressure wave.

The measured and calculated wave movement was compared and used to identify the deficiency (location and magnitude of leaks and air bubbles).

1.3 Objective of the research

To develop and tests an infrastructure assessment technique that would:

- Define the location and
- Extent of deficiencies (leaks and air bubbles) in a water supply system

This would be an innovative procedure, available at a low cost and contributing to the status assessment and optimal use of existing infrastructure.

1.4 Layout of report

The report consists of the following chapters and annexure:

Chapter 1: Introduction (This chapter)
Chapter 2: Literature Review
Chapter 3: Experimental work
Chapter 4: Field work
Chapter 5 Development of evaluation techniques
Chapter 6 Conclusions
Chapter 7: References

Appendices

Appendix 2A: List of the supporting literature included on the compact disc
Appendix 3A: Overview of experimental work conducted by author and graduate students at the University of Pretoria
Appendix 3B: B16 Pipeline Surge (*.P2K) files
Appendix 4A: Hobo Data Recordings at Arendsnes 18 July 2009
Appendix 4B: Graphical presentation of recorded pressure variations at Arendsnes Pipeline
Appendix 4C: Dataq Recordings at Arendsnes 18 July 2009
Appendix 4D: Spread sheet files for the analyses of the Arendsnes wave propagation

2 Literature review

2.1 General

The most important variables that could influence the hydraulic capacity of pipelines are the variation in the roughness parameter (ageing, partial failure of liner systems, corrosion) and the ineffective de-aeration of the pipe. The influence of air/bubbles and leaks is discussed in the following paragraphs to provide a better understanding of the hypothesis of this research study and to indicate that inverse transients might be used to identify the presence and magnitude of air bubbles and leaks in pipelines. The wave characteristics of pipelines and the wave propagation are also discussed to provide further background to the process of inverse transients. The presence of air in water mains is first discussed, followed by a review of the influence of leaks on the performance of pipelines.

2.2 The presence of air in pipelines

2.2.1 Problems associated with air in pipelines

Problems associated with ineffective de-aeration of pipelines and the impact it has on the hydraulic performance of pipeline systems is as follows (Kirkland, 2002):

Reduced flow. When a pipeline is charged with water, dissolved air will accumulate locally in the high parts of the pipeline and will reduce the pipeline diameter at that point. **Figure 2-1** illustrates the reduction in pipe diameter as a result of air present in the pipeline. If the velocities remain low (lower than 2 m/sec), the high point will generate a head loss through the constriction that will reduce the flow.

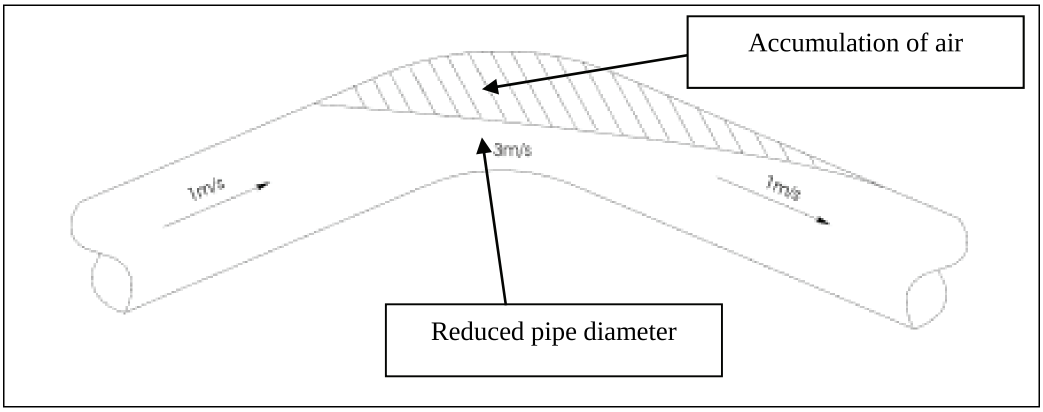

Figure 2-1: Accumulation of air and the associated reduction in pipe diameter.

Increased pump operating costs. The previously mentioned head loss at the high parts of the pipeline forces the pump to work harder in order to achieve the required performance.

Water hammer. The discharge of an air-water mixture through an orifice can lead to significant pressure surges if the two-phase flow is in the slug flow regime. A much greater pressure is required to discharge the air-water mixture through an orifice than is required for the gas, resulting in a rapid fluctuation in pressure.

Corrosion. Air that accumulates in the high points of the pipeline will subject the valves and metallic pipeline to concentrated oxygen that will cause corrosion at these points. Corrosion will weaken these components and shorten their lifetime.

During normal operating conditions, the presence of air in the pipeline will have a negative effect on the discharge capacity of the system and it is therefore essential to remove all the air from the system. During transient conditions, there are certain advantages in the presence of free air in a pipeline. The free air has the ability to reduce induced pressure spikes by compressing the air (deformation energy required) and decrease the wave celerity (Wylie & Streeter, 1978).

2.2.2 Ways in which air can enter a system

Air in a pipeline can arise for various circumstances (Van Vuuren, 1990) as summarized below:

Filling of the pipeline: During the filling of a pipeline, large volumes of air can be trapped in a system. When the pipeline is not flowing full and the flow is increased, air might become trapped in the system.

Pumps: Low suction pressures at the pumps could lead to a release of air from solution.

Vortices at the pump or pipe intake: The presence of free surface vortexes could have a big influence on the amount of air intake into the system. The depth of submergence of the intake, the inlet geometry and the flow rate determines the formation of vortexes.

Air separation: When water enters a low-pressure zone, the dissolved air present in the water will be released from solution in the form of small air bubbles. In general, about 3% (by volume) of air in solution is present in the water (Wylie & Streeter, 1978). The dissolved air will be released from solution as air bubbles if the temperature rises or pressure drops below certain levels. Zlecke &

Keller (Van Vuuren, *et al*, 2004) documented that the rate at which air dissolves under almost all conditions, is much slower than the rate at which it can be released.

If a sudden pressure drop occurs in a liquid with a certain gas content in solution, super saturation and thus gas release can occur. The amount of gas released depends in a linear manner on the pressure drop below the governing saturation level. The equation of 'state for gases' governs the variation of gas content α with pressure and is expressed under isothermal conditions as $\alpha.p = \alpha_i.p_i$ ($_i$ = initial conditions). Although the mass density of the liquid is hardly modified, the free gas content will drastically change the compressibility of the mixture and thus have a significant effect on the pressure wave celerity (Bollaert & Schleiss, 2001).

2.2.3 Dissolved air

An understanding of the way in which dissolved air is released from the water in the pipeline is of great importance. The presence of dissolved air in a pipeline usually becomes apparent when the water appears milky or white in colour. When this milky water is left to settle in a glass, it will become translucent. This phenomenon is often seen in borehole installations where the water reaches high temperatures. If the water then travels along the pipeline, dissolved air can be a major problem. The following could be indicative of situations that cause air to dissolve in the water (Kirkland, 2002):

- *Pump station*. If the fittings on the inlet to transfer pumps are not tightly sealed, air may be drawn into the pipe. This is apparent especially where the pump suction is working under vacuum conditions. When a pump is drawing water from lower water levels, it could possibly draw a vortex into the suction line and introduce a moderate amount of air.

- *Friction along the pipe length*. Friction is generated between the water and the inner wall of the pipe as the water travels along the length of the pipeline. When the water containing air moves at high velocities, large amounts of air can accentuate water hammer conditions, which often occur at high velocities.

- *Changes in velocity*. Where pressure reducing valves or globe valves are installed along the pipeline, a change in the velocity of the water might occur. At this specific point the water expands downstream of the pressure reducing valve and small pockets of dissolved air may be released. This is especially applicable to large diameter pressure reducing valves with a turn down ratio (TDR) greater than 4:1 as illustrated in **Figure 2-2**.

Where :

Change in velocity

$V_2 < V_1$

and

$P_2 > P_1$

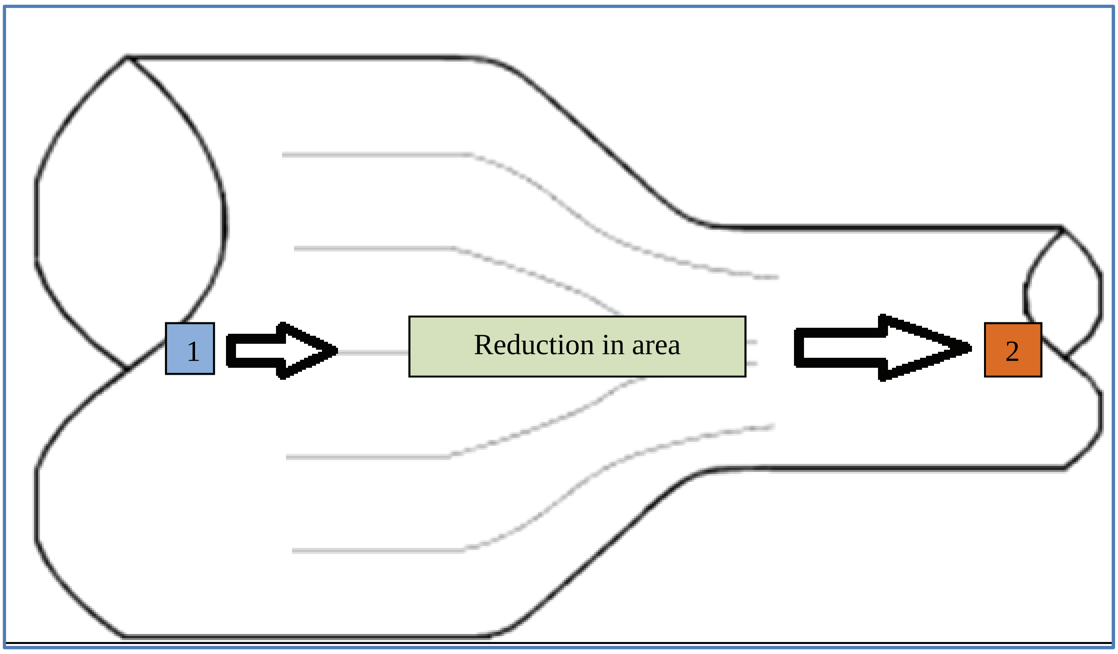

Figure 2-2: The change in velocity as a result of an expansion in pipe diameter.

2.2.4 Effective de-aeration of pipelines

There are various procedures for de-aerating pipelines. The mechanical and hydraulic methods are discussed below.

2.2.4.1 Mechanical de-aeration

Although sufficient outlets are available to release air in normal distribution systems, it is important to consider the effects of free air on the properties of the system. It is imperative that air accumulating at the high parts of a pipeline is effectively released through an air valve.

A poor understanding of air valves often leads to incorrect installation. The detailed operation of three different types of air valves are described below (Kirkland, 2002):

- *Large orifice air valve*. This valve is often referred to as a kinetic air valve and the valve's prime purpose is to release large amounts of air during the filling of a pipeline. These valves are mostly sized for the intake of air. The valve should also be sized for filling the pipe to ensure that the air volumes leaving the orifice do not exceed a specific velocity that will cause the valve to close before the air is adequately released. The valve should allow air to enter the pipe during drainage to prevent the pipe from collapsing due to negative pressure in the line. The size of the air valve may also have an effect on the rate of drainage when emptying the pipeline. The pressure on the surface of the upper orifice of the valve will create a force exceeding the buoyancy of the float. When the pressure in the system drops, the float will fall allowing air to enter the pipeline.

- *Small orifice air valve*. This valve is often called an automatic air valve and its purpose is to release small quantities of dissolved air from the pipeline when it is under pressure. This ensures that the pipeline remains fully charged and avoids many of the problems caused by air pockets in the pipeline. This valve can also be used as a kinetic valve in smaller pipes to release air during filling and also to introduce air during draining of the pipes.

- *Combined valve*. This valve is commonly referred to as a double orifice or double acting valve as it incorporates both the kinetic and automatic functions. These two functions are generally cast into the same housing and which can sometimes incorporate an isolation valve.

2.2.4.2 Hydraulic de-aeration

The water velocities in the majority of pipelines vary between 0.5 and 1.5 m/s. It is possible that dissolved air released from the water will travel along the pipeline – as long as there is not a significant negative gradient in a pipeline. High velocities are required to transport air in pipelines with large inverse slopes. Therefore it is important to release the air before a downward bend in a pipeline through the use of an automatic orifice air release valve. . The automatic orifice air release valve is needed to release dissolved air from the high parts of the pipeline (Kirkland, 2002).

The threshold velocities for a given pipe with a certain slope where the air bubble becomes unstable and is transported through the pipeline were developed by Kalinske and Bliss and Wisner (Van Vuuren *et al*., 2004). These are the most commonly used equations to indicate the velocity required to transport the air through the pipeline:

$$\frac{Q_L^{\ 2}}{gD^5} = 0{,}707 \tan\phi$$

Equation 2-1

Where:

Q_L	=	Required flow rate (m^3/s)
D	=	Pipe diameter (m)
ϕ	=	Slope of pipeline (degrees)

And

$$v_c = \sqrt{gD}\left(\ 0{,}25\sqrt{\sin\phi} + 0{,}825 \ \right)$$

Equation 2-2

Where:

v_c	=	Critical velocity required for the removal of air (m/s)

In a recent study (Van *Vuuren et al.*, 2004) the following relationship was determined to hydraulically transport air.

$$V_{\min} = a\sqrt{gD}\,\theta^b$$

Equation 2-3

Where:

V_{min}	=	Minimum velocity required to transport air (m/s)
a	=	Constant value (determined for a medium size bubble) = 0,2178
θ	=	Slope of the pipe (degrees)
b	=	Constant value (determined for a medium size bubble) = 0,4007
g	=	Gravitational acceleration (m/s^2)
D	=	Internal pipe diameter (m)

2.2.5 Air valve selection

Software has been developed for optimizing air valve selection. The following points simplify some of the factors to consider when selecting a valve for a specific location (Kirkland, 2002):

- *Pump station:* A high turbulence zone occurs downstream of the pump and there is a possibility that any air present will dissolve into the water. It is therefore critical to release the air before it enters the pipeline. An automatic orifice valve should be located at the high collection point of the pipeline where the velocity is at its lowest. A combination of air valves should be used where the pipeline is travelling downwards.

- *High peaks in the pipeline:* The peaks, distances and height differences between valves should be tabulated. Scour points, pipe diameters and classes of pipes play an important role in kinetic valve selection. The wall thickness and pipe diameter relationship indicates the differential air pressure acceptable at the air valve. This also ensures that the pipe does not exceed it safe working vacuum conditions. The topography and the filling rate of the pipeline are needed to calculate the correct orifice size. The air in the pipeline is not necessarily released at the same rate as the rate at which the pipeline is filled with water. The velocity will increase as the pipeline extends because of the compressibility of the air.

- *Locations of direction change and varying velocity:* The following table indicates a rule of thumb that can be used in the selection of combined air release valves for different pipe diameters. The data may not necessarily be the same for all manufacturers and is specifically based on ARI air release valves. The selection is based on having air valves located along a pipeline with a spacing of 500 metres. This ensures that vacuum conditions will not stress the pipe during drainage. A correct analysis should be made to confirm valve selection.

2.3 Leaks in pipelines

It has been reported that each of the following leak detection methods have disadvantages and advantages depending on the circumstances under which they are applied (Xiao-Jian Wang *et al.*, 2002). The dampening of the transient wave method provides satisfactory results under most conditions.

The other procedures that have been proposed include: reflected wave and timing methods; volume balance methods; pressure or flow deviation methods; acoustic methods; pig-based monitoring and on-line surveillance methods; frequency analyses methods; inverse techniques and generic algorithm methods (Xiao-Jian Wang et al, 2002).

2.4 Transients in pipelines

Transient pressures/water hammer can cause damage to pipelines. It occurs as a result of sudden changes in water pressure (pressure shock) that leads to the unsteady flow of water in the pipeline. Water hammer occurs when there is a sudden change in the velocity of the moving water, resulting in a thumping sound within the pipe. A thorough analysis on water hammer and pressure surges should be performed and used to inform the design of a pipeline system.

Changes in the steady-state operating conditions of a water system are usually caused by (Van Vuuren, 1990):

- The closure of a valve in the system;
- Suddenly starting up or shutting down of a pump;
- Unpredictable circumstances (such as a pipe burst or power failure); and
- Sudden variation in demand.

Water is essentially non-compressible but elastic and when one of the changes discussed above occurs, all the energy carried by the water has to be transferred somewhere else. This energy then creates a brief, but large, pressure spike in the water. The pressure spike can easily double or triple the water pressure in the system. It occurs so fast that a regular pressure gauge will not register these pressure fluctuations. The pressure spike passes as a shock wave through the pipe at speeds typically in the range of 300-1200 m/s. This creates stresses in the pipe and the pipe can be weakened every time the water hammer occurs (Stryker, 2003).

Water hammer pressures are influenced by various variables. According to Stryker, the following variables are important to find the source of the water hammer problem:

- The length of the pipe;
- The wave speed in the pipe;
- The speed at which the valve is closed or partially closed;
- The initial velocity of the water.

2.5 Wave movement and pressure surge theory

2.5.1 Unsteady compressible flow

The inertia forces in a system increase as the rate of the valve opening or closing increases. A shock wave is created that travels through fluid at the speed of sound (symbol c). The mechanism of compressibility transforms the kinetic energy of the fluid into elastic energy (upholding the principle of conservation of energy). If the disturbance is created downstream, the fluid upstream of the wave is still flowing at its original pressure, velocity and density. The pressure of a shock wave within a rigid pipe is described below in **Figure 2-3**, which represents a pipeline connected to a reservoir and sudden closure of at the end of the pipeline (Chadwick & Morfett, 1998).

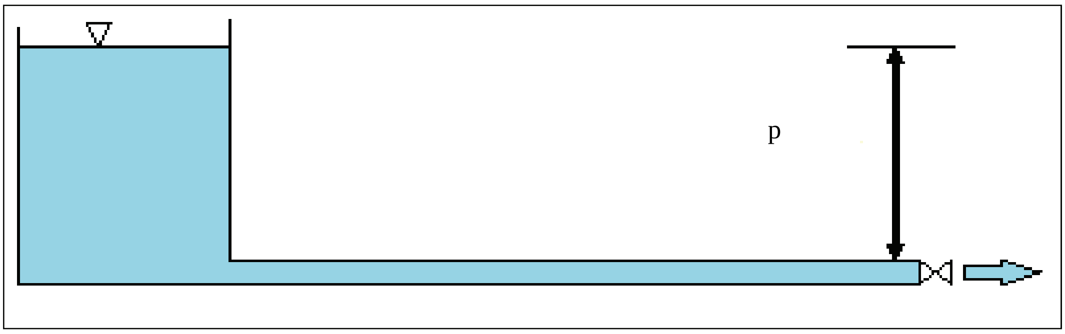

(a) Instant of valve closure (t = 0, where t = time after closure)

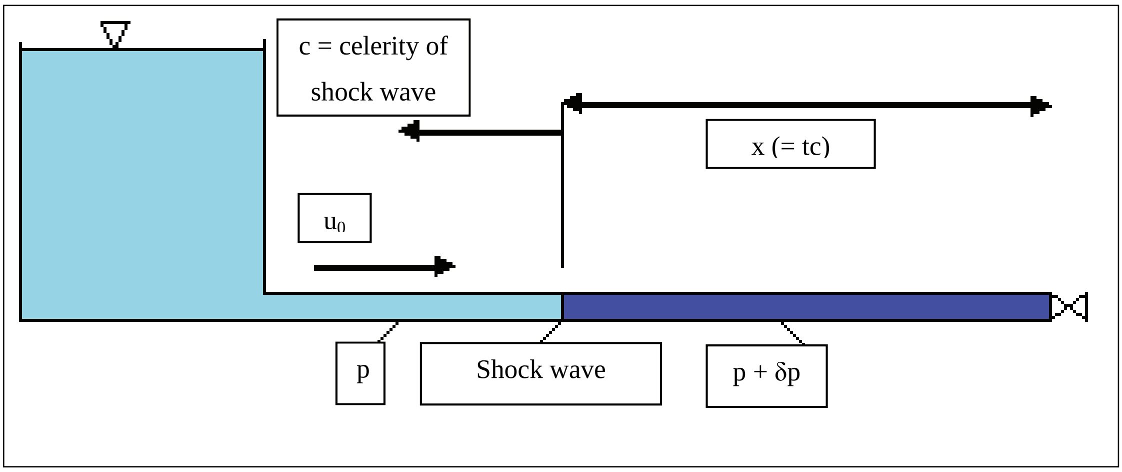

(b) Passage of shock wave (t = x/c)

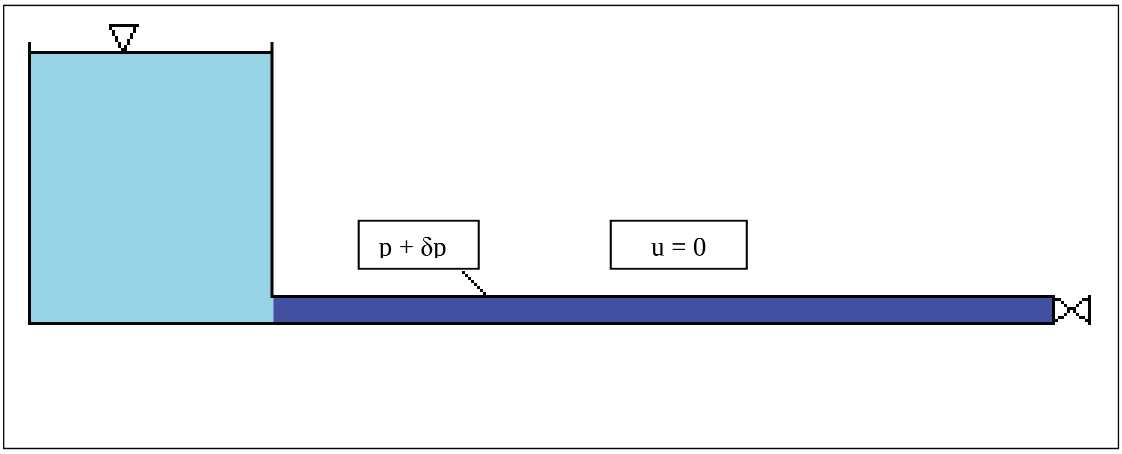

(c) Fluid compressed throughout the pipe (t = L/c)

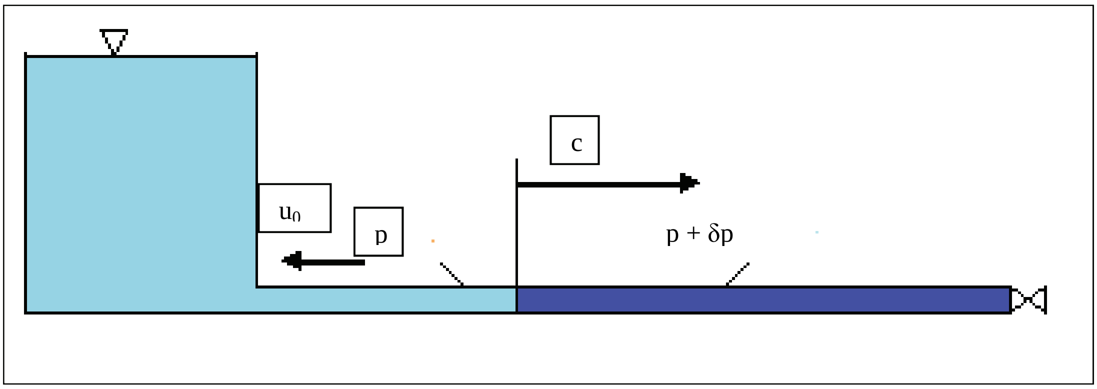

(d) Decompression (L/c < t < 2L/c)

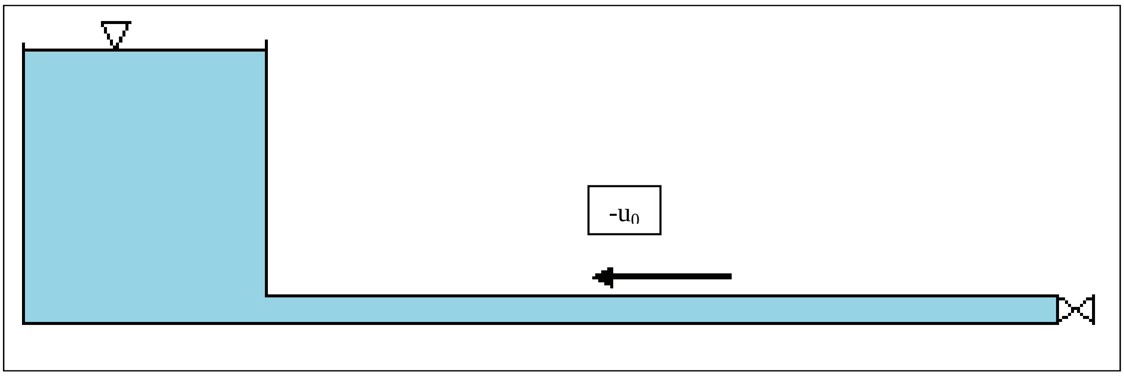

(e) Fluid decompression throughout the pipe (t = 2L/c)

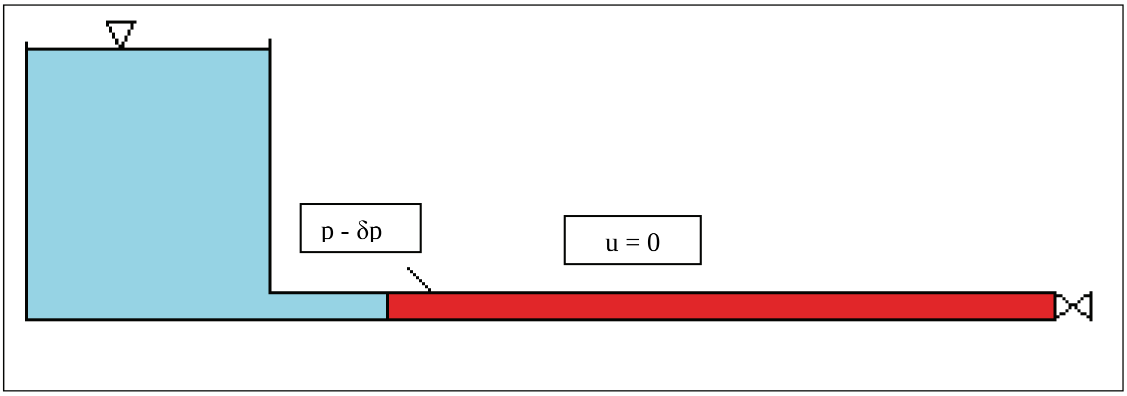

(f) Negative pressure almost throughout the pipe (t < 3L/c)

Figure 2-3: Propagation of a shock wave in a pipeline (Chadwick & Morfett, 1998).

*Discussion of **Figure 2-3**:*

(a) The valve closes, generating a shock wave.

(b) The shock wave travels along the pipeline. The fluid in-between the shock wave and the valve is compressed and the pressure rises to p + δp.

(c) The pipe is filled with pressurised fluid when the wave arrives at the reservoir.

(d) Since the reservoir level remains unchanged, there is an imbalance at the pipe-reservoir interface. A decompression wave is generated which travels back along the pipeline towards the valve. The fluid in-between the wave and the reservoir are now at its original p, but u is reversed. The fluid on the valve's side of the wave is still at $p + \delta p$.

(e) The valve will serve as a dead end (if closed). When the decompression wave arrives at the valve, negative pressure is generated and a negative shock wave is produced. The fluid in-between the valve and the wave is at rest, but now under negative pressure $p - \delta p$. The fluid in-between the wave and the reservoir is still at p and the flow is still reversed.

(f) When the negative pressure wave arrives at the reservoir, the pipeline pressure is lower than the pressure in the reservoir and the fluid flows from the reservoir into the pipe. Theoretically the velocity is now restored to its original magnitude and direction. This is only true since hydraulic losses were not taken into account.

The cycle (a) to (f) repeats itself until all the energy has been lost due to friction and deformation energy.

2.5.2 Basic theory of transient flows

A change in the steady-state operating conditions of a fluid is communicated to the system through pressure waves propagating from the point in the system at which the change in the steady flow condition was imposed (Van Vuuren, 1990). After some time, the system attains a new state of equilibrium.

The rate of change of the flow rate determines the applicable method to be employed in calculating the value of the pressure variance and the wave propagation. It can be assumed that the rate of change is proportional to the degree of compressibility of the fluid. In non-compressible fluids and non-elastic pipes, changes in flow conditions are instantaneously transmitted through the system. The analysis based on this assumption is referred to as the rigid column theory (Van Vuuren, 1990).

Control systems are often required to implement operational variations in systems with high pressures and high flow rates. When compared to measured values, the compressibility of the fluid as well as the elasticity of the systems needs to be considered in order to provide valid results. This theory is referred to as the elastic theory (Van Vuuren, 1990).

2.5.3 The rigid column theory

When Newton's second law is applied to represent the deceleration of a rigid water column in a pipeline, the following relationships is applicable for the pressure rise associated with the closure of a valve at the end of a pipeline:

$$\Delta H = \frac{L}{g} \cdot \frac{dv}{dt}$$

Equation 2-4

Where:

$\frac{dv}{dt}$	=	presents the change of flow velocity, dv, over a period of time, dt;
A	=	Cross sectional area of the pipeline (m^2)
L	=	Length of the pipeline (m)
ΔH	=	Pressure fluctuations (m)

The rigid column theory provides acceptable results for the pressure fluctuations resulting from a valve closure if, $dt > \frac{L}{60}$ where *dt* equals the time-lapse in seconds between the two equilibrium stages and L (m) is the length of the pipeline (Van Vuuren, 1990).

2.5.4 The elastic theory

This theory is based on the assumption that a pressure wave will propagate along the pipeline at a rapid, but finite rate wherever a disturbance occurs. Propagation of the pressure wave results in compression of the fluid and the deformation of the pipeline as the wave moves through the system. When the elastic theory is utilised in determining the magnitude of transient pressures, the elasticity of the pipeline can either be neglected in the rigid pipe theory or it can be taken into account in the elastic pipe theory (Van Vuuren, 1990). The following two variations of the pressure-flow-relationships are then obtained:

2.5.5 The elastic (rigid pipe) theory

$$\Delta P = \rho \cdot c \cdot \Delta V$$

Equation 2-5

Where:

ΔP	=	Pressure fluctuations (N/m^2)
c	=	Wave celerity for pipe (m/s)
ρ	=	Unit mass of water (kg/m^3)
ΔV	=	Change in flow velocity (m/s)

The wave celerity can be determined by:

$$c = \sqrt{\frac{K}{\rho}}$$

Equation 2-6

Where:

K	=	Bulk modules of water (N/mm^2)

This relationship is referred to as Joukowsky's law (Van Vuuren, 1990).

2.5.6 The elastic pipe theory

The principle of preservation of energy shows that:

$$c' = c \cdot \frac{1}{\sqrt{1+\left(\frac{K}{E}\right)\left(\frac{D}{t}\right)}}$$

Equation 2-7

Where:

c'	=	Wave celerity for an elastic pipe (m/s)
K	=	Bulk modulus of water (N/mm^2)
E	=	Elasticity of pipe material (N/mm^2)
D	=	Pipe diameter (m)
t	=	Wall thickness of the pipe (m)

2.6 The effect of free air on transient pressures

Entrapped air can have either beneficial or detrimental effects on a pipeline. These effects depend on the amount of air, the two-phase control of the air-water mixture and the cause and properties of the transient pressure.

2.6.1 Benefits of free air on transient pressures

The elasticity of the air present in an air-water mixture can cause a significant reduction in water hammer pressures and can also lead to a decrease in the wave celerity. This dampening effect of free air on pressure surges as a result of the compressibility of the air can be reflected in the calculation of the wave celerity.

For a pipeline without the presence of free air (Van Vuuren, 1990):

$$c = \sqrt{\left(\frac{K}{\rho}\right)\frac{1}{1+\left(\frac{K}{E}\right)\left(\frac{D}{t}\right)}}$$

Equation 2-8

For a pipeline with the presence of free air (Van Vuuren, 1990):

$$c' = c \cdot \sqrt{\frac{1}{1+\frac{c_2 \cdot m}{p^2}}} \qquad \text{With} \qquad c_2 = \frac{R \cdot T \cdot K}{1+\frac{K \cdot D}{E \cdot t}}$$

Equation 2-9

Where:

c'	=	Wave celerity (m/s)
K	=	Bulk modulus of water (N/mm^2)
E	=	Elasticity of pipe material (N/mm^2)
D	=	Pipe diameter (m)
t	=	Wall thickness of the pipe (m)
ρ	=	Density of water (kg/m^3)
c_2	=	Constant
m	=	Mass of free air per unit mix (kg/m^3)
p	=	Absolute pressure (N/m^2)
R	=	Gas constant (J/kg·K)
T	=	Temperature (Kelvin)

Figure 2-4 indicates the relation between the wave celerity and the percentage of air present in a system for different water pressures (Wylie & Streeter, 1978).

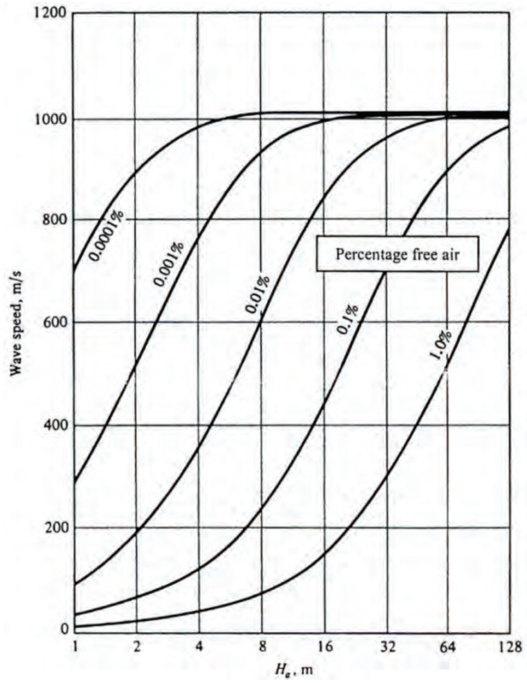

Figure 2-4: Wave speed for an air-water mixture (Wylie & Streeter, 1978)

2.7 Detecting leaks in pressurised pipes by means of transients

2.7.1 Background

Limited information is currently available on the subject of inverse transients with specific reference to determining the existence and location of free air in a pipeline. The study therefore draws on the available knowledge concerning the use of inverse transients to detect the existence and location of leaks in a pipeline.

Hydraulic transients can be considered as a valuable tool for obtaining information on specific hydraulic properties. When a hydraulic transient propagates through the pipeline, like a ‘probe’, it is affected by specific properties or irregularities within the pipeline. The analysis of such a transient will potentially provide valuable information on these properties and irregularities in the pipeline. The recordings of pressure transients should therefore indicate the existence of an air pocket, a leak or a malfunctioning check valve (Jönsson, 2001).

The need exists for an effective method to obtain information regarding the properties in a pipeline in order to detect the irregularities that could be indicative of leaks. Experiments need to be safe and controlled. This can be done by suddenly opening or closing a valve and monitoring the pressure responses of the network. The measured pressure/flow signal can provide information on the leak and layout status of the pipeline. The signal on the ‘normal’ part of the pipeline can be used to calibrate the rest of the network and to assess the influence of leaks. This is masked by random noise and measurement errors, reflections from irregularities, unknown demands and is attenuated and transformed by friction steady or unsteady states (Ivetic & Savic, 2002).

Results obtained in a laboratory study and in operative pipes (Jönsson from Brunone & Ferrante, 2002) showed the appropriateness of unsteady-state tests in the detection of pipe leaks. In these tests relative small overpressures were sufficient and the risk of damaging the pipes under testing was relatively small. The pressure signal was registered in one section of the pipeline (measured section) and the technique under discussion was then used in the operative sections (Brunone & Ferrante, 2002).

A large number of leak detection methods currently exist. Physical systems used (e.g. ground-penetrating radar, acoustic leak-detection, infrared spectroscopy) are very sophisticated and fairly reliable, but also very costly. A simple, cheap and reliable method for the detection of leaks would be of great economic value (Kapelan *et al.*, 2003). Liggett and Chen introduced the method of inverse transient analysis for the detection of leaks. In contrast with steady-state problems, transient events can provide large amounts of data required for successful calibration (Kapelan *et al.*, 2003).

2.7.2 Traditional techniques used for leak detection

There are many different techniques that can be used to determine the existence and location of leaks in a pipeline. Most originated from the field of oil and gas. The techniques most commonly used are (Brunone *et al.*, 2000):

- *Hydrostatic method*: This technique involves the pressurising of a pipeline and the reviewing of the pressure drop in the isolated section. Another procedure entails the comparison of the continuity of mass transfer.

- *Acoustical method*: This technique uses the correlation between acoustic sounds generated by high velocity and the liquid pressure in the pipeline to detect leaks in the pipeline.

- *Inverse steady-state method*: This method requires extensive data to be commercially viable due to the dynamics in water systems (Pudar & Liggett, 1992).

2.7.3 Leak analysis in pipes using inverse transients

Leak analyses in pipes through the use of transients form part of the Transient Analysis Methods which are based on the transmission and reflection properties of pressure waves (Jönsson *et al.* from Brunone *et al.*, 2000).

A leak has three effects on the pressure graph (Brunone *et al.*, 2000):

- Firstly, when the decaying (negative) pressure wave reaches the leak, a reflection wave and a translation wave are generated at the leak. The reflection waves travels towards the origin of the negative pressure wave. This increases the value of the pressure at that instance and results in a disturbance in the downward pressure leg, which can be observed on the pressure time plot at the point where the negative pressure wave was created (**Figure 2-5**). The further the leakage is from the point where the negative pressure wave was generated the longer it will take for the disturbance to be noticed on the pressure time graph. Similar variations will be seen at all locations where the pressure are monitored between the position where the negative wave was generated and the location of the leak. The amplitude of the wave increases as the dimension of the leak increases. The time difference between the initial wave and the reflected wave can be determined and the location of the leak can then be calculated through **Equation 2-10**. The cycle period of the pipeline can be determined by using a graph similar to **Figure 2-5**. If the length of the pipeline is known, the celerity at which the transient travels can be determined with the following formula:

$$c = \frac{2 \cdot L}{\Delta t}$$

Equation 2-10

Where:

c	=	Wave celerity (m/s)
L	=	Length of the pipeline (m)
Δt	=	Time difference between the initial wave and the reflected wave (s)

- Secondly, leaks cause distortions in the oscillatory peaks and troughs after the main pressure rise has occurred.

- Thirdly, a disturbance in the oscillating pressure pattern resulting from the reflection wave generated at the leak.

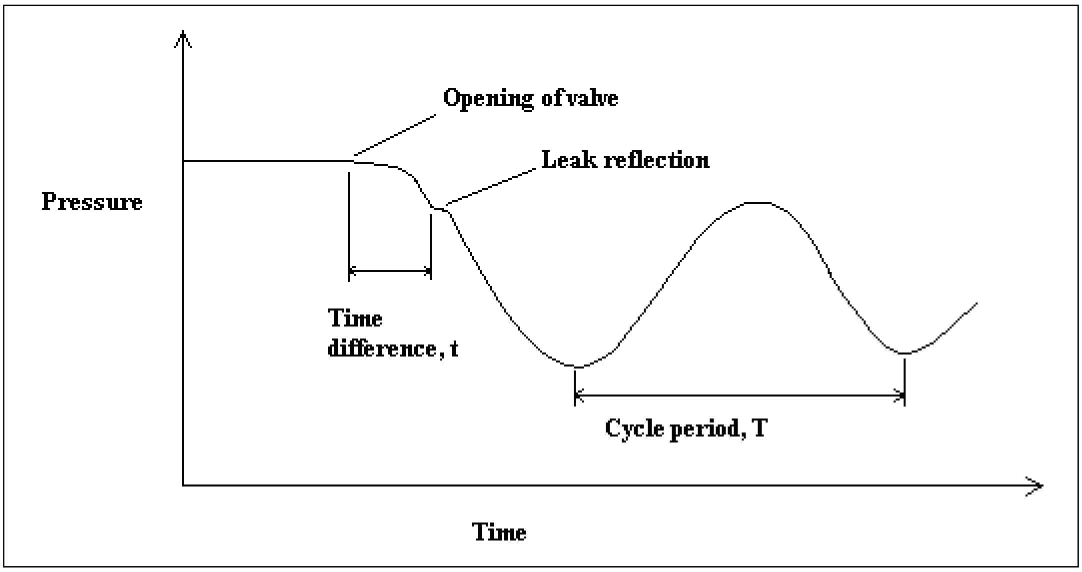

Figure 2-5: Basic theory of leak detection

The measured pressure signal can be compared with either the predictions of a numerical model for the same transient or the experimental values previously obtained.

The procedure for leak detection in pipelines using inverse transient analysis consists of the following steps (Kapelan *et al*, 2003):

- Introducing of an artificial transient, either by changing the flow or head at a specific location e.g. opening or closing of a valve;

- Observation of pressures and flows variation (if possible) at a number of locations in the system;

- Comparison of the recorded and simulated pressure variations;

- Identification of the deficiencies from the results.

The author (Kapelan *et al*, 2003) suggested that periodic calibration and review of the transient model should be conducted to incorporate the changes which have been imposed on the system (pipe replacements and extensions).

3 Theoretical modelling of the system

3.1 Introduction

Prior to the start of this study some experimental work had been carried out by the author, reviewing the use of induced transients in experimental setups with the objective to determine the potential use of this technique in the evaluation of deficiencies in water transfer systems.

The experimental work was limited to the use of inverse transients to evaluate the effect of the presence of localised trapped air volumes and artificial leakages in pipelines and what their effect is on the propagation of pressure waves. Small bore pipes (50 mm to 100 mm diameter) were tested.

Appendix 3A contains details of tests that were conducted during the period 2004 to 2009.

The theoretical review on a number of system precedes the experimental work which is described in Chapter 4. In the following paragraphs the B16 pipeline is theoretically reviewed to establish the influence of a leak and an air bubble on the transient waves.

3.2 Theoretical assessment of the B16 pipeline

3.2.1 Introduction

Pipelines were identified to be reviewed theoretically by using the appropriate surge analyses software with the intention of obtaining comparative results for the pipelines with and without deficiencies (air bubbles and leaks) in the system.

In the following section the B16 pipeline of Rand Water is discussed. The influence of leakage and air bubbles was reviewed separately.

3.2.2 Leakage influence on pressure waves in B16

A Surge model was set up for the B16 pipeline to be able to conduct a theoretical assessment of the influence of leaks and air bubbles on the pattern of the pressure waves in the pipeline at different locations**. Figure 3-1** reflects the simplified profile that was used for the surge analyses while

Figure 3-2 presents the schematic system layout (Node numbers) that was used in the surge analyses. Details of the profile are provided in **Table 3-1.**

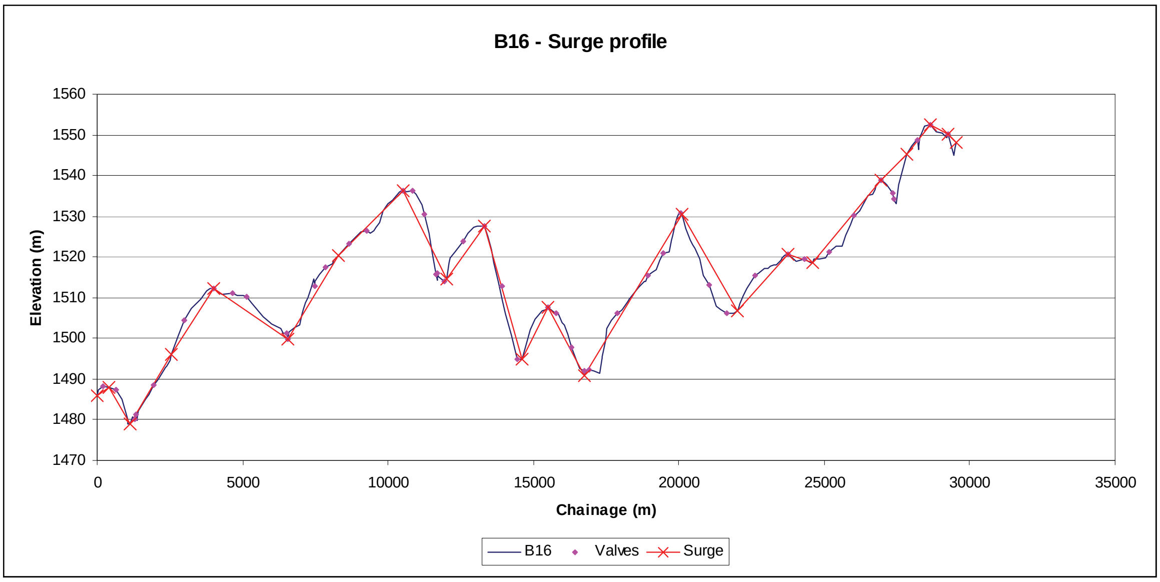

Figure 3-1: The profile used for the surge analyses on the B16 pipeline

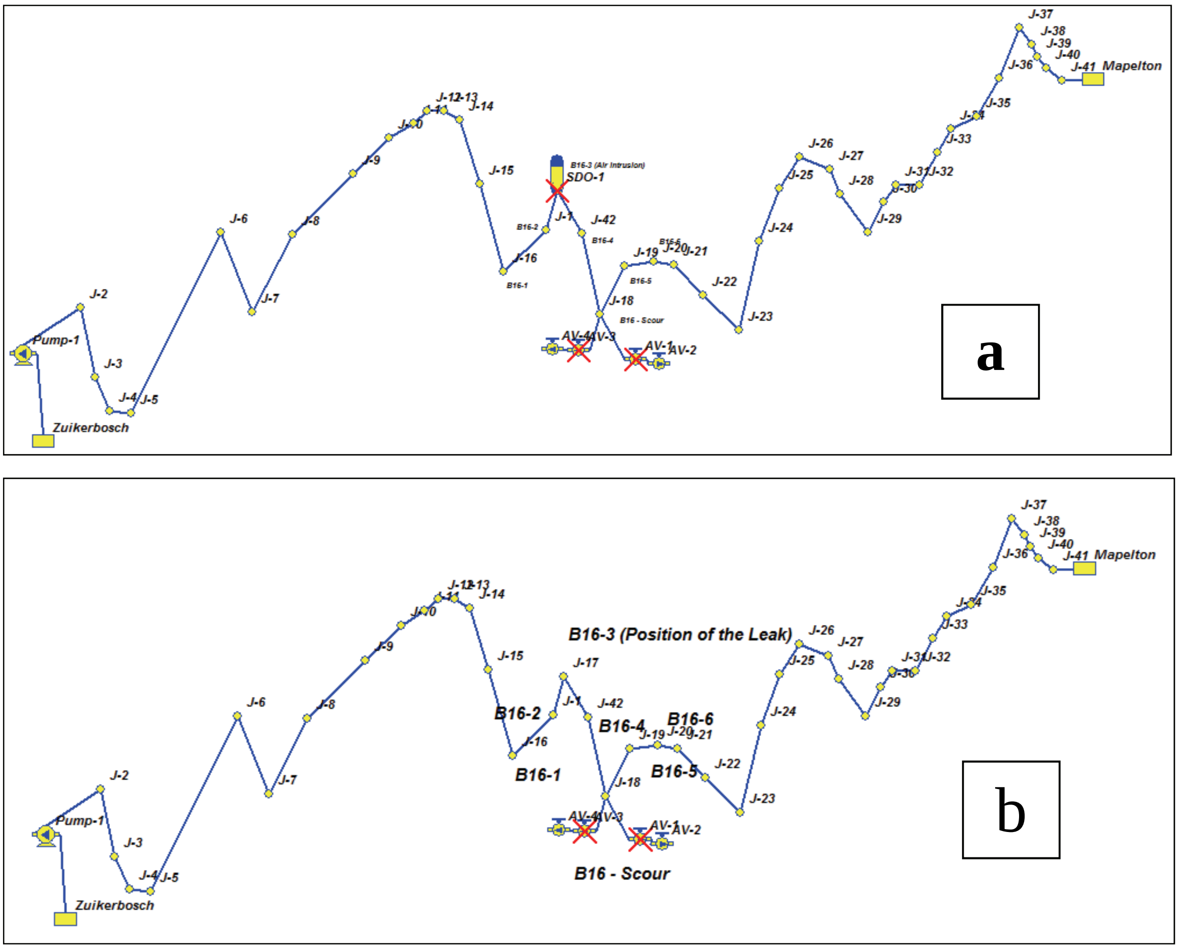

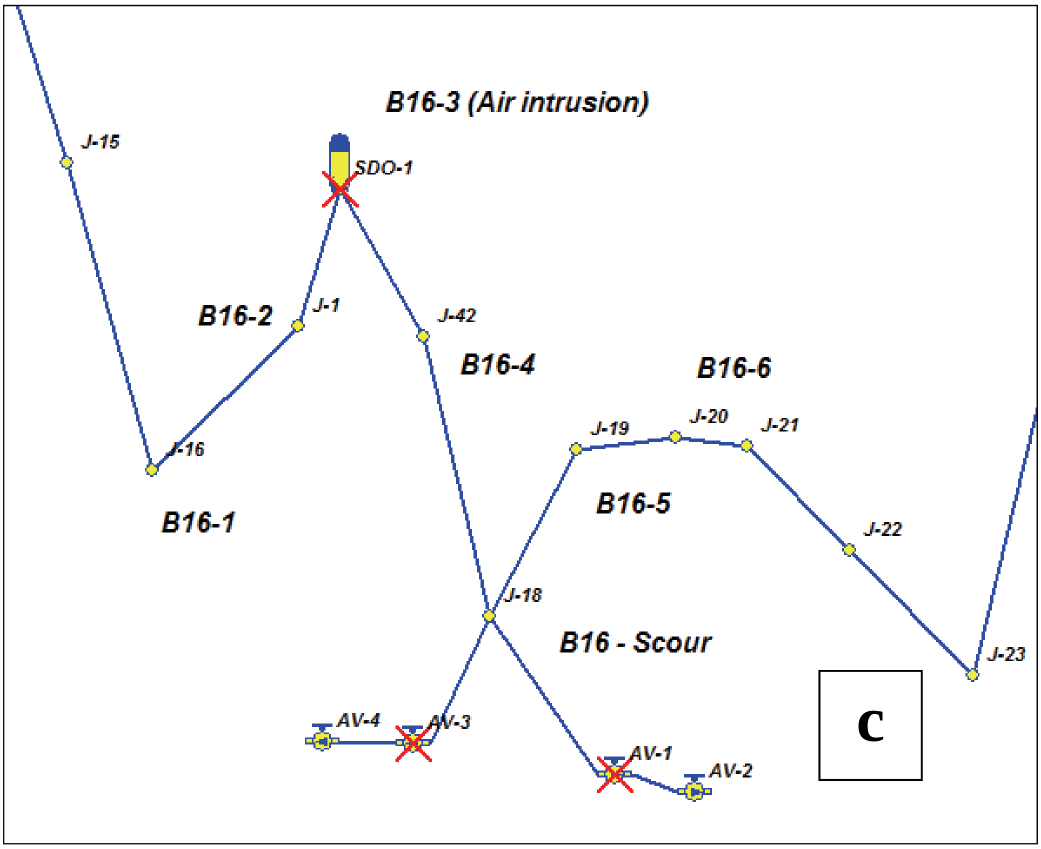

Figure 3-2: Schematic layout (a and b) of the surge models for B16 with the details of the pressure recording positions (c)

Table 3-1: Details of the surge profile for B16

Node		Chainage (m)	Elevation (m)	Pipe length (m)
J-1		0,00	1485,81	
J-2		400,00	1487,85	400,00
J-3		1150,00	1479,05	750,00
J-4		2561,65	1495,90	1411,65
J-5		4000,00	1512,25	1438,35
J-6		6575,00	1499,85	2575,00
J-7		8300,00	1520,30	1725,00
J-8		10500,00	1536,30	2200,00
J-9		12000,00	1514,60	1500,00
J-10		13300,00	1527,65	1300,00
J-11		14600,00	1494,95	1300,00
J-12		15500,00	1507,70	900,00
J-13		16770,00	1490,80	1270,00
J-14		20100,00	1530,40	3330,00
J-15		22000,00	1506,75	1900,00
J-16		23750,00	1520,50	1750,00
J-17		24581,10	1518,60	831,10
B16-3	Location where the air was introduced (Node J-17).			
J-18		26956,68	1538,75	2375,58
	Location where the negative pressure wave was generated.			
J-19		27827,81	1545,20	871,13
J-20		28630,12	1552,50	802,31
J-21		29250,00	1550,24	619,88
Mapleton		29545,39	1548,18	295,39

Table 3-2 summarises the surge analyses that were conducted to review the influence of a leak on the surge propagation while **Figure 3-3** to **Figure 3-6** reflect comparative head time relationships at certain locations for the analyses that were performed.

Table 3-2: Surge analyses to reflect the influence of a leak on the pressure wave propagation

Analysis	Flow rate (m^3/s)	Leak details		Reference on the figures below	Induced negative wave	
		Node	Leakage (l/s)		Node	Induced flow (l/s)
B16 CN	3,206	J-13	0	Prev	J-18	870
B16 CN Leak	3,206	J-13	350	New	J-18	870

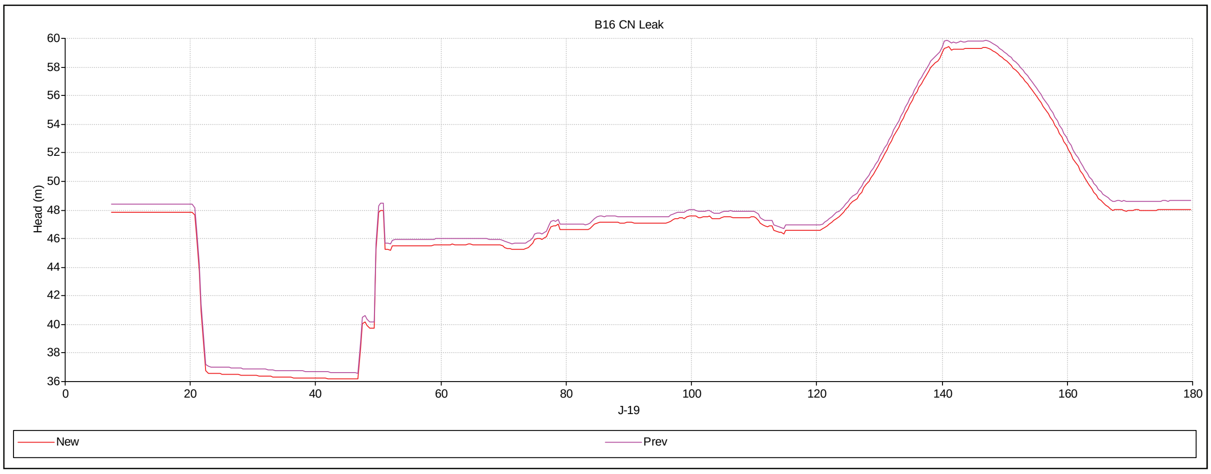

Figure 3-3: Pressure head time relationship at Node J-20 (B16-6)

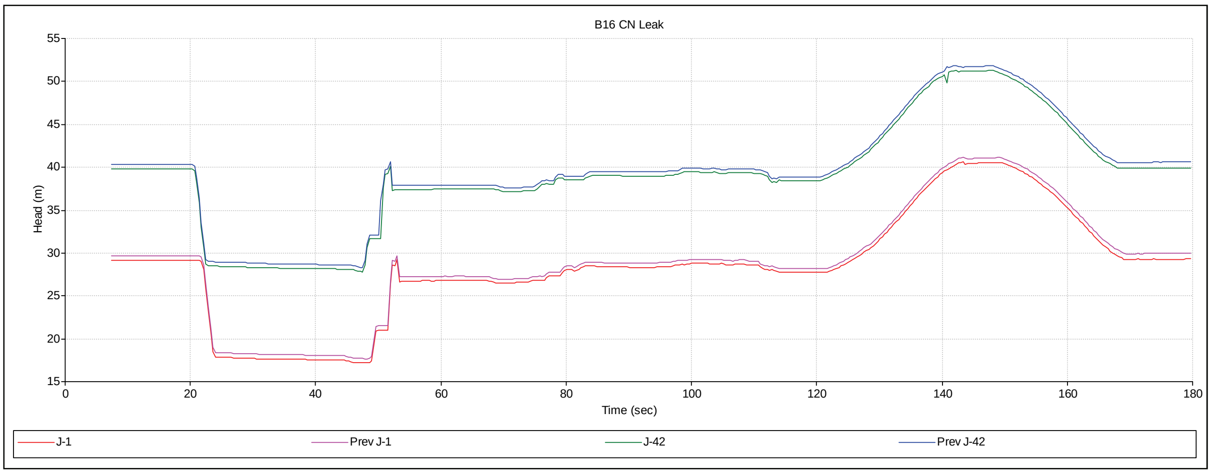

Figure 3-4: Pressure head time relationship at Nodes J-42 (B16-4) and J-1 (B16-2) (The "Prev" result is when there was no leak – Analysis B16 CN Leak)

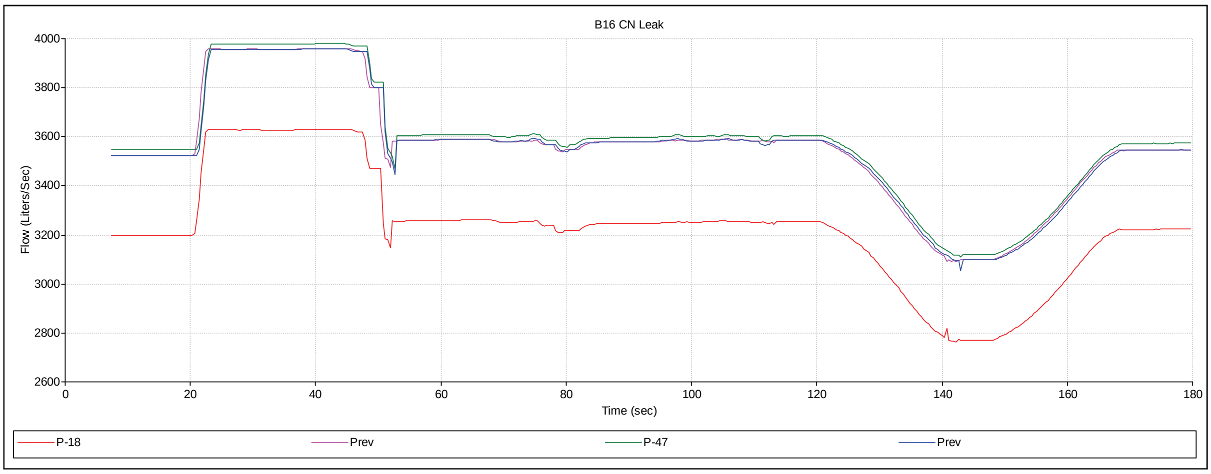

Figure 3-5: Flow rate time relationship in pipes on both sides of the leak at node J-17 (Leak)

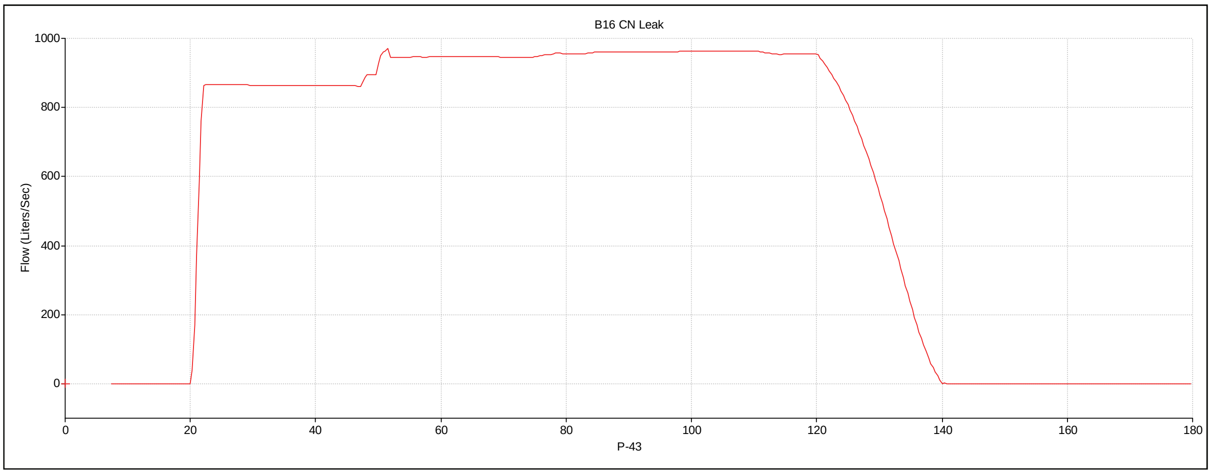

Figure 3-6: Flow rate time relationship at node J-15 where the negative wave is created

These results reflect that the influence of a small leak (less than 10 % of the flow in the pipeline) will be difficult to detect in the B16 pipeline.

3.2.3 Air bubble influence on pressure waves propagation in the B16 pipeline

Table 3-3 reflects the analyses that were performed to evaluate the influence of an air bubble on the movement of the pressure wave.

Table 3-3: Surge analyses reflecting the influence of an air bubble on the pressure wave propagation in the pipeline

Analysis	Flow rate (m^3/s)	Air bubble		Reference on the figures below	Induced negative wave	
		Node	Volume air (normal m^3)		Node	Induced flow (l/s)
B16 EN	3,206	J-17	0	Prev	J-18	870
B16 EN Air	3,206	J-17	2,1		J-18	870

Figure 3-7 to **Figure 3-11** reflect comparative head time relationships at certain locations for the analyses that were performed.

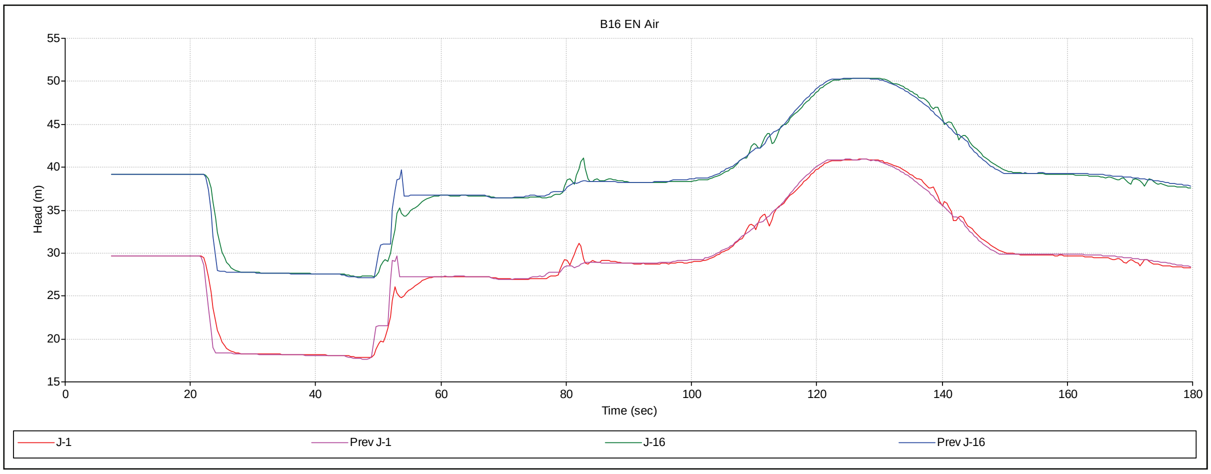

Figure 3-7: Pressure head comparison at J-1 (B16-2) and J-16 (B16-1) when an air bubble of 0 m3 (Previous) and 2,1 m3 has been captured at Node J-17

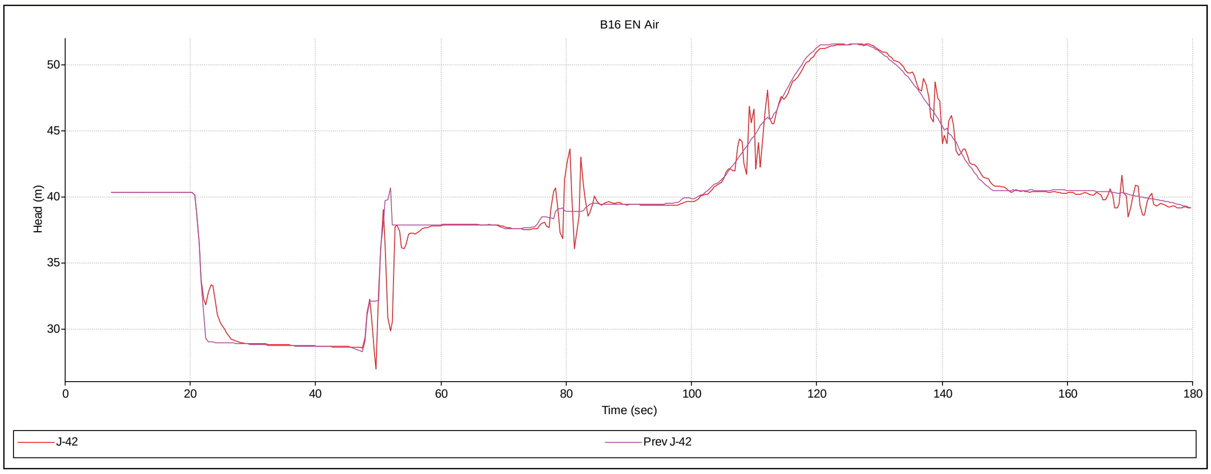

Figure 3-8: Pressure head comparison at J-42 when an air bubble of 0 m^3 (Previous) and 2,1 m^3 has been captured at Node J-17

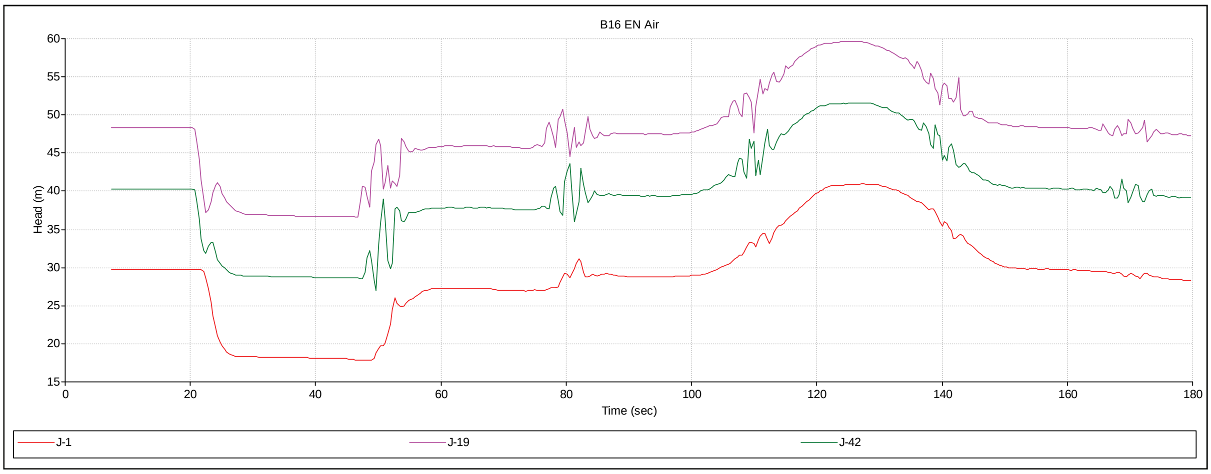

Figure 3-9: Pressure head comparison at J-1, J-19 and J-42 when an air bubble of 2,1 m^3 has been captured at Node J-17

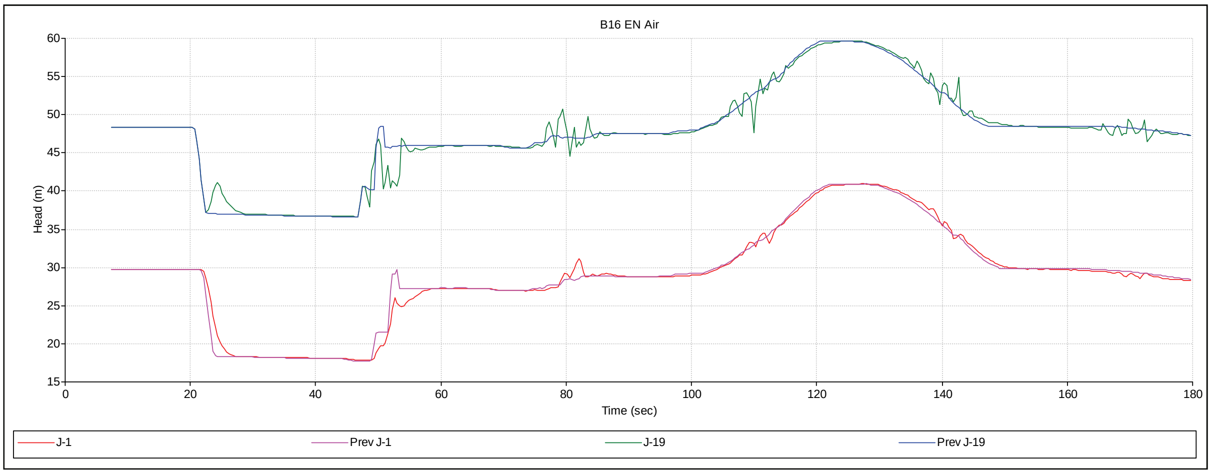

Figure 3-10: Pressure head comparison at J-1 and J-19 when an air bubble of 2,1 m^3 has been captured at Node J-17 (Result "Prev" no air at J-17)

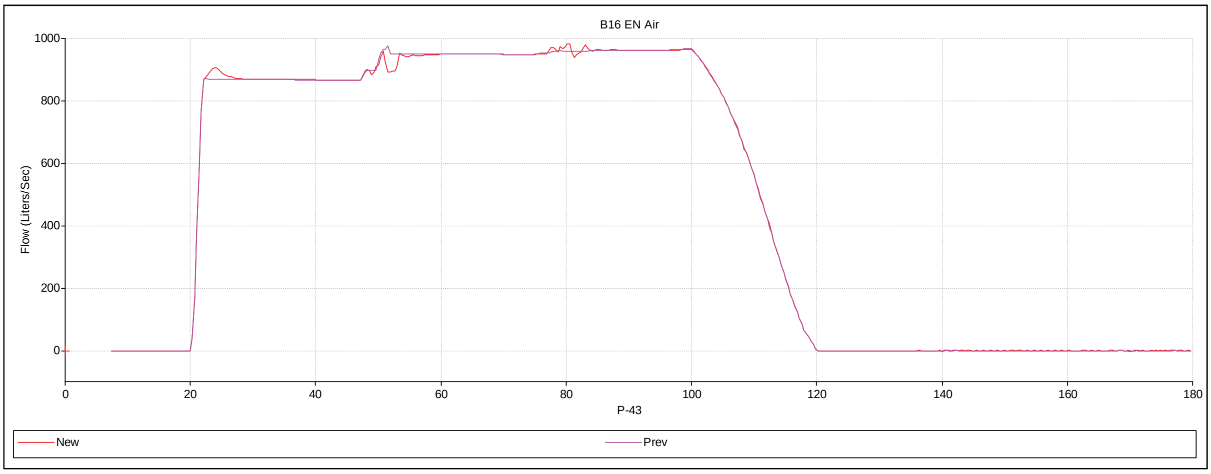

Figure 3-11: Flow rate-time comparison at J-43 when an air bubble of 2,1 m^3 has been captured at Node J-14 and no leak at J-13 (Result "Prev" was with no air at J-17)

The following observations can be made from these simulated results:

- The pressure time relationships will reflect that the reflecting wave originated from the air bubble (**Figure 3-7**, **Figure 3-8** and **Figure 3-10**);

- These pressure fluctuations are noticeable any position on the side of the air bubble where the transient has been incorporated (**Figure 3-9**); and

- The flow rate at the point where the discharge is generated reflects an increase which is associated with the deformation energy which is released from the air bubble.

These results confirm that the influence of air on the change in the wave propagation is much more prominent than the influence of a leak on the wave pattern.

The theoretical analyses reflect that:

- **Leaks of about 10% the flow rate can be detected, while**
- **An air bubbles volume to discharge rate of 10% is clearly detected in the results.**

It can therefore be concluded that the presence or air bubbles are easier detected than leaks in pipelines.

The SURGE2010 data files for the analyses are listed in Appendix 3B and are included on the accompanying CD.

4 Field work

4.1 Introduction

The emphasis in this research is to **generate a negative pressure wave in a system and by tracking the wave movement and its variation, the location of leaks and air bubbles can be identified.**

The methodology requires the installation of pressure transducers and data recorders to capture the propagation of induced pressure waves. The frequency of the pressure recordings directly influences the accuracy to locate a deficiency in a pipeline. A number of pipelines were reviewed. The following results are discussed below:

- **Arendsnes pipeline in the Tshwane Metropolitan Supply Area;**
- **The B16 pipeline of Rand Water; and**
- **The Kuthala to Kendal Pipeline of the Department of Water Affairs.**

The field tests conducted on the Arendsnes pipeline were to assess the influence of artificially generated leaks and air pockets on the wave propagation in the pipeline, while the field tests on the B16 pipeline were to assess the presence of an introduced air bubble in the pipeline. In the case of the Kuthala to Kendal pipeline (will be referred to as the Kuthala Pipeline) different normal operating scenarios were reviewed from which the locations of air pockets were determined.

The results for the three pipelines are discussed independently in the following paragraphs.

4.2 Arendsnes Pipeline – Tshwane Metropolitan Municipality

4.2.1 Introduction

Experience obtained from preliminary experimental work, indicated that inverse transients can be used to determine the location of deficiencies by assessing the anomalies of the pressure time plots. **Figure 4-1** is a simple presentation of the pressure-time plot, indicating the influence of a leak on the pressure-time plot (Refer to Chapter 2).

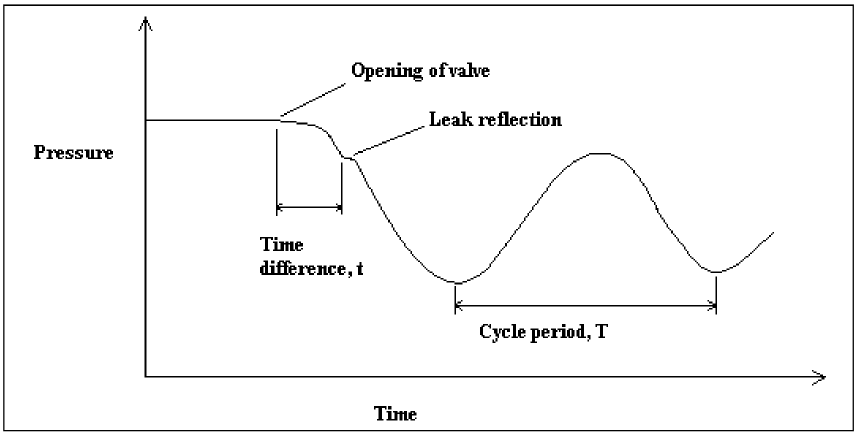

Figure 4-1: Simplified pressure-time plot indicating the influence of a deficiency (leak) on the relationship

Based on this notion, pressure recordings were conducted to review the wave propagation in the pipeline with an entrapped air bubble and different artificially generated leak rates.

The nodes where instrumentation was installed for the inverse transient tests on the Arendsnes pipeline are reflected in **Figure 4-2**. The artificially generated leak was introduced at node AN4, while the air was introduced at node AN3 because node AN2 was inaccessible.

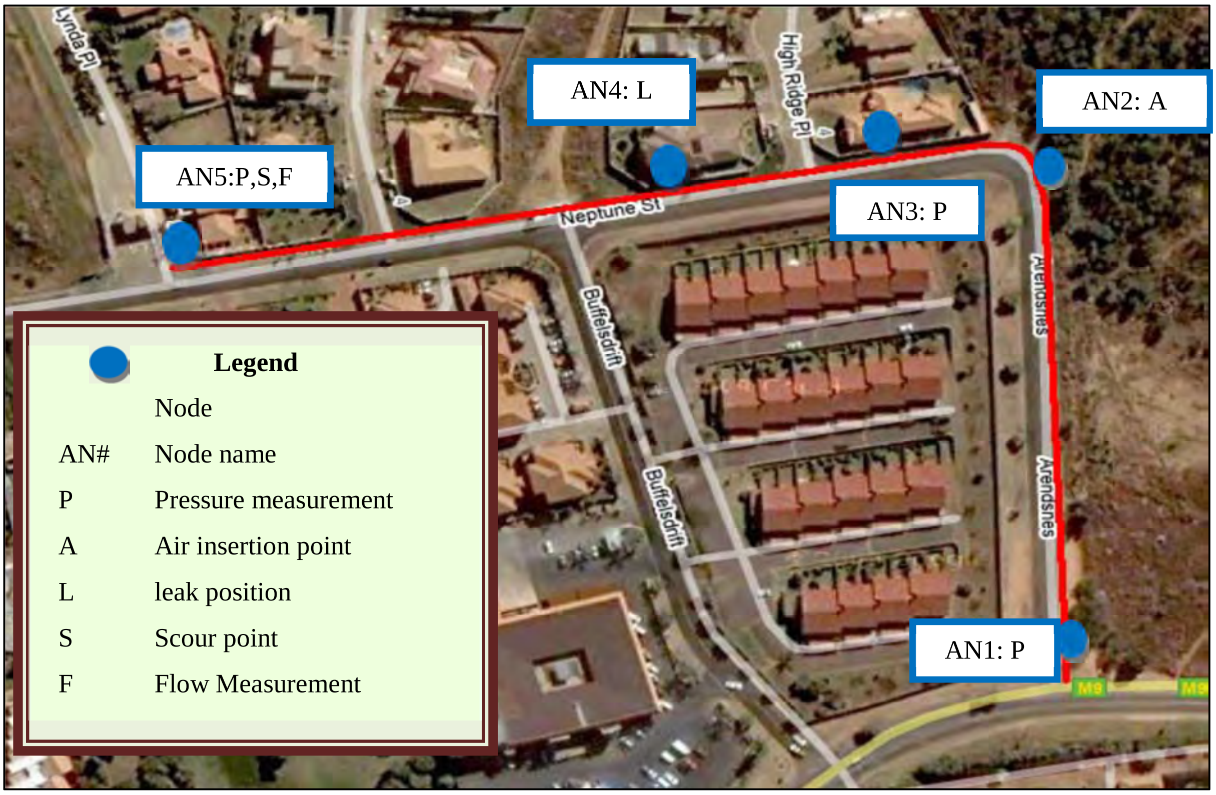

Figure 4-2: Positions where instrumentation was installed on the Arendsnes pipeline

Details of the pressure transducers and data loggers that were used are reflected in **Table 4-1**.

Table 4-1: Arendsnes – Pressure transducers and data loggers' details

Node	Distance between nodes (m)			Pressure transducers	Manufactured of Data loggers and Identification		Measurement frequency
	Start	End	Distance		Type	ID	
AN5 #	*AN5*	*AN3*	446,45	16 Bar Absolute	Hobo	2044486	1 Hz
				25 Bar Gauge	Dataq	489B2FAC	10 Hz
Leak	*AN5*	*Leak*	263,91	*None*			
AN3	*AN3*	*AN1*	382,54	16 Bar Absolute	Dataq	48AC594F	10 Hz
				10 Bar Gauge	Hobo	2229541	1 Hz
AN1	*AN1*	*T-junction*	26,5	10 Bar Absolute	Hobo	2010102	1 Hz
				16 Bar Absolute	Dataq	489B4101	10 Hz
Total section	*AN5*		855,49	*None*			

Note:

 # Location where the flow was introduced to generate the pressure wave.

Table 4-2 indicates the tests which were performed on 18 June 2009.

Table 4-2: Tests conducted on the Arendsnes pipeline

System configuration	Test	Start time
Arendsnes current system	N1	13:15
	N2	13:19
	N3	13:25
Small Leak	Ls1	13:31
	Ls2	13:34
	Ls3	13:38
Large leak	LL1	13:42
	LL2	13:45
	LL3	13:48
Intermediate leak	IL1	13:53
	IL2	13:58
	IL3	14:01
Air	Air1 or AT1	14:27
	Air2 or AT2	14:29
	Air3 or AT3	14:32

Table 4-3 indicates the different leaks which were introduced at node AN4.

Table 4-3: Details of the leaks which were introduced at node AN4

Leak	Time to fill bucket	Leak rate (l/s)
Small	3 minutes and 19 seconds	0,553 l/s
Large	41 seconds	2,68 l/s
Intermediate	1 minute and 32 seconds	1,196 l/s

4.2.2 Results from the slow data recordings (1 Hz) (Hobo data loggers)

4.2.2.1 Introduction

The Hobo data loggers were located at each of the pressure measurement sites (**Figure 4-2**). At each of these locations data was also recorded at a higher frequency using a Dataq data logger. The recording rate of the Hobo data loggers is 1 Hz, while that of the Dataq recordings were conducted at 10 Hz.

A graphical presentation of the recorded data sets (at 1 Hz) at the different nodes (AN5, AN3 and AN1) is illustrated in **Figure 4-3** to **Figure 4-5**.

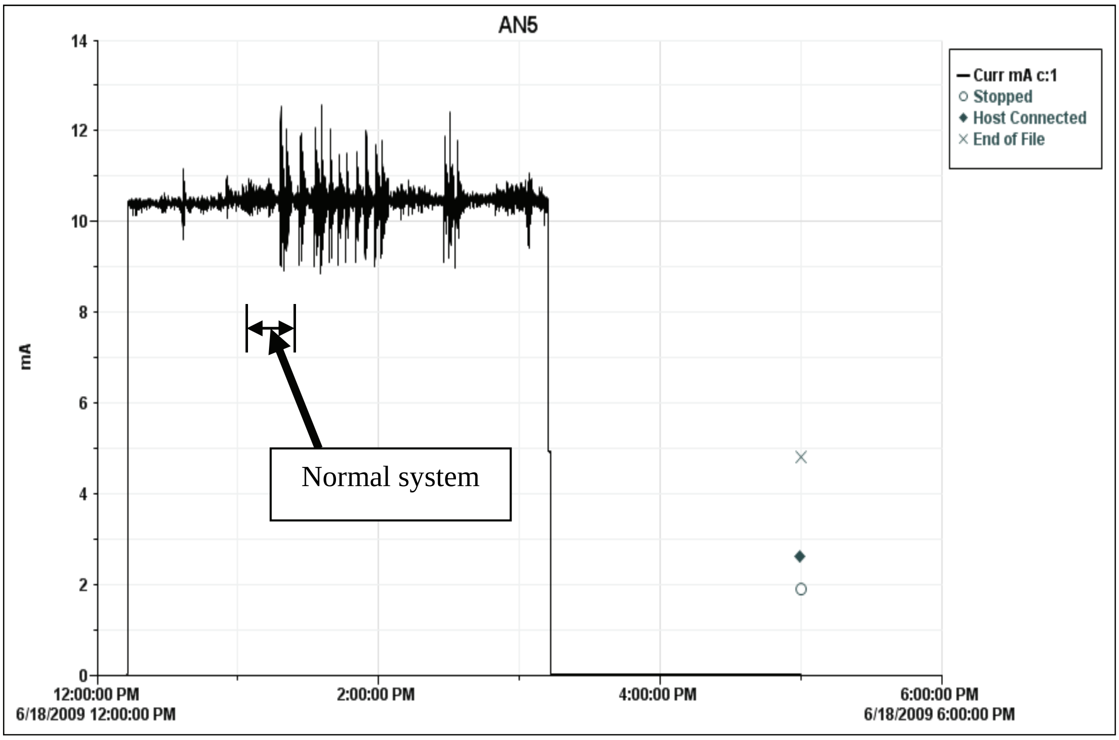

Figure 4-3: Hobo data – Graphical presentation of the recorded data at AN5

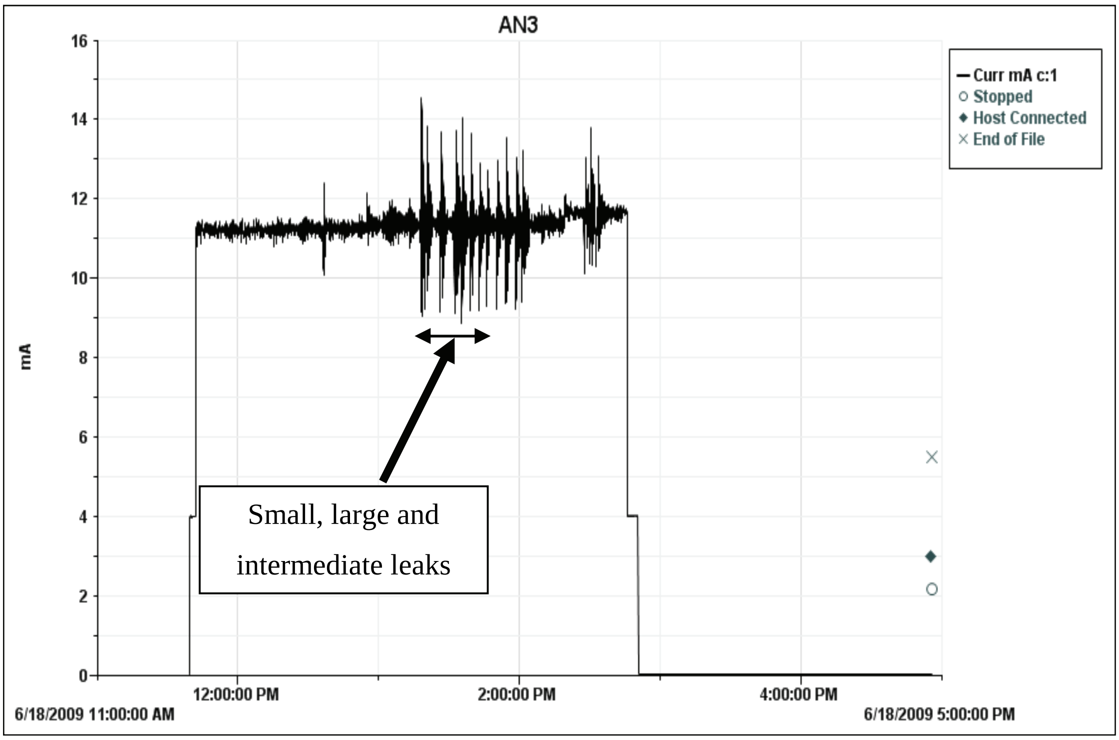

Figure 4-4: Hobo data set – Graphical presentation of the recorded data at AN3

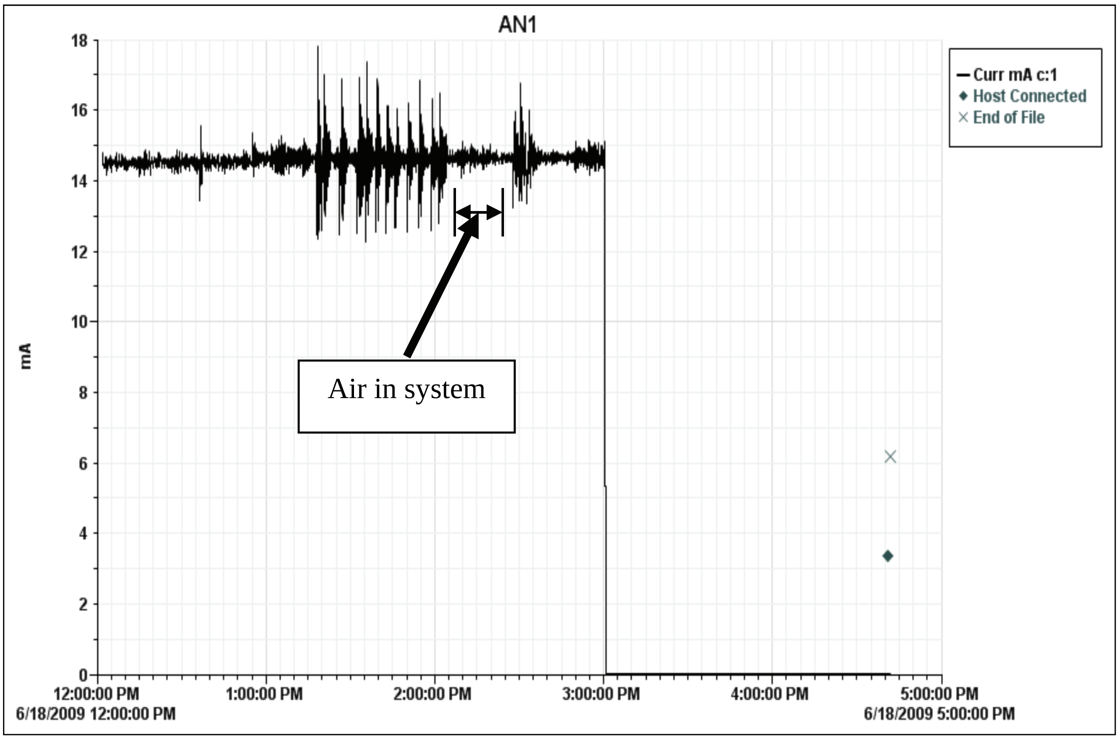

Figure 4-5: Hobo data set – Graphical presentation of the recorded data at AN1

All 15 generated pressure spikes can be identified on each of the recorded data sets resulting from the inverse transient pressures that were generated. The recorded data sets are included in electronic format in **Appendix 4A**.

The first 3 pressure waves were recorded on the **current system** (indicated as events 1 to 3), followed by the 3 pressure waves corresponding to a small leak being introduced onto the system (at node AN4) (events 4 to 6), then the next 3 waves represent the tests for a large leak (at node AN4) (events 7 to 9), followed by the next 3 pressure fluctuations representing the conditions associated with an intermediate leak (events 10 to 12). The final 3 pressure fluctuations represent the effect of the introduction of 2 Kg of air into the system just downstream from the isolated air valve at node AN2 (events 13 to 15). The distances between the recording nodes are schematically reflected in **Figure 4-6.**

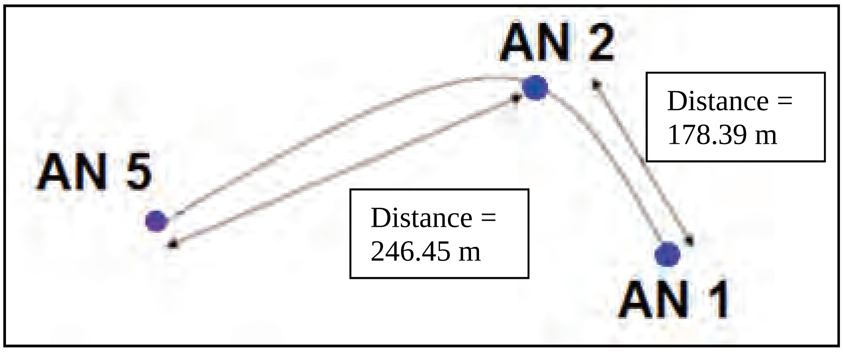

Figure 4-6: Schematic layout of the pressure recording nodes on the Arendsnes pipeline

The analyses for the slower recording frequencies (Hobo recorders capturing data at 1 Hz) are not discussed here. The relative short distance between the recording positions requires a higher frequency for the data recordings to be able to accurately define the pressure fluctuations.

The graphical results illustrated in **Figure 4-9** to **Figure 4-11** reflect the pressure on the vertical axis in milliamp and the time on the horizontal axis in seconds. The pressure reducers recorded pressures in milliamps and these milliamp values were converted to pressure head, utilising linear relationships for the pressure rating of the transducer (normally Bar). The pressure transducer's ratings, indicated in **Table 4-1**, were used in the calculation of the pressures. The output of 4 to 20 milliamp for the Hobo recorders and the 0 to 2 Volt output of the Dataq recorders were used to convert the recorded data to pressures.

The results from the faster recordings (Dataq recorded at 10 Hz) are reflected below.

4.2.3 Results obtained from the field tests conducted on the Arendsnes pipeline

4.2.3.1 Introduction

The Dataq data loggers were positioned at the locations along the pipeline identified in **Figure 4-2** where the pressures were recorded on Dataq data loggers at a frequency of 10 Hz. These data loggers have a resolution of 16 bits. Since these Dataq data loggers record at 10 Hz, the data records are extensive and the appropriate sections need to be extracted.

4.2.3.2 Recorded flow data for the field tests at Arendsnes

The release of flow from the pressurised system was recorded at a frequency of 1 Hz, using a FUJI ultrasonic flow meter. reflects the instrumentation while the recorded flow rate variation is provided in.

Figure 4-7: Flow recording equipment (Fuji)

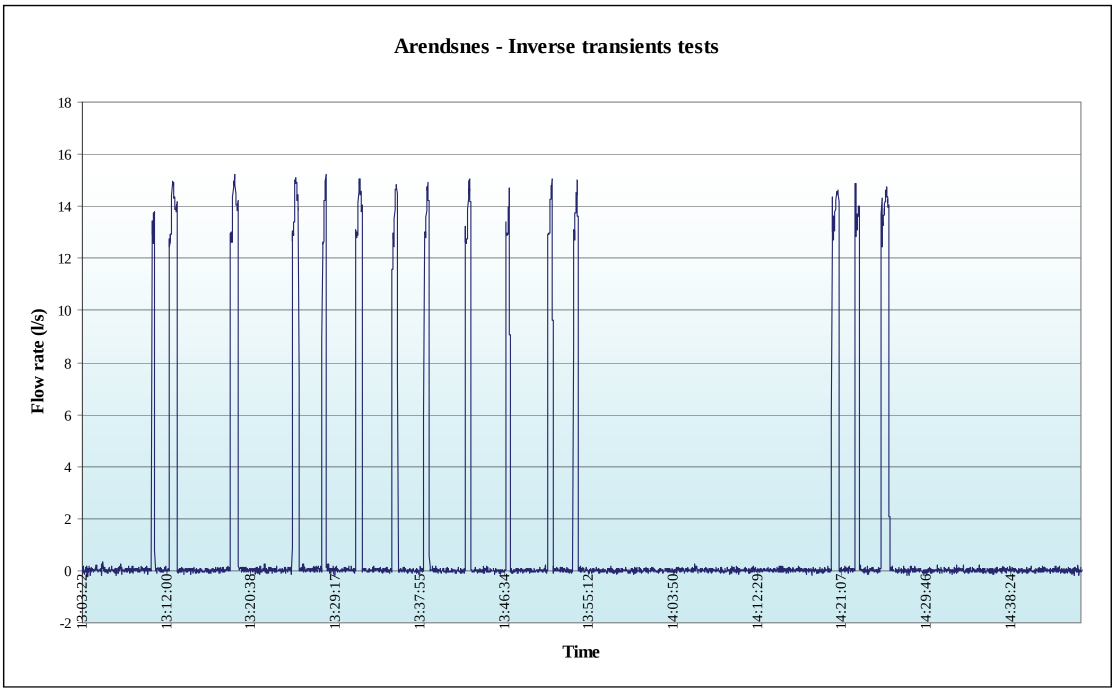

Figure 4-8: Recorded induced flow rate at AN5

The maximum recorded flow rate was 15,23 l/s. reflects the relationship between the flow rate used to induce the pressure surge for the various tests.

Table 4-4: The flow rates at AN5 used to generate the negative pressure spike

System	Reference on graphs	Test	Maximum flow rate (l/s)	Duration of release
Current (N)	1	NT1	13,80	
	2	NT2	14,93	
	3	NT3	15,23	
Small leak (Ls)	4	SLT1	14,93	
	5	SLT2	15,22	
	6	SLT3	15,04	
Large leak (LL)	7	LLT1	14,75	
	8	LLT2	14,93	
	9	LLT3	15,07	
Intermediate leak (LI)	10	ILT1	14,72	
	11	ILT2	15,02	
	12	ILT3	15,00	
Air	13	AT1	14,47	
	14	AT2	14,89	
	15	AT3	14,76	

4.2.3.3 Recorded pressure head variations (Arendsnes Pipeline)

The data sets were reviewed and the data for each of the tests identified in
Table 4 2 were extracted. **Figure 4-9** to **Figure 4-17** provide the pressure head variation for the different the tests that were undertaken (**Table 4-2**). The first tests without the artificial leak or air introduced into the pipeline are referred to as the “Normal state”.

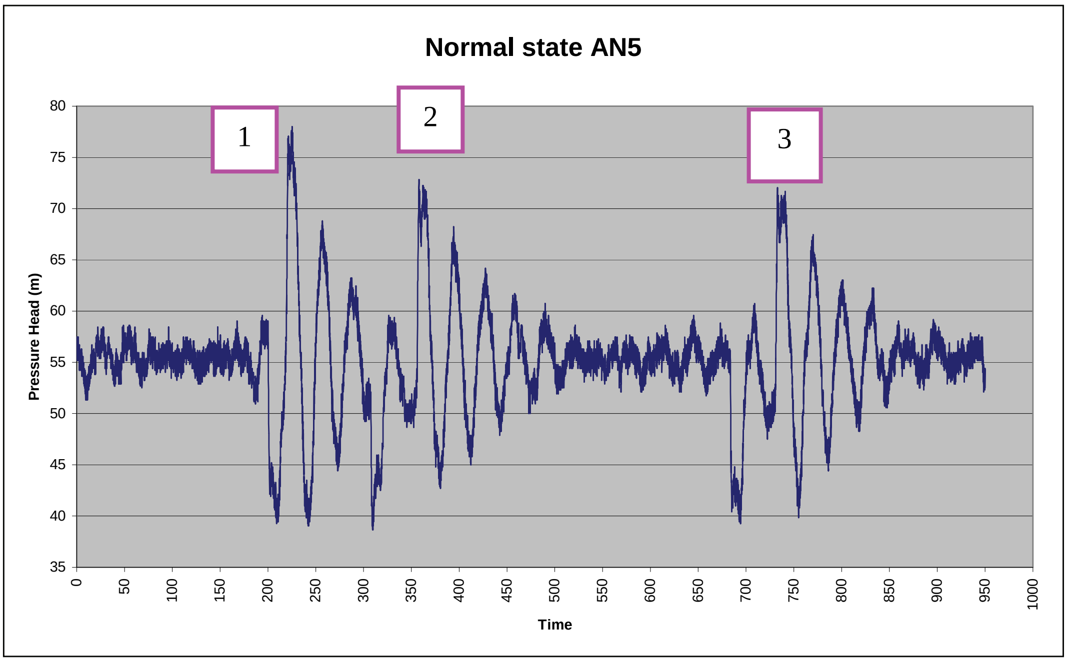

Figure 4-9: Dataq pressure recording – Current system AN5

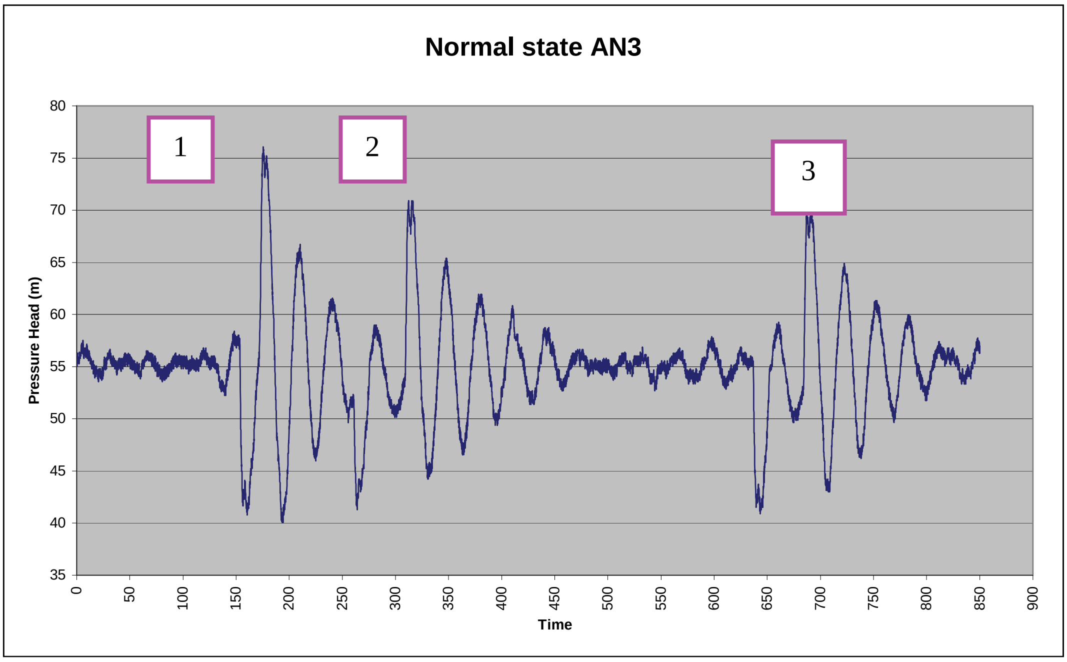

Figure 4-10: Dataq pressure recording – Current system AN3

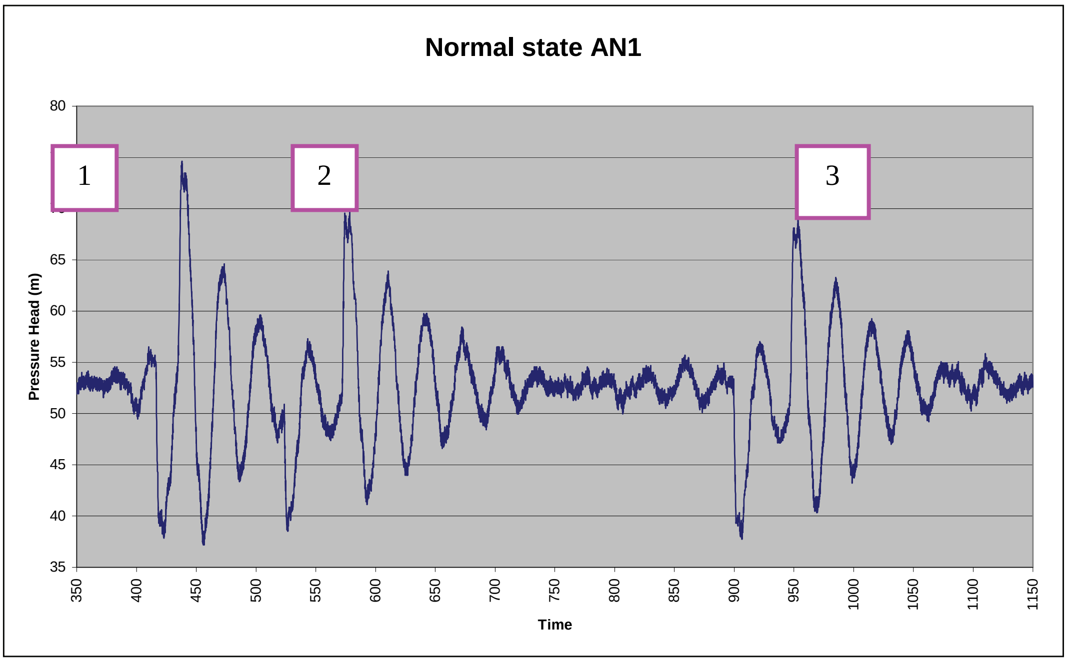

Figure 4-11: Dataq pressure recording – Current system AN1

The Dataq recorded pressure fluctuation for the tests for the different leakage rates are reflected in **Figure 4-12** to **Figure 4-14** and are referenced as "Leakage events".

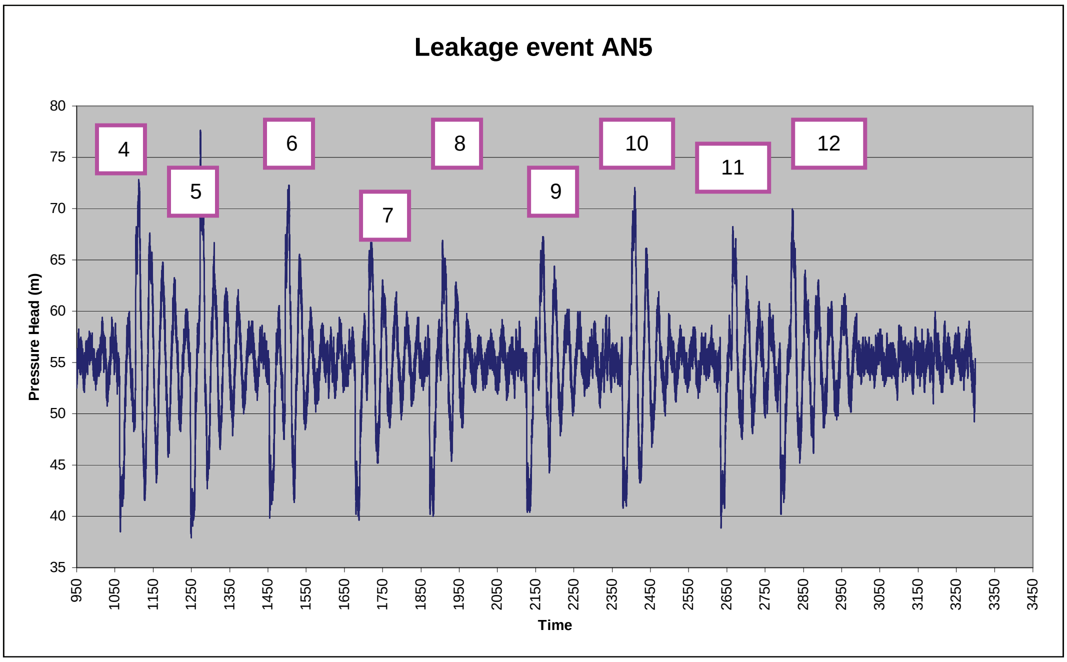

Figure 4-12: Dataq pressure recording at AN5 for the tests where leaks were artificially introduced at node AN4

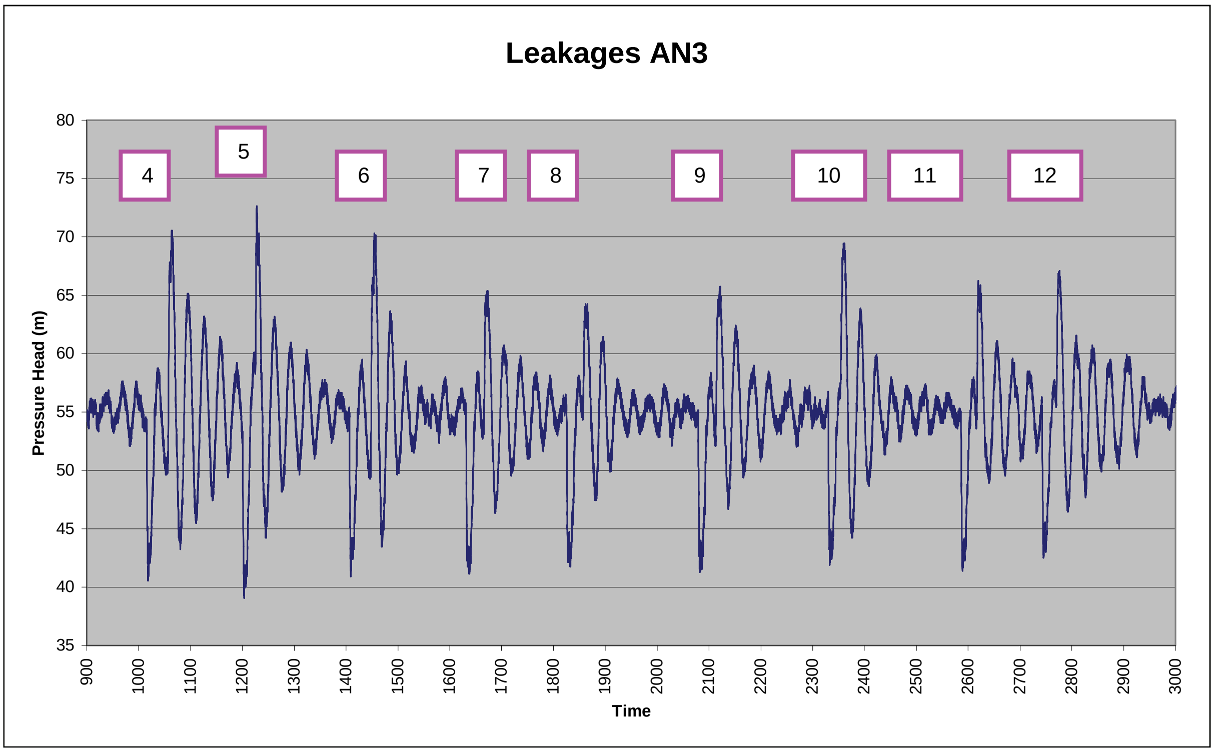

Figure 4-13: Dataq pressure recording at AN3 for the tests where leaks where leaks were artificially introduced at node AN4

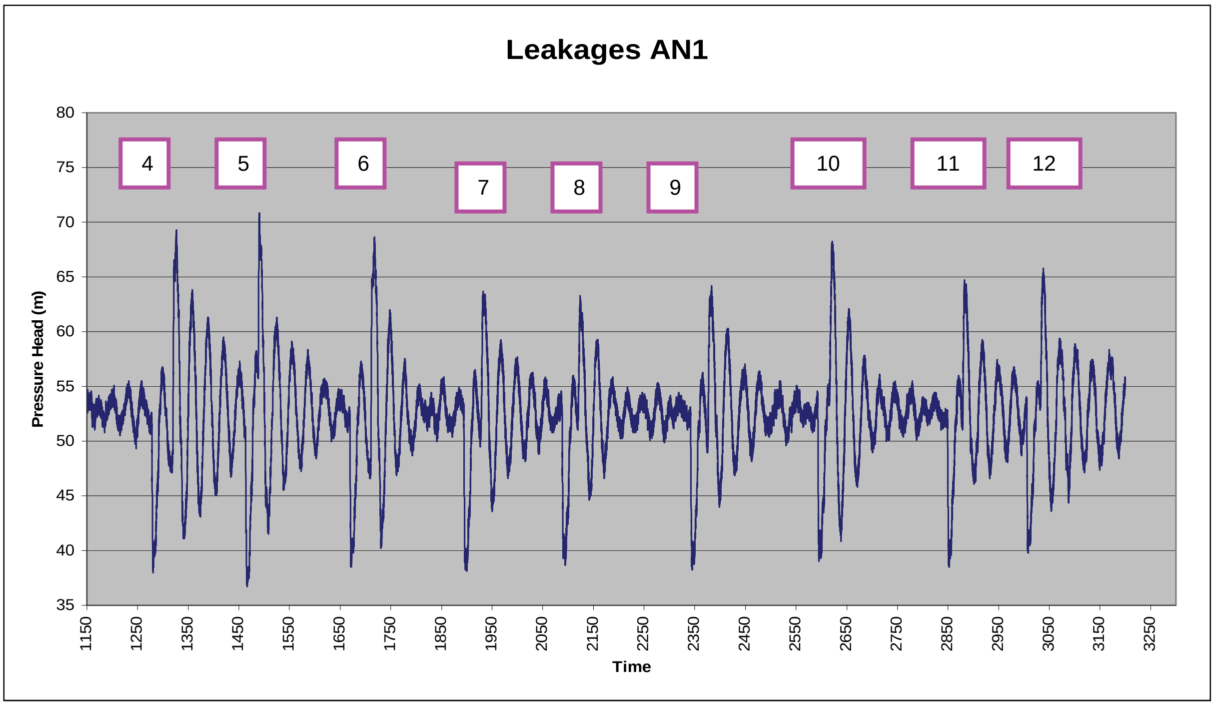

Figure 4-14: Dataq pressure recording at AN1 for the tests where leaks where leaks were artificially introduced at node AN4

The recorded data for the tests conducted with the air in the system, are graphically presented in **Figure 4-15** to **Figure 4-17**.

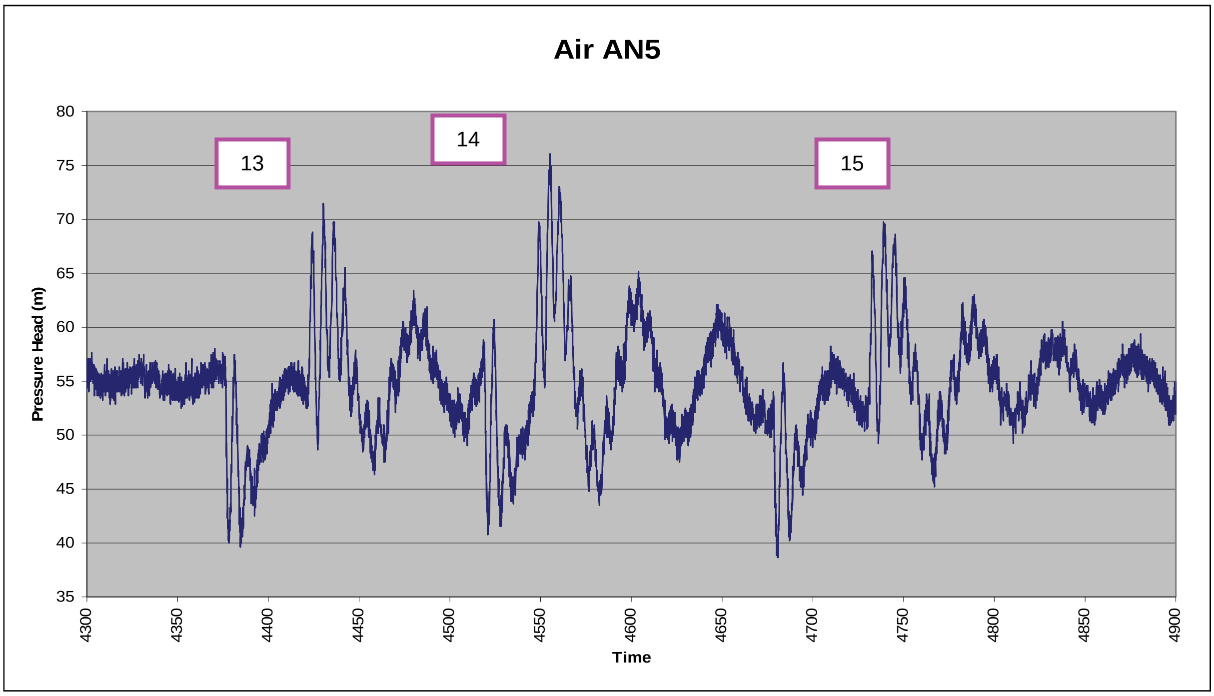

Figure 4-15: Data recorded pressure variation at AN5 for the tests when air was present in the pipeline at node AN2

Figure 4-15 now shows a fast variation of the measured pressures, indicating the reflection of the wave from the air bubble. The same variation is not noticeable in any of the recordings for the leak tests reflected in **Figure 4-12** or **Figure 4-14**.

Furthermore it is significant to notice the difference in the pressure fluctuations between **Figure 4-15** and that of **Figure 4-16** and **Figure 4-17**. The reason for this is that the reflection wave is recorded at node AN5, while the pressure wave transferred upstream from the air bubble (upstream) at node AN3 towards node AN1 is characterised by the translation wave. This is graphically reflected on the next page in Table 4-5.

Table 4-5: Influence of an air bubble during the movement of a pressure wave in a pipeline

Time	Pressure wave movement	Discussion
Before the negative pressure wave is introduced.	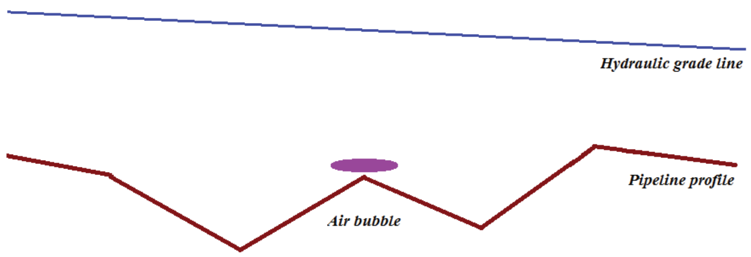	Normal pressure condition.
Negative pressure wave introduced	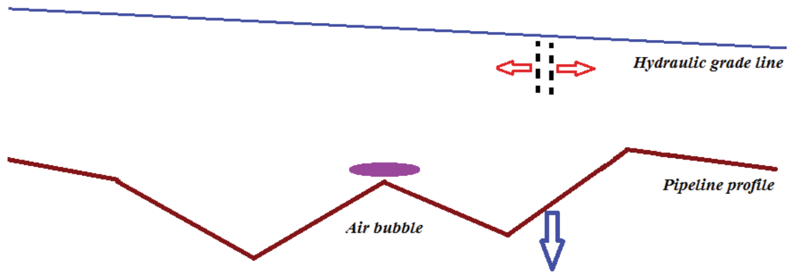	Negative pressure wave moves upstream and downstream.
Time elapsed = c/L_1	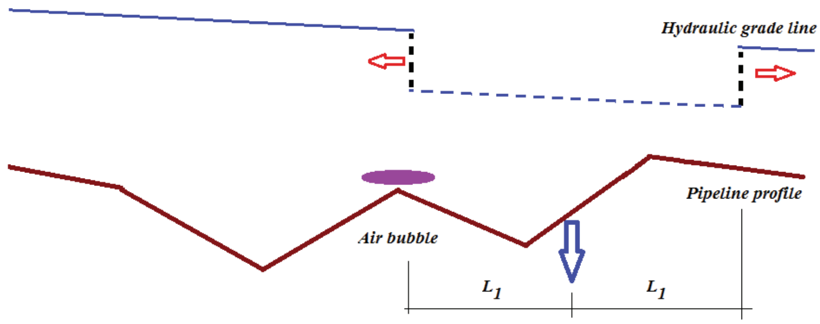	The pressure wave alters the pressure condition along the pipeline.
Time elapsed = C/L_2	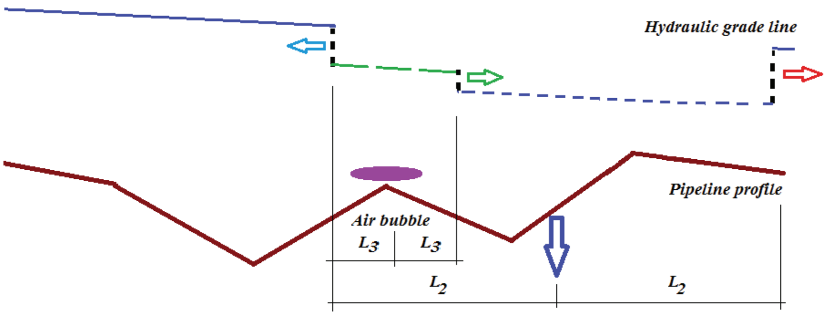	A positive wave is reflected from the air bubble and moves downstream to the point where the negative wave was generated. The translation wave moving upstream from the position of the air bubble is of a lesser value that the wave that was originally generated.

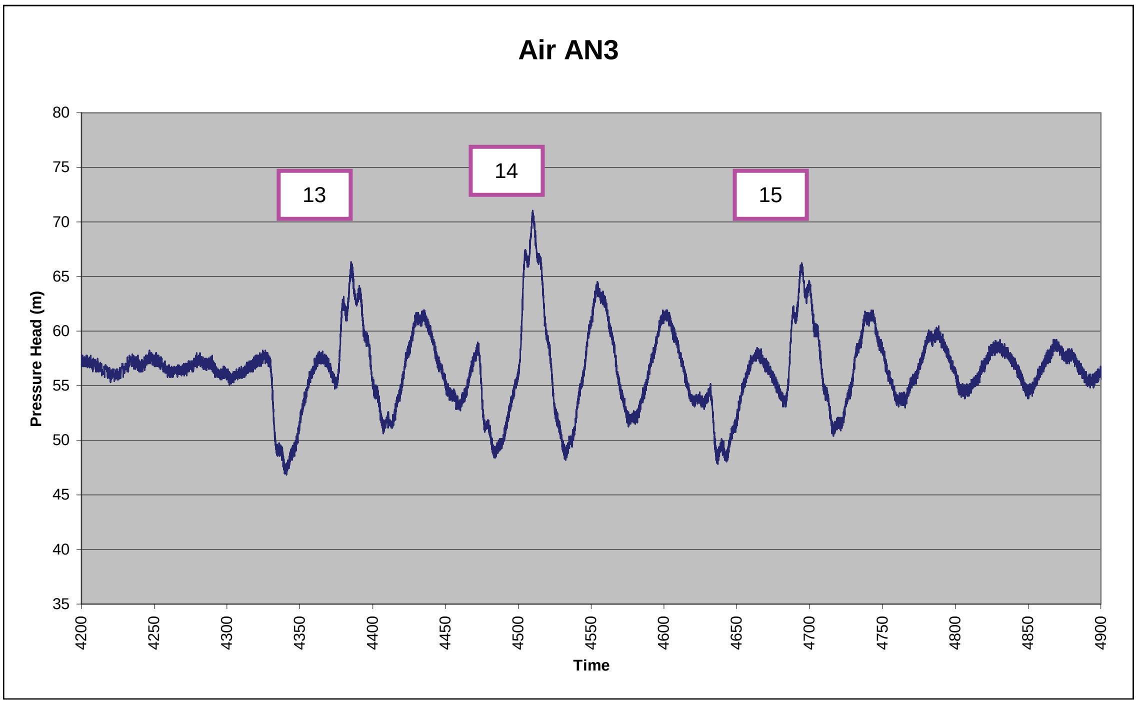

Figure 4-16: Dataq recorded pressure variation at AN3 for the tests when air was present in the pipeline at node AN2

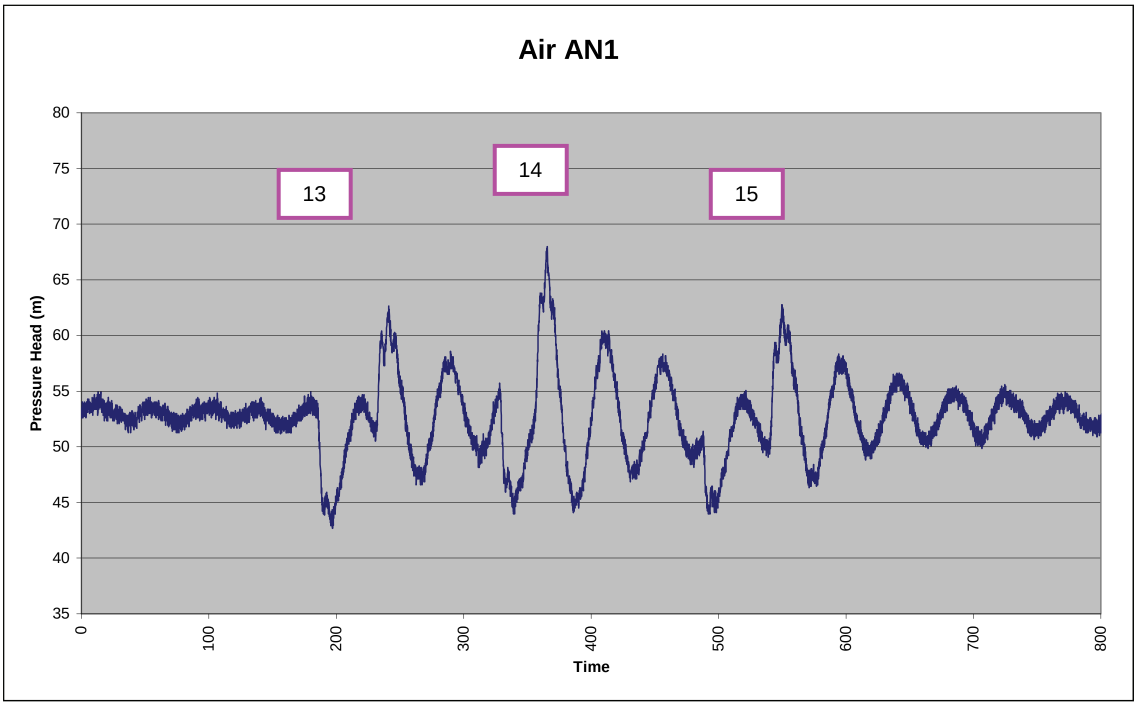

Figure 4-17: Dataq recorded pressure variation at AN1 for the tests when air was present in the pipeline at node AN2

The wave periods for the different test runs were determined as indicated in **Figure 4-18**. These were then evaluated for the different tests and the results are graphically presented in **Figure 4-19**.

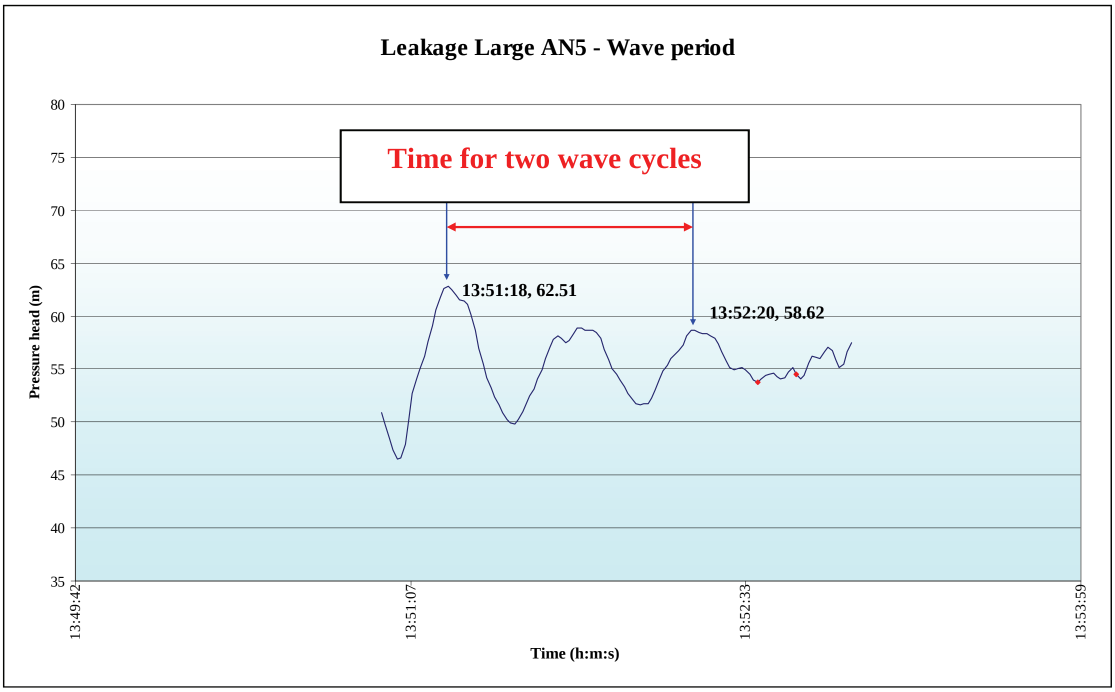

Figure 4-18: Determination of the wave period

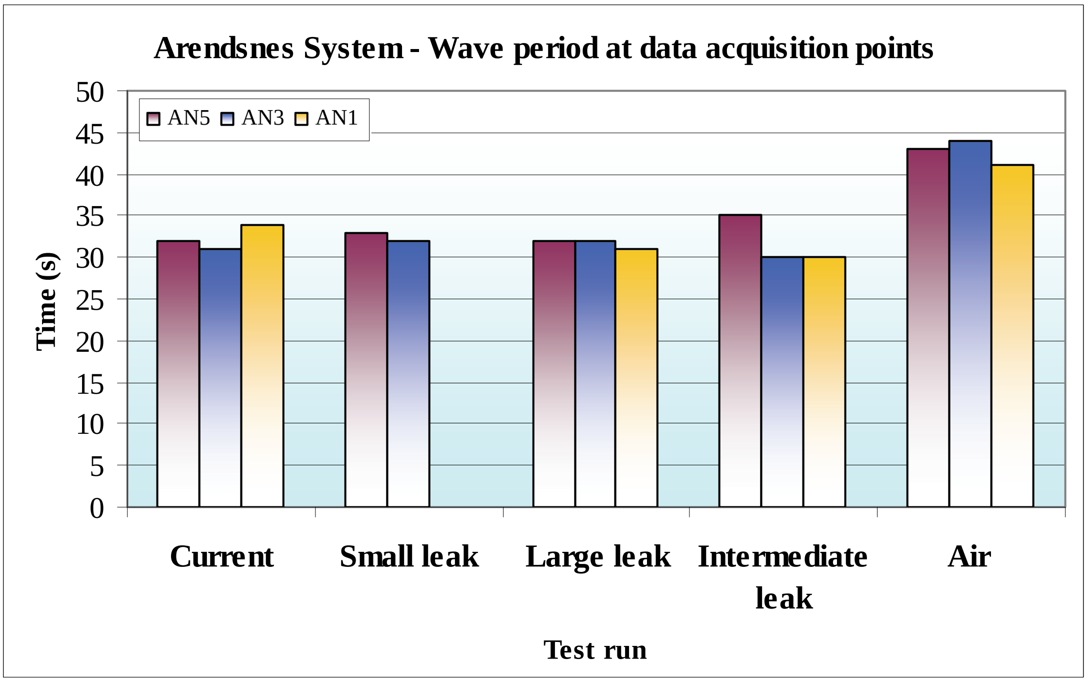

Figure 4-19: Measured wave period for the different tests conducted for the Arendsnes pipeline

<u>The period of the wave propagation is significantly altered by the presence of a small air pocket and hence the ineffective de-aeration of a pipeline can be established by the use of inverse transients.</u>

Figure 4-20 reflects two oscillating wave patterns. The longer one is associated with the systems pressure fluctuation and the shorter one is probably associated with the oscillation in the isolated section between AN5 and the T-section at the connection with the main pipe in Rigel Avenue (Refer to **Figure 4-2**).

Figure 4-20 reflects the pressure fluctuation at node AN5 when air is captured at node AN2.

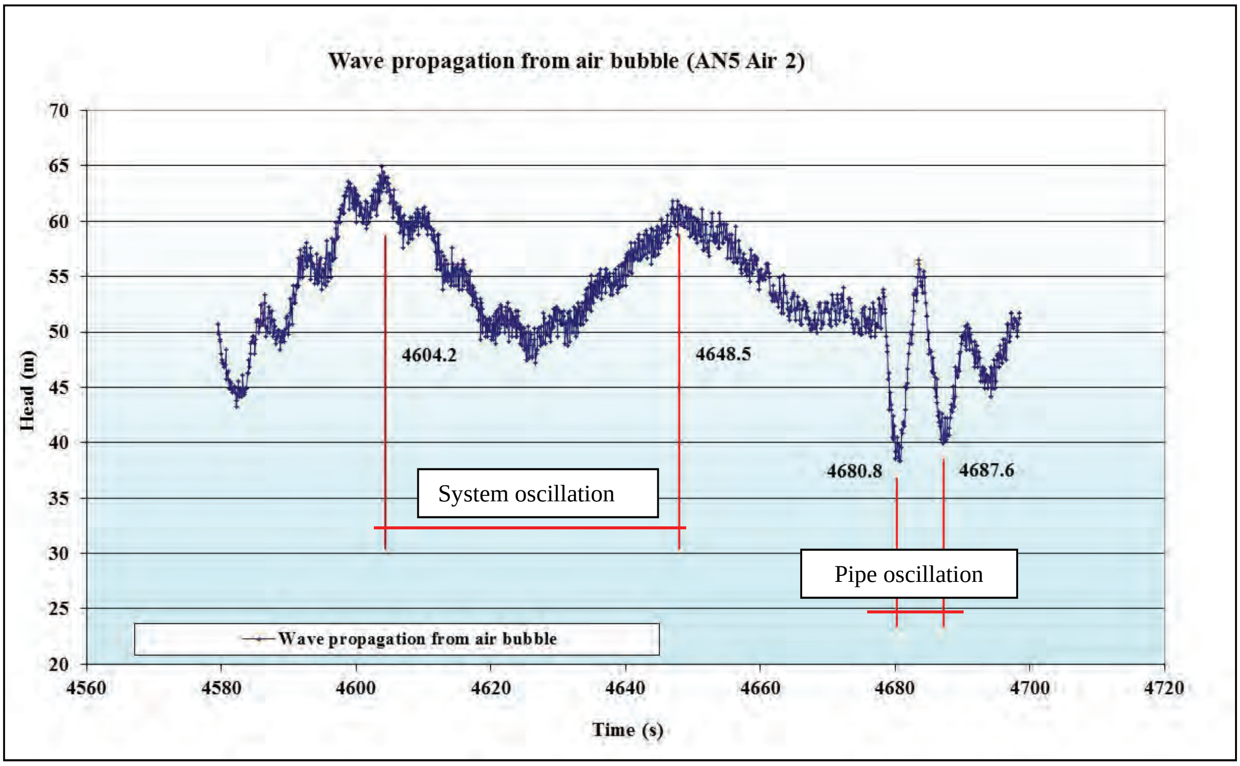

Figure 4-20: Time it takes for the reflection wave from the air bubble

The reflection wave (from the location of the air bubble) produces a high pressure due to the deformation energy which is released by the expanding air bubble. This type of wave pattern reflects the presence of an air bubble and hence inverse transients can be used to establish if pipelines have been fully de-aerated. **Appendix 4B** contains all the recorded pressures which were obtained during the field work.

4.2.3.3 Review of the pressure variance

The recorded head-time graphs were reviewed with specific focus on the first downward leg to assess whether the head-time graphs at node AN5 due to a reflection wave were affected by the specific deficiency (either the artificially created leak at node AN4 or the air bubble which was introduced at node AN3), be it a leak or an air bubble in the pipeline.

Based on the understanding that at the deficiency the reflection wave will travel downstream towards AN5 and that an altered wave will travel upstream (translation wave) towards AN1, the pressure variance at AN5 is now assessed in more detail.

All the graphical results for the downward leg of all the tests are however in **Appendix 4B**.

Figure 4-21 to **Figure 4-23** reflect the recorded head-time relationship at AN5 for the tests that were conducted for the Large leaks (refer to **Table 4-2**). The figures indicate the moving average of 2 points. In these figures the vertical lines have the following meaning:

- Blue dashed line – Opening of valve to indicate the start of the negative pressure wave at node AN5
- Red dashed line – Reflection from the leak (node AN4)
- Black dashed line – Reflection from the connection with the pipeline in Rigel avenue (near node AN1)

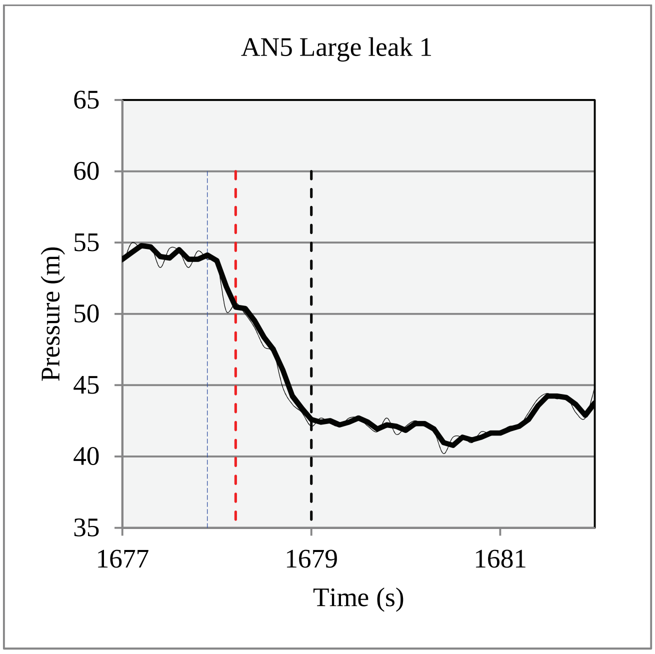

Figure 4-21: Head-time relationship at AN5 indicating the reflection wave on the downward leg – Test with Large Leak (LL1)

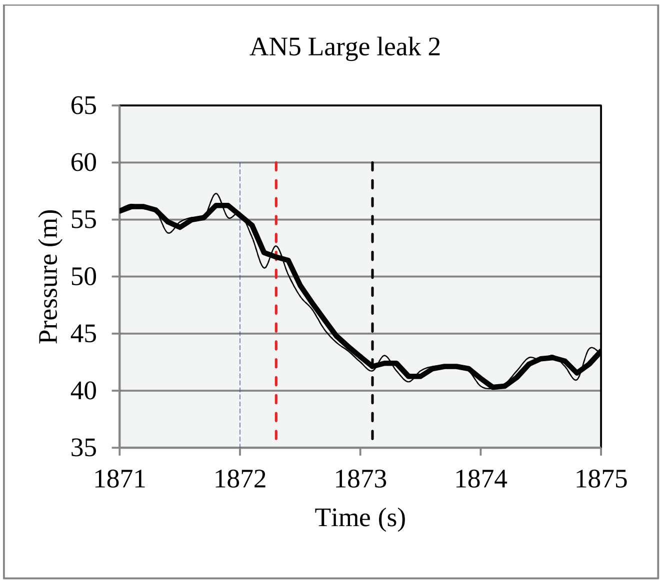

Figure 4-22: Head-time relationship at AN5 indicating the reflection wave on the downward leg – Test with Large Leak (LL2)

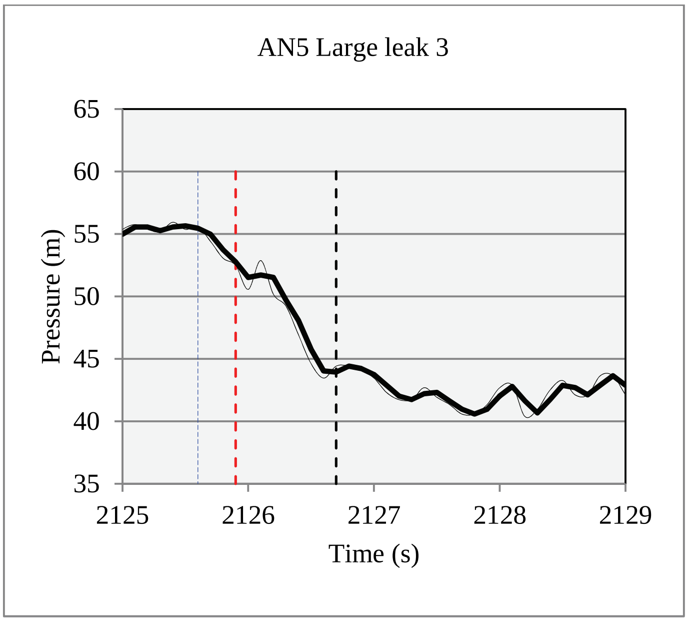

Figure 4-23: Head-time relationship at AN5 indicating the reflection wave on the downward leg – Test with Large Leak (LL3)

In all these figures it is possible to calculate the origin of the leak which is situated 115,5 m away from AN5 if the celerity is 770 m/s. The calculations are based on the identifiable change in the pressure time plot at the AN5. It might not always be easy to detect this change which necessitates the recording of pressures at a number of locations between the point where the pressure wave was introduced and the expected location of the deficiency in the pipeline.

Figure 4-24 and **Figure 4-25** reflect the recorded data at AN5 for two tests (Air 1 and Air 3) that were conducted after 2,7 kg of air has been introduced to the pipeline.

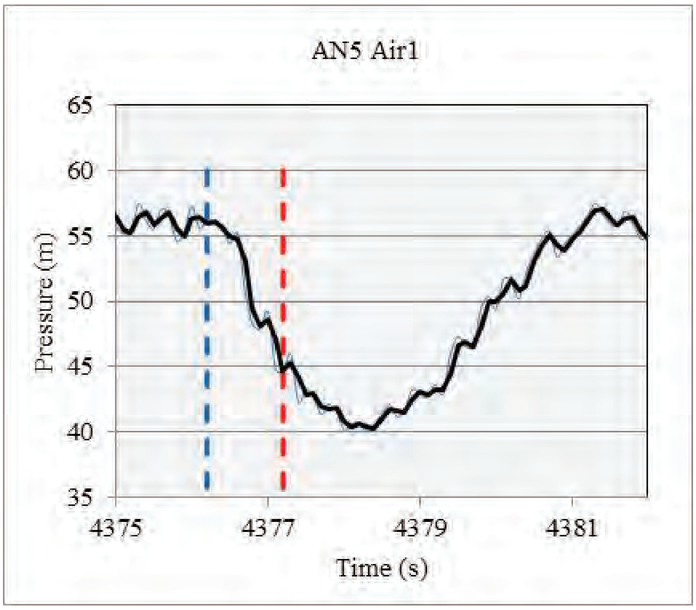

Figure 4-24: Head-time relationship at AN5 indicating the reflection wave on the downward leg – Test with Air Bubble (Air 1)

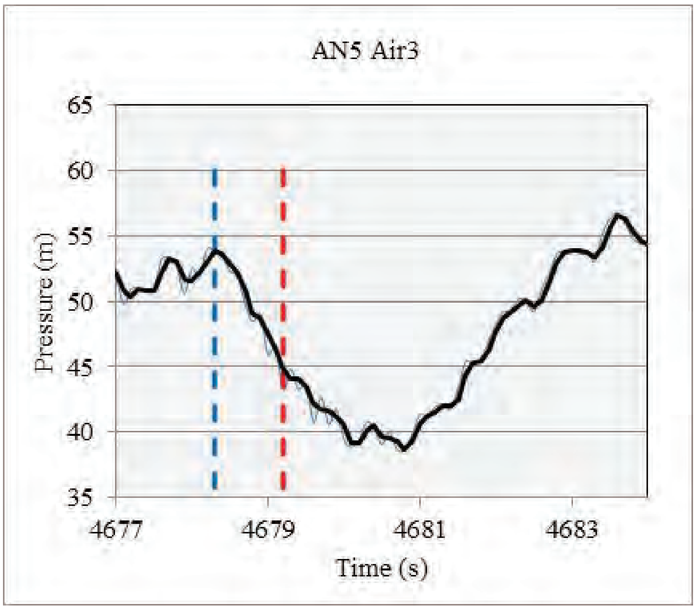

Figure 4-25: Head-time relationship at AN5 indicating the reflection wave on the downward leg – Test with Air Bubble (Air 3)

Knowing that a wave will be reflected from the bubble at AN3 towards AN5, the time it will take to travel to node AN5 since the point in time when the negative pressure wave has been created at node AN5, can be calculated.

Table 4-6 reflects the different wave celerities which were used to conduct the sensitivity analyses of the required time for the reflection wave to be travelling from node AN3 (air bubble) to node AN5.

Table 4-6: Different wave celerities used in the assessment of the reflection wave from the air bubble at node AN3

Celerity reference	Celerity speed (m/s)
C1	600
C2	800
C3	1000

The smoothed graph of the head time data was plotted (pink line) to assist with the identification of the point on the downward leg of the head-time graph where the slope changes. This point represents the time when reflected or rebounded wave reaches AN5.

Figure 4-26 and **Figure 4-27** reflect the expected time for the reflection wave from an air bubble at Node AN3 to reach node AN5. Included on **Figure 4-26** and **Figure 4-27** vertical lines have been included for the different wave celerities identified in **Table 4-6.**

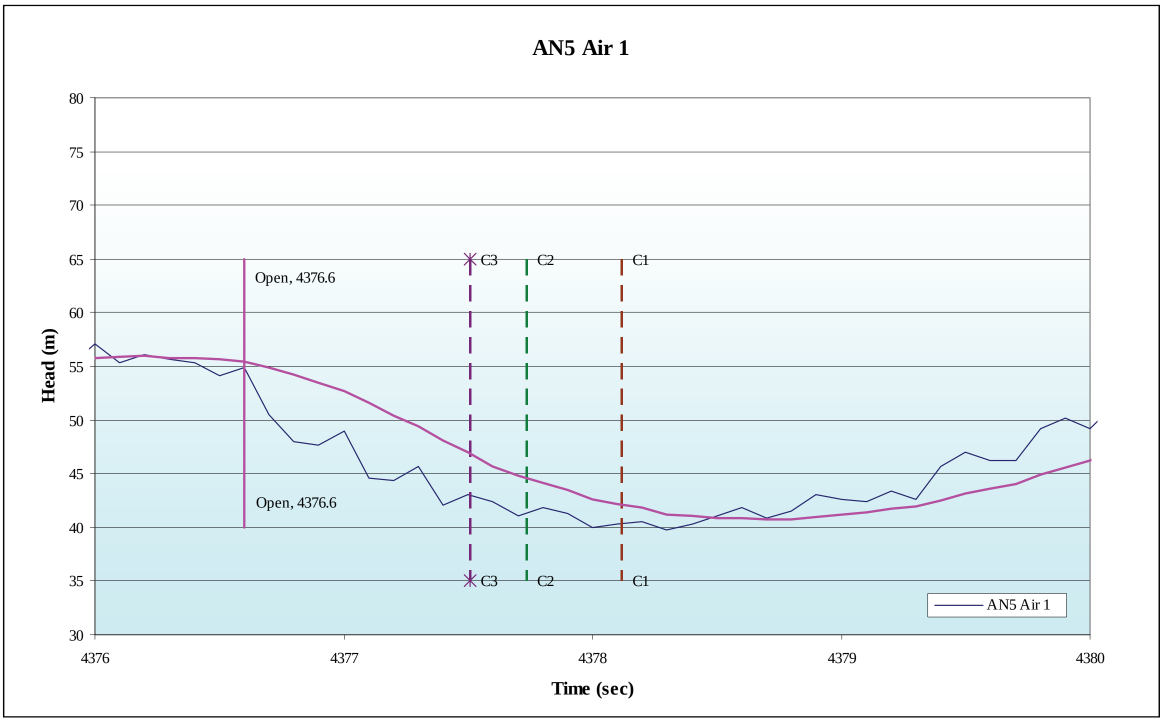

Figure 4-26: Head-time relationship at AN5 indicating the reflection wave from the air bubble on the downward leg of the relationship – Test with air bubble (Air 1 or AT1)

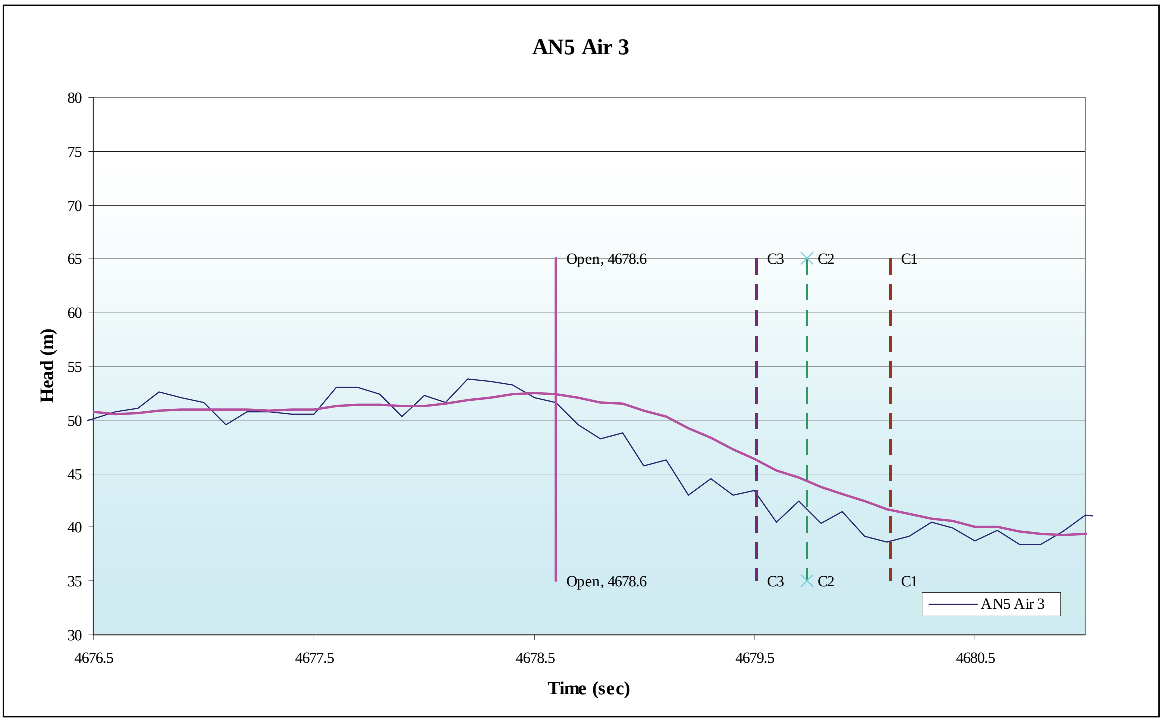

Figure 4-27: Head-time relationship at AN5 indicating the reflection wave from the air bubble on the downward leg of the relationship – Test with air bubble (Air 3 or AT3)

A realistic celerity of 800 m/s in **Figure 4-26** and **Figure** 4-27 above indicates the position of the bubble from which the pressure wave is reflected.

4.2.4 Conclusion from the test conducted on the Arendsnes Pipeline

The results obtained, indicated that leakages and air pockets alter the pressure wave magnitude and the pressure oscillation period as the pressure wave propagates through the pipeline.

In can thus be concluded that for the field tests conducted at Arendsnes:

- The influence on the pressure wave occurs on the "down" leg of the induced pressure wave, due to the relative positions where the pressures have been recorded and the time to generate the negative wave (flow rate variation),

- A leakage (induced at node AN4) reflects a pressure spike back to the position where the inverse transient was introduced at node AN5. This reflection wave will reach the point where the inverse transient has been introduced after some time laps which could be used to determine the location of the leak;

- Air pockets returns a more profound positive pressure wave in comparison to a reflection wave from a leak, on the downward leg of the pressure spike and dampens the transient pressure wave progressing beyond the location of the air bubble, resulting that the pressure spike and the pressure drop values are substantially less than those generated by the valve setting (which generate the inverse transient) in the normal operational (de-aerated system) state of the pipeline. Air pockets also reduce the celerity resulting in a prolonging of the wave period (**Figure 4-19**).

4.3 Khutala Pipeline

4.3.1 Introduction

The Khutula to Kendal Pipeline (referred to in this report as the Khutala Pipeline) was constructed in the 1970s to supply water to the Kendal Coal Power Station. The pipeline is part of the transfer system (Usuthu-Vaal) which transfers water from the Morgenstond and Jerigo dams to a series of pumps stations and reservoirs to the water shed at Rietspruit Reservoirs. From here the water gravitates via the reservoirs at Davel to the reservoirs at Khutala Pump Station. From here the water is finally pumped to a reservoir at Kendal Power Station, completing its journey of roughly 200km. The Khutala pipeline is a 750 mm diameter steel pipe with a bitumen liner and a fibre bitumen coating and has a length of 31 km.

On 25 February 2010 a dynamic test was conducted on a section of the Khutala pipeline. **Figure 4-28** reflects the positions (KU1 to KU4) where the pressure recordings were conducted.

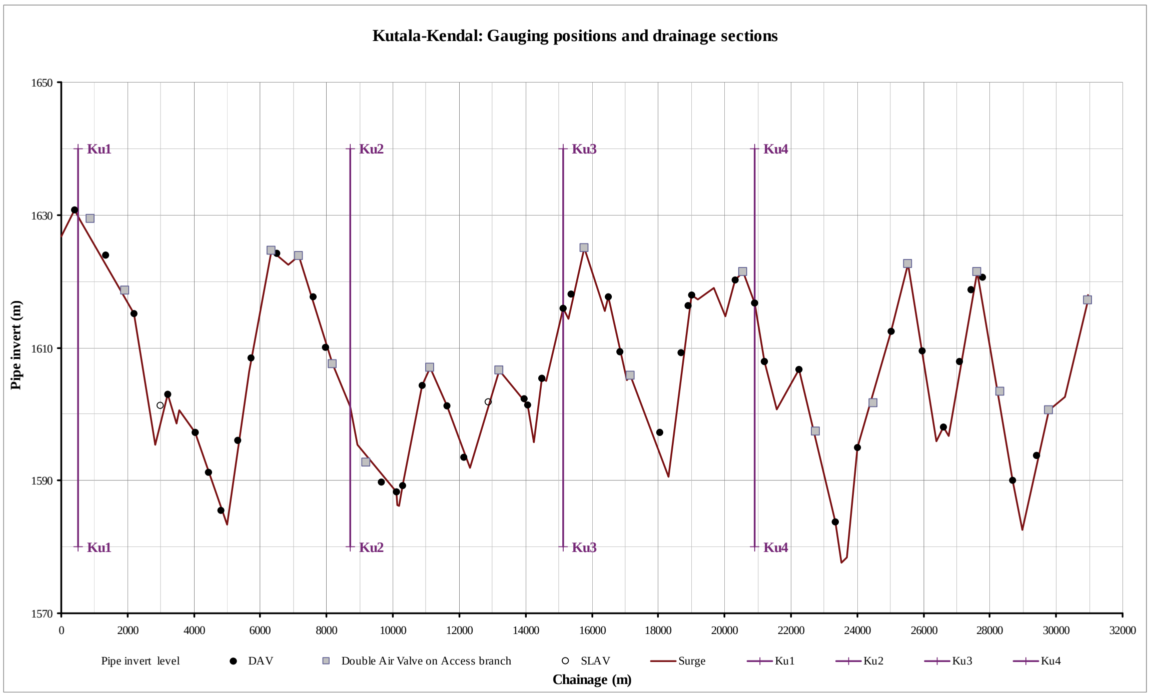

Figure 4-28: Longitudinal profile of Khutala pipeline

The purpose of the pressure transducers was to capture the pressure variations resulting from the operational changes. The location of the air valves is shown in **Figure 4-29.**

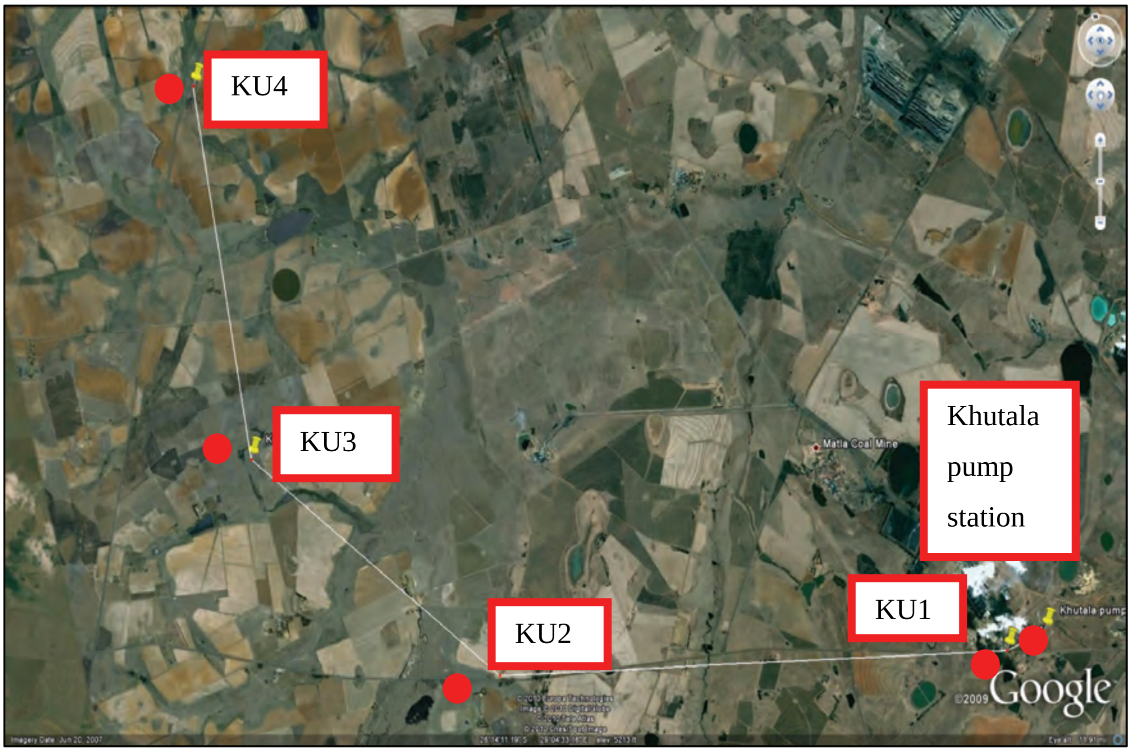

Figure 4-29: Layout of Khutala pipe and pressure transducers

Figure 4-30 reflects typical details of the pressure recordings on one of the air valves. It is clear that the air valve operates at low heads, resulting in leakage into the valve chamber.

Figure 4-30: Typical details of the installation of the pressure recording equipment

4.3.2 Test methodology

Personnel of the Department of Water Affairs assisted with the installation of the pressure recording equipment and testing of the Khutala Pipeline. As mentioned above, four air valves were chosen for the installation of pressure transducers. **Table 4-7** highlights some details of the recording positions.

Table 4-7: The type of air valves for each test location

Pressure recording position (Gauging point)	Chainage (m)	Elevation (m)	Type of air valve
Ku1	500,2	1629,1	Double air valve
Ku2	8725,13	1601,1	Single small air valve
Ku3	15125,4	1615,96	Double air valve
Ku4	20900,1	1616,86	Double air valve

At each gauging point two pressure transducers and two data logger were installed. Details of the pressure transducers used are indicated in **Table 4-8**.

Table 4-8: Pressure transducers used to record the pressure variations on the Khutala pipeline

Node	Pressure transducer range	Data loggers	Frequency
Ku1	5 Bar G	Hobo	1 Hz
	5 Bar G		
Ku2	16 Bar A		
	10 Bar G		
Ku3	4 Bar G		
	4 Bar G		
Ku4	4 Bar G		
	4 Bar G		

All the required steps were taken to ensure that the data recording equipment was functional. The flow was recorded in a manhole just downstream from the pump station where a Fuji Portaflow ultra sonic flow meter was installed (**Figure 4-31**).

Figure 4-31: Fuji Portaflow flow meter

Three pumps are installed in the Kuthala Pump Station. **Figure 4-32** reflects the general layout of the pump station.

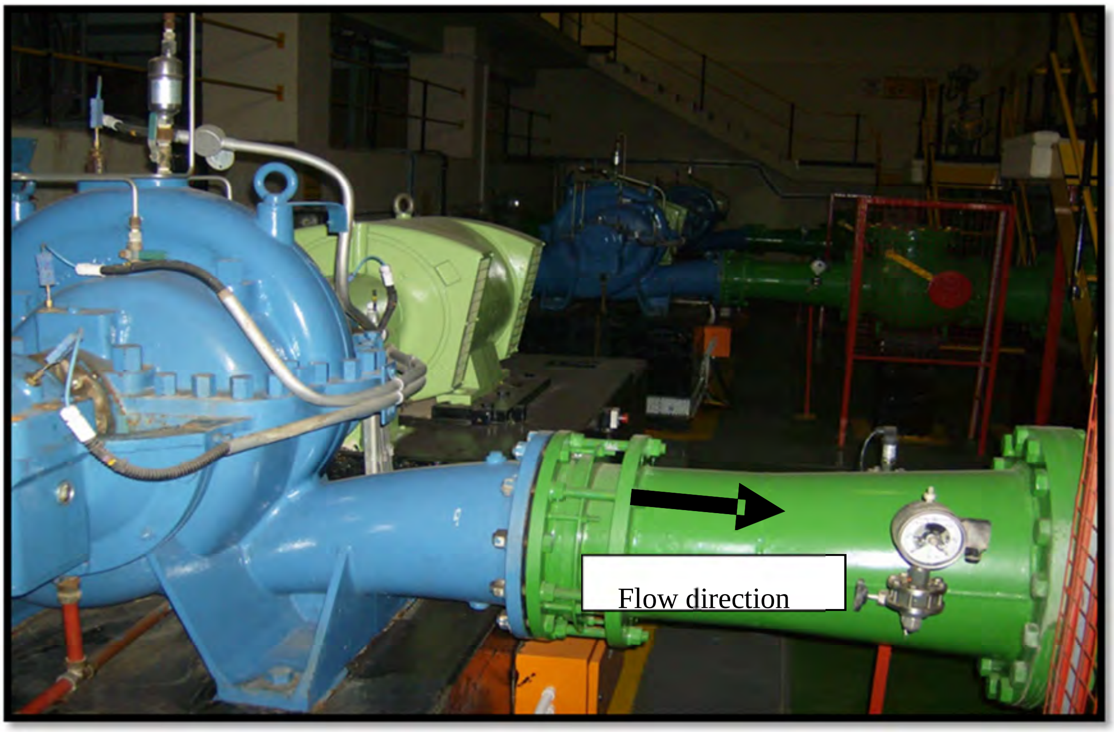

Figure 4-32: Some details of the layout of the Kuthala Pump Station

Water can gravitate from Kuthala to Kendal, making this a booster pump station which has to overcome the additional friction loss for higher pumped discharges. Normally one pump will be running and the second pump will be switched on when the demand requires it. The third pump functions as a standby unit. All pumps are controlled from a central control switch board.

During the pressure recordings, the pumps were switched on and off as is reflected in **Table 4-9**.

Table 4-9: Khutala Pump Station – Variable operating conditions

Event	Pump 1	Pump 2	No. of pumps running	Time
1	Off	Off	0	14:00
2	Switched on	Off	1	14:42
3	Running	Switched on	2	14:52
4	Controlled stoppage	Running	1	15:27
5	Switched on	Running	2	15:32
6	Trip	Running	1	15:35

The pressures were recorded at all the data acquisition points. However, the recording at Ku2 only captured the first section of the data set, probably due to some bad contact or battery failure (rain on the day of the field tests).

4.3.3 Recorded pressure data

The hobo data loggers were set to record data at a frequency of 1 Hz. **Figure 4-33** to **Figure 4-35** reflect the complete recorded data set at Ku1, Ku3 and Ku4.

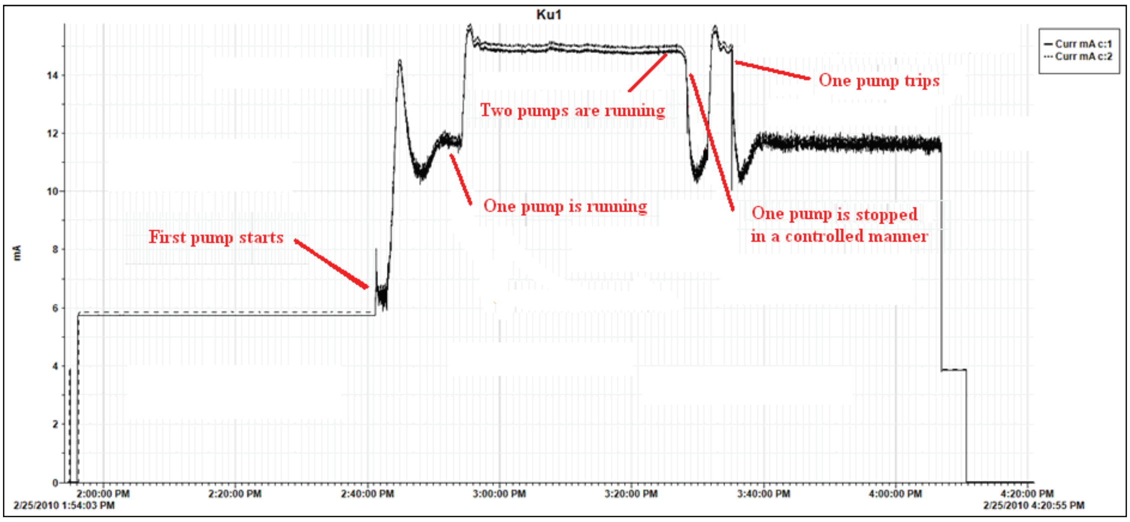

Figure 4-33: Ku1 hobo data logger data for Khutala

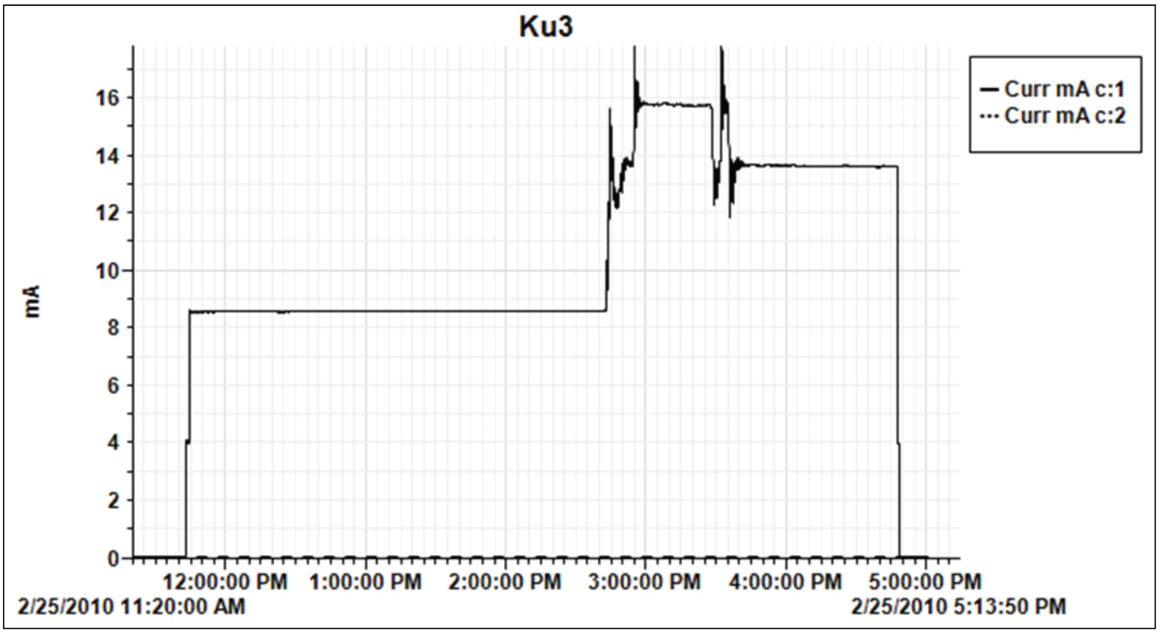

Figure 4-34: Ku3 hobo data logger data for Khutala

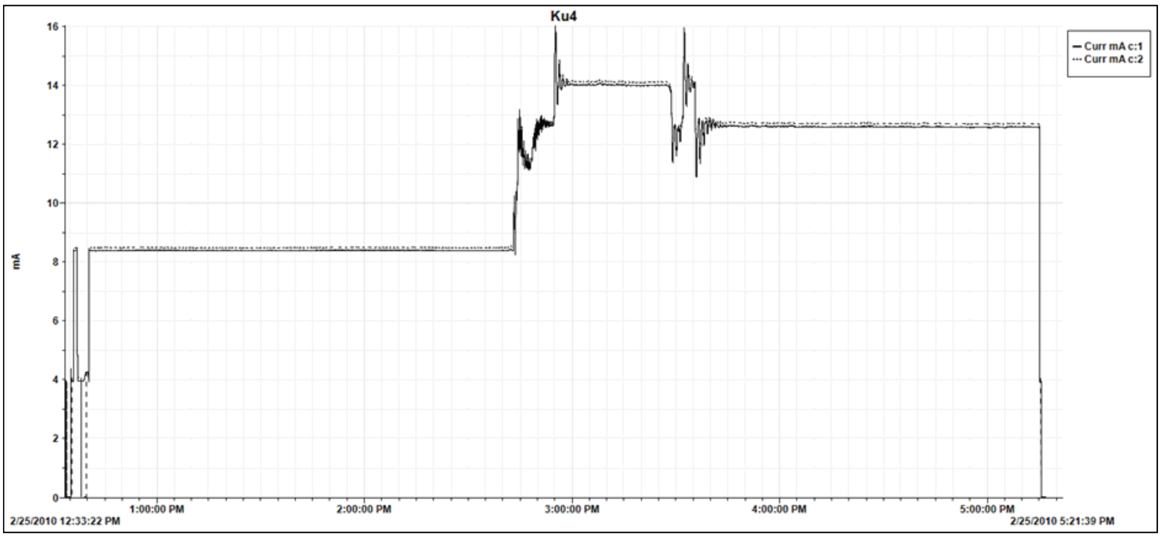

Figure 4-35: Ku4 hobo data logger data for Khutala

Three pressure spikes can be seen on the pressure graphs displayed above. These pressure variations coincide with the changes to the operation of the system that was detailed in **Table 4-9**.

Figure 4-36 reflects the longitudinal profile and the minimum static head (blue line on level of Kendal Reservoir).

As was mentioned before, the Kuthala Kendal pipeline can either gravitate or can be boosted by the operation of the pumps in the Kuthala Pump Station. During the period of no pumping it is possible that the higher sections of the pipeline (A1 to A4) may drain (**Figure 4-36)**.

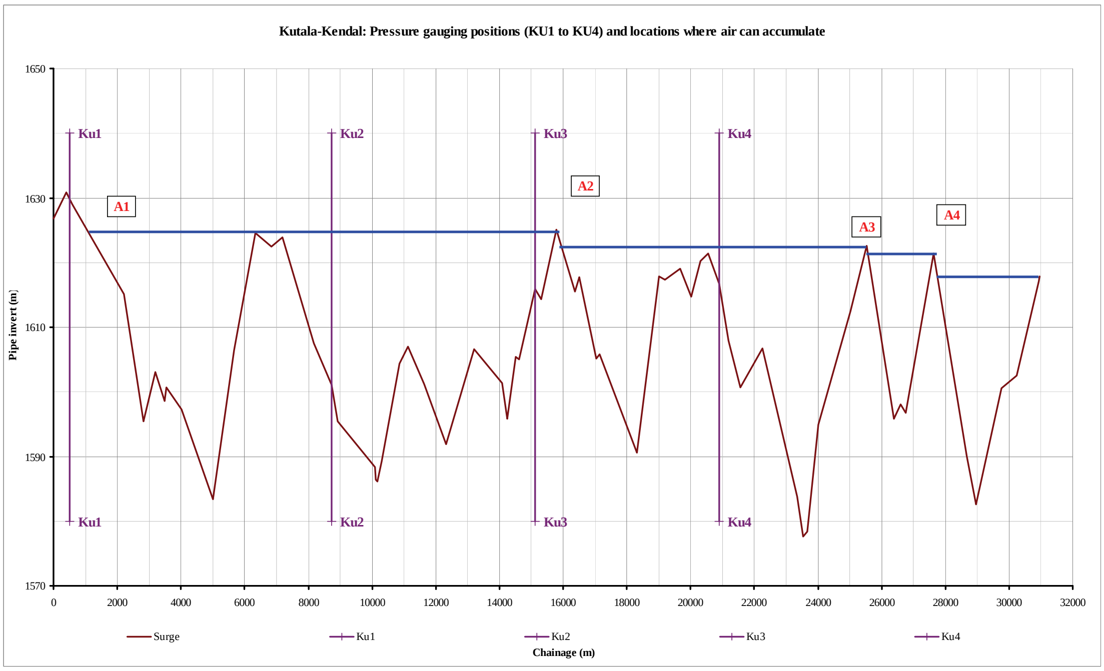

Figure 4-36: Sections of the Kuthala Kendal Pipeline where air might accumulate

Table 4-10 reflects the flow rates which were recorded for the different events.

Table 4-10: Recorded flow rates during the field tests

Event	Pump 1	Pump 2	Recorded flow rate (l/s)	Time
1	Off	Off	0	14:00
2	Switched on	Off	385	14:42
3	Running	Switched on	385 to 580	14:52
4	Controlled stoppage	Running	580 to 385	15:27
5	Switched on	Running	385 to 580	15:32
6	Trip	Running	580 to 385	15:35

When a pump starts, the air should be expelled through the air valves or be transported hydraulically towards Kendal Reservoir. **Table 4-11** shows the minimum required flow rate to hydraulically transport the flow (Van Vuuren *et al.*, 2004).

Table 4-11: Calculated flow rate to hydraulically transport air

Section downstream from air pocket	Diameter (m)	Negative slope (degrees)	Required velocity to transport different size air bubble hydraulically			Minimum flow rate to transport the air (l/s) #
			Large	Medium	Small	
A1	0,75	0,5001	0,590	0,448	0,450	198,9
A2	0,75	0,917	0,738	0,571	0,564	249,1
A3	0,75	1,800	0,946	0,748	0,725	320,3
A4	0,75	2,755	1,107	0,887	0,849	375,1

Note: Relationship in accordance to Van Vuuren et al (2004)

The relationship which is used to determine the required velocity to hydraulically transport the air (certain bubble size) is given by (*Van Vuuren et al (2004)*:

$$V_{min} = 0,2703\sqrt{gD}\,\theta^{0,368}$$

Equation 4-1

Where:

V_{min} = Minimum velocity required to transport air (m)

g = Gravitational acceleration (m/s^2)

D = Internal pipe diameter (m)

θ = Slope of the pipe measured from the horizontal (degree)

From Table 4-11 it is clear that the air will eventually be hydraulically removed from the pipeline. However if the pipeline has been partially drained it will take some time to recharge the whole pipeline. It is therefore possible that downstream of A1 and A4 some air might have been present in the Khutala Pipeline.

Table 4-12 (separate page**)** indicates the recorded pressures as Pump 1 was switched on (Event 2). The pressure oscillations at Ku3 and Ku4 downstream from Ku1 (A1) are significantly different. Furthermore the period for the pressure oscillation at Ku4 (33 seconds) is longer than the period at Ku3 (22,5 seconds), indicating that air downstream from Ku3 is most likely, extending the oscillation frequency experienced at Ku3.

Table 4-12: Recorded pressure as pump one is started (Event 2)

Location of the recording	Pressure variation
Ku1	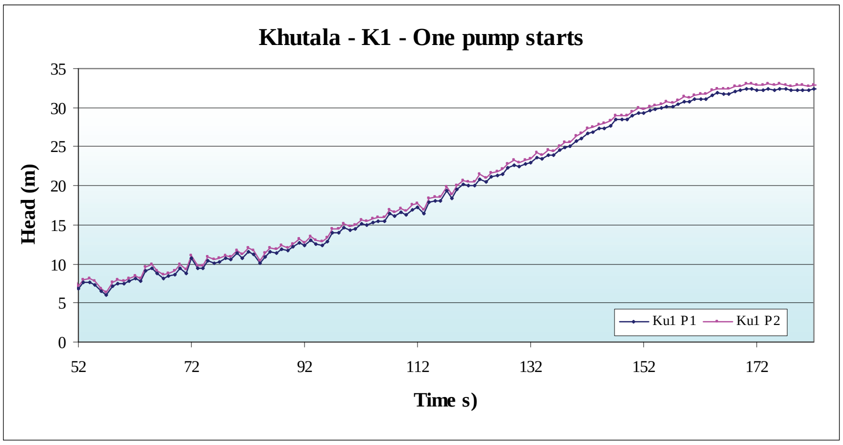
Ku3	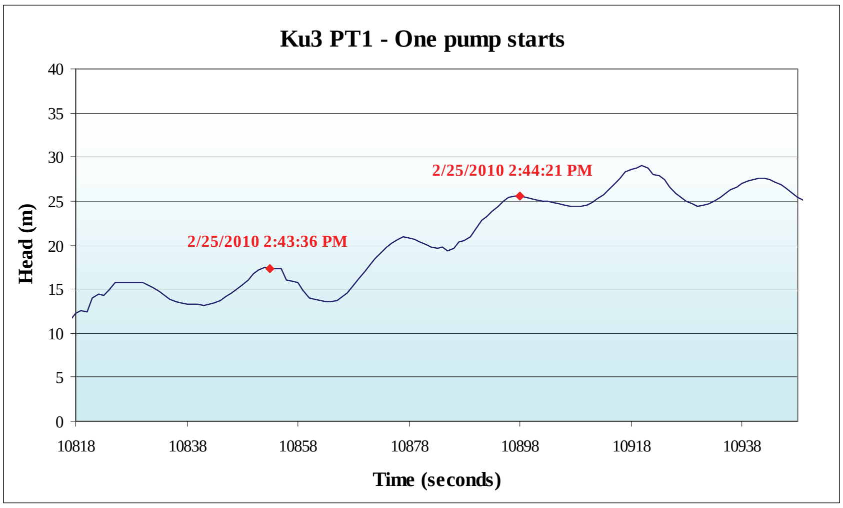
Ku4	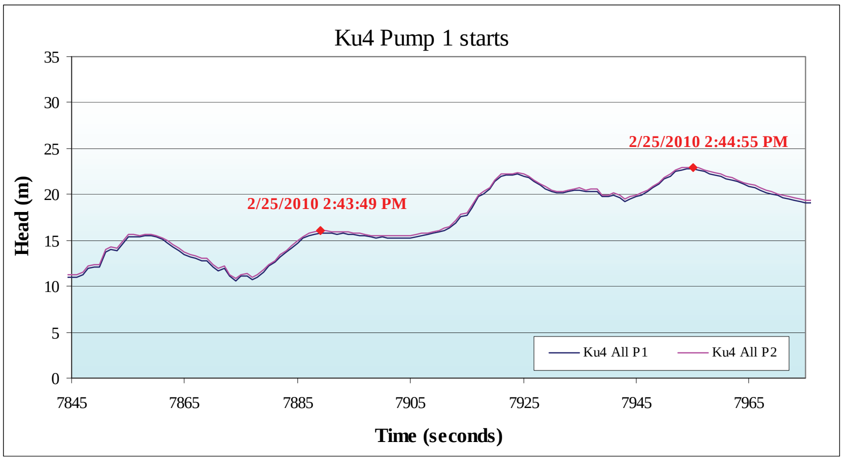

What is further noticeable, as is shown in the graphs in **Table 4-13**, is that the instability on the upward leg of the head-time graph of the recorded pressures at Ku3 and Ku4 are similar.

Table 4-13: First upward leg at Ku3 and Ku4 when the first pump is started (Event 2)

Recorded pressure fluctuation at Ku3
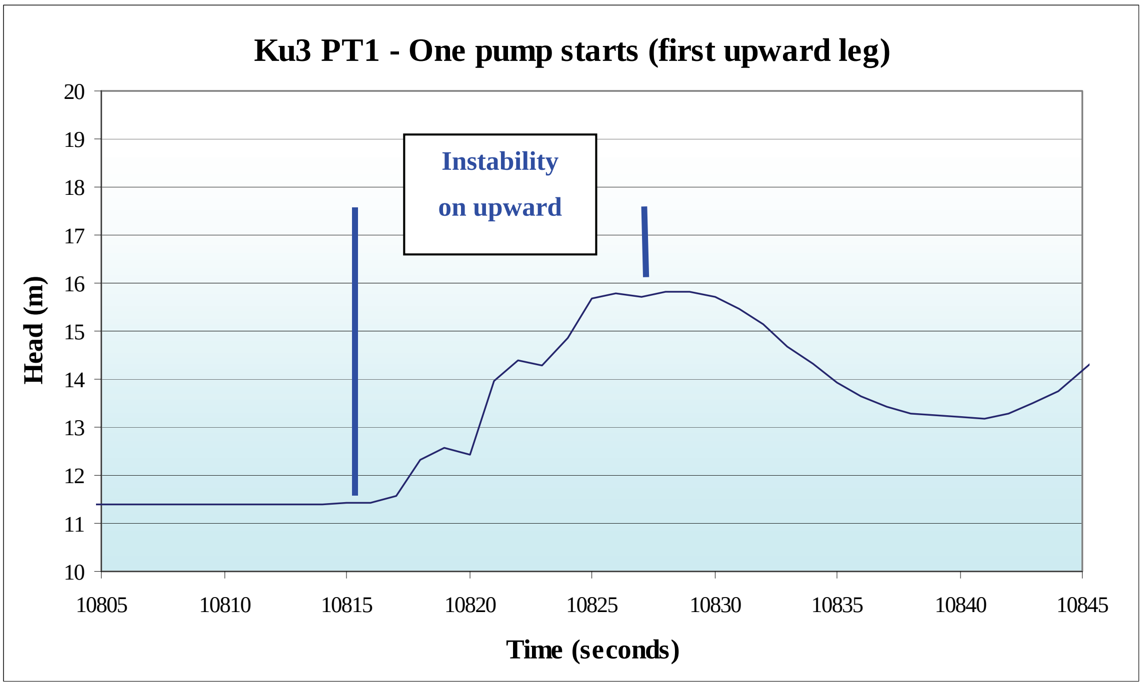
Recorded pressure fluctuation at Ku4
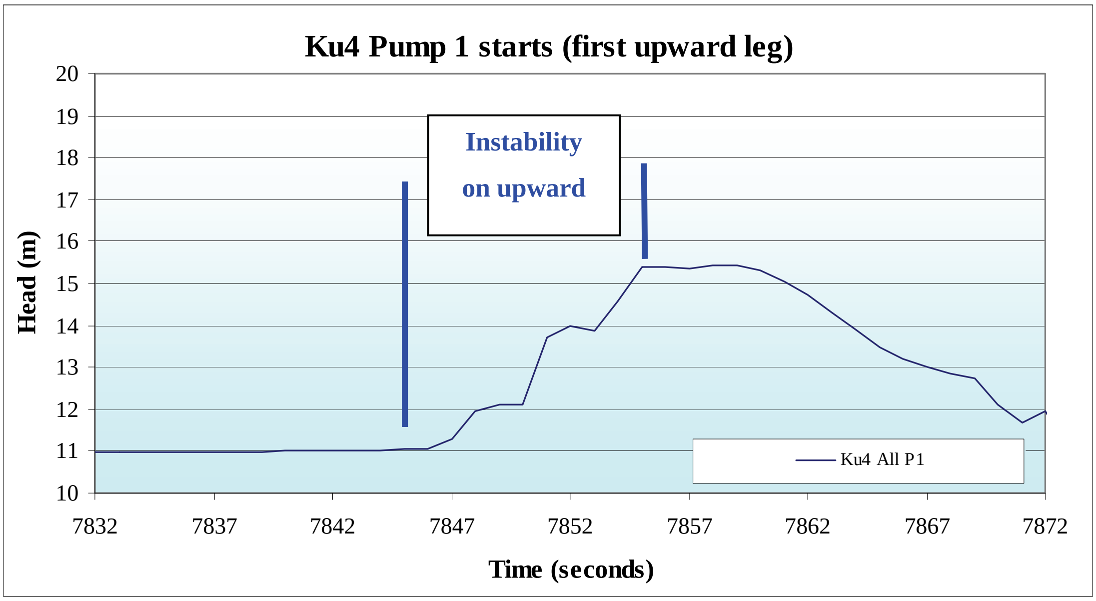

This pressure instability is generated upstream from both Ku3 and Ku4 and downstream from Ku1, since the pressure fluctuations are not visible on the head-time graph of Ku1 and it is most likely that the instability originated at the air bubble at **A1** (**Figure 4-36**).

Further analyses of the pressure variation at Ku3 and Ku4 reveal that another instability occurs on both the head-time graphs of Ku3 and Ku4, but that the time step between the first occurrence and the re-occurrence of the head instability is different (longer) at Ku3 than at Ku4 as is reflected in **Table** 4-14. The first rebounded head instability at Ku3 occurred about 36 seconds after the head instability was first spotted at Ku3, while at Ku4 the rebounded instability is noticeable about 25 seconds after it first occurred at Ku4.

Table 4-14: Head time instability when the first pump is started on the Khutala Pipeline

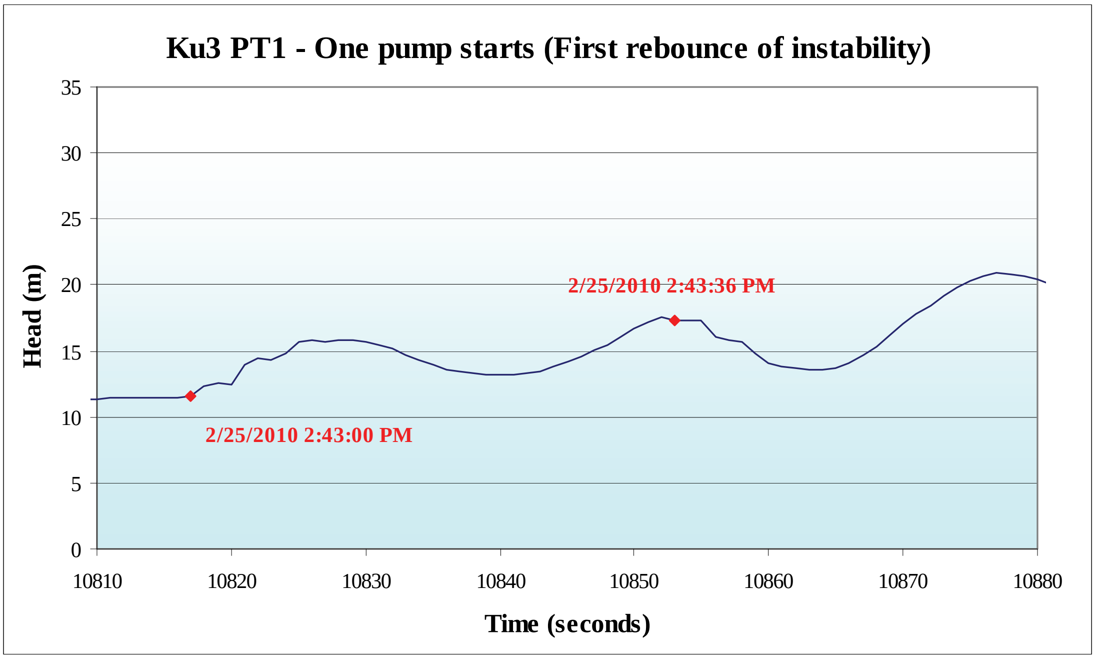

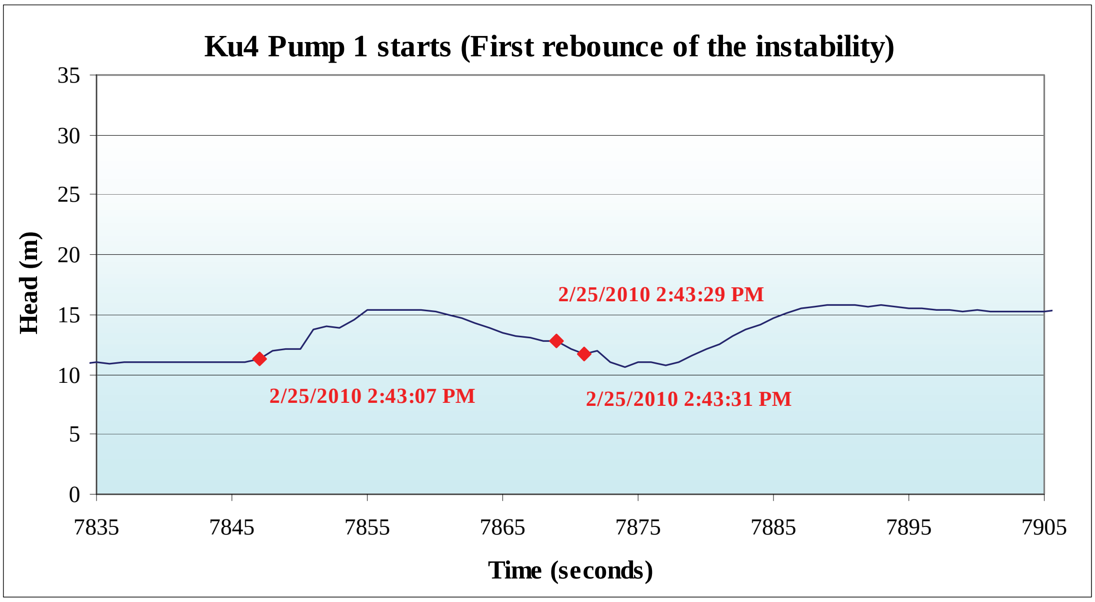

This indicates that the reflecting or rebounding of the first head instability has to be generated downstream from Ku4.

It was calculated that at an average celerity of 850 m/s, the instability reflected from the end of the pipeline (at Kendal). From the assessment thus far it could be concluded that there was an **air bubble between Ku1 and Ku3** which resulted in the first instability in the run-up head-time graphs noticed at Ku3 (and later at Ku4). The energy losses between the different pressure gauging points were analysed which confirmed this finding. **Table 4-15** indicates the calculated absolute roughness for the different flow rates.

Table 4-15: Calculated absolute roughness for the different flow rates in the Kuthala Pipeline

Pipeline section		Number of pumps in operation	Distance between the start and end of the pipeline section (m)	Flow	Calculated roughness, k_s (mm)	
Start	End				Barr	Colebrook/ White
Ku1	Ku2	1	8150	0,385	1,898	1,896
Ku2	Ku3		6400		4,703	4,700
Ku3	Ku4		5775		0,003	0,002
Ku1	Ku4		20325		1,225	1,222
Ku1	Ku2	2	8150	0,58	Data at Ku2 was lost	
Ku3	Ku4		5775		0,001	0,0005
Ku1	Ku3		14550		1,599	1,597
Ku1	Ku4		20325		0,624	0,623

Figure 4-37 reflects the calculated grade lines for the two different flow rates introduced in the Khutala Pipeline.

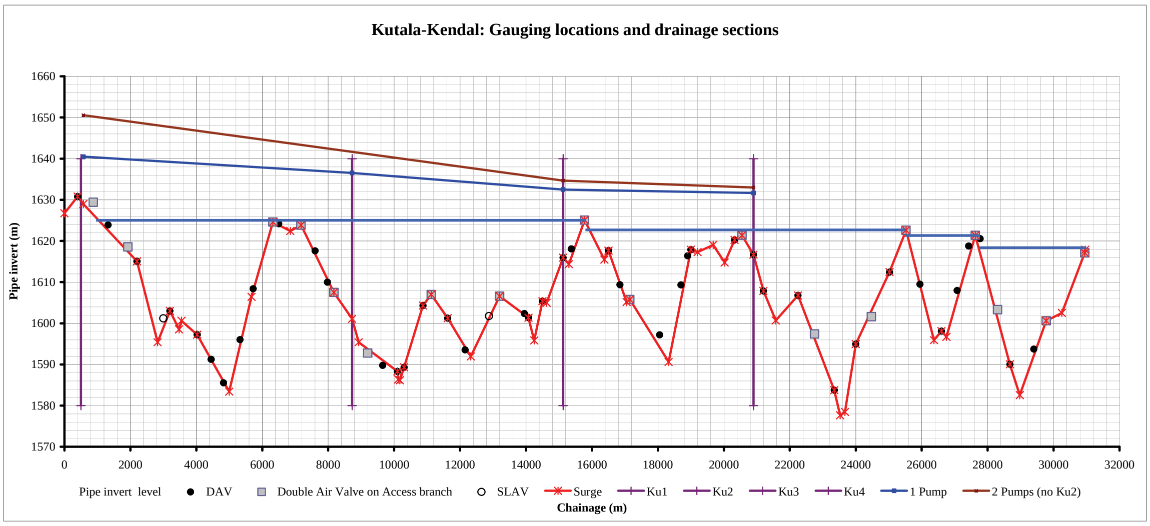

Figure 4-37: Hydraulic grade lines for different flow rates in the Khutala Pipeline

These calculated grade lines, confirm that the location of the air bubble is between Ku1 and Ku3 and more specifically between Ku1 and Ku2.

It can therefore be concluded from the field tests conducted on the Khutala-Kendal pipeline, that:

- It is possible to define the origin of the deficiency in a pipeline by comparing the recorded pressure fluctuations at the different recording positions and the hydraulic grade lines;
- The origin of and consequences of the reflection or rebounding pressure wave could be determined with higher accuracy if the data is recorded at higher frequency; and
- If air is captured in the pipeline, the head instability in relation to the residual head for a specific operating condition is much more significant for lower flow rates than for higher flow rates.

4.4 Assessment of the B16 Pipeline (Rand Water)

4.4.1 Introduction

The B16 pipeline runs parallel to the B8 line from Slangfontein to Mapleton and was constructed in 2005. The pipeline material is steel with various wall thicknesses along the profile and a Cement Mortar liner. The diameter of the pipeline is 2300 mm.

It was reported in **Section 3.2** that a Surge model was set up for the B16 pipeline to be able to conduct a theoretical assessment of the influence of leaks and air bubbles on the pattern of the pressure waves in the pipeline at different locations**. Figure 4-38** reflects the simplified profile that was used for the surge analyses while **Figure 4-39** presents the schematic system layout (Node numbers) that was used in the surge analyses. Details of the profile are provided in **Table 4-16**.

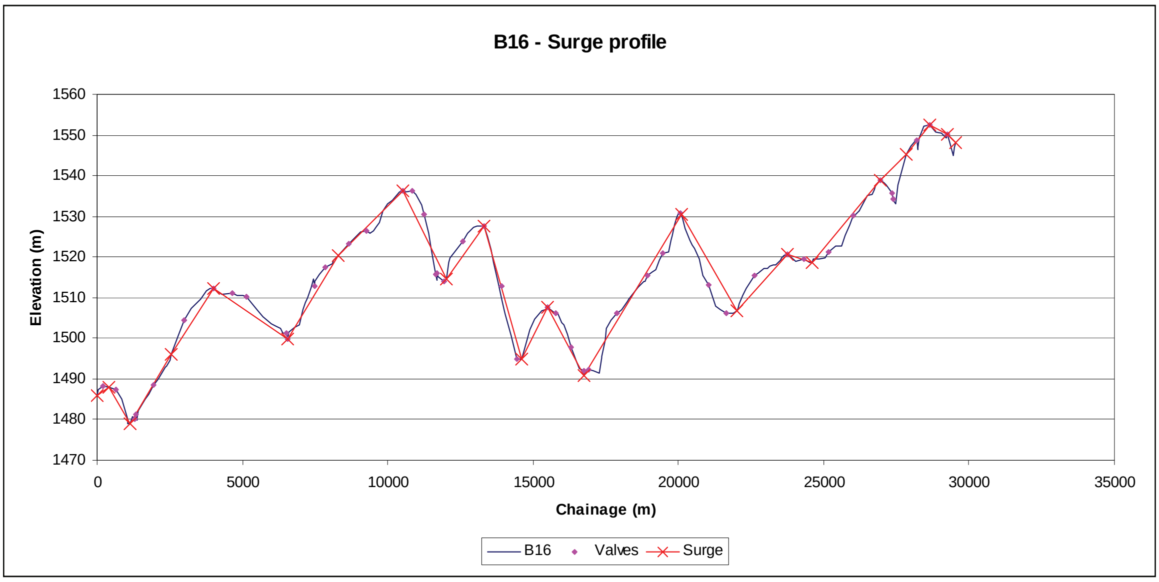

Figure 4-38: The profile used for the surge analyses on the B16 pipeline

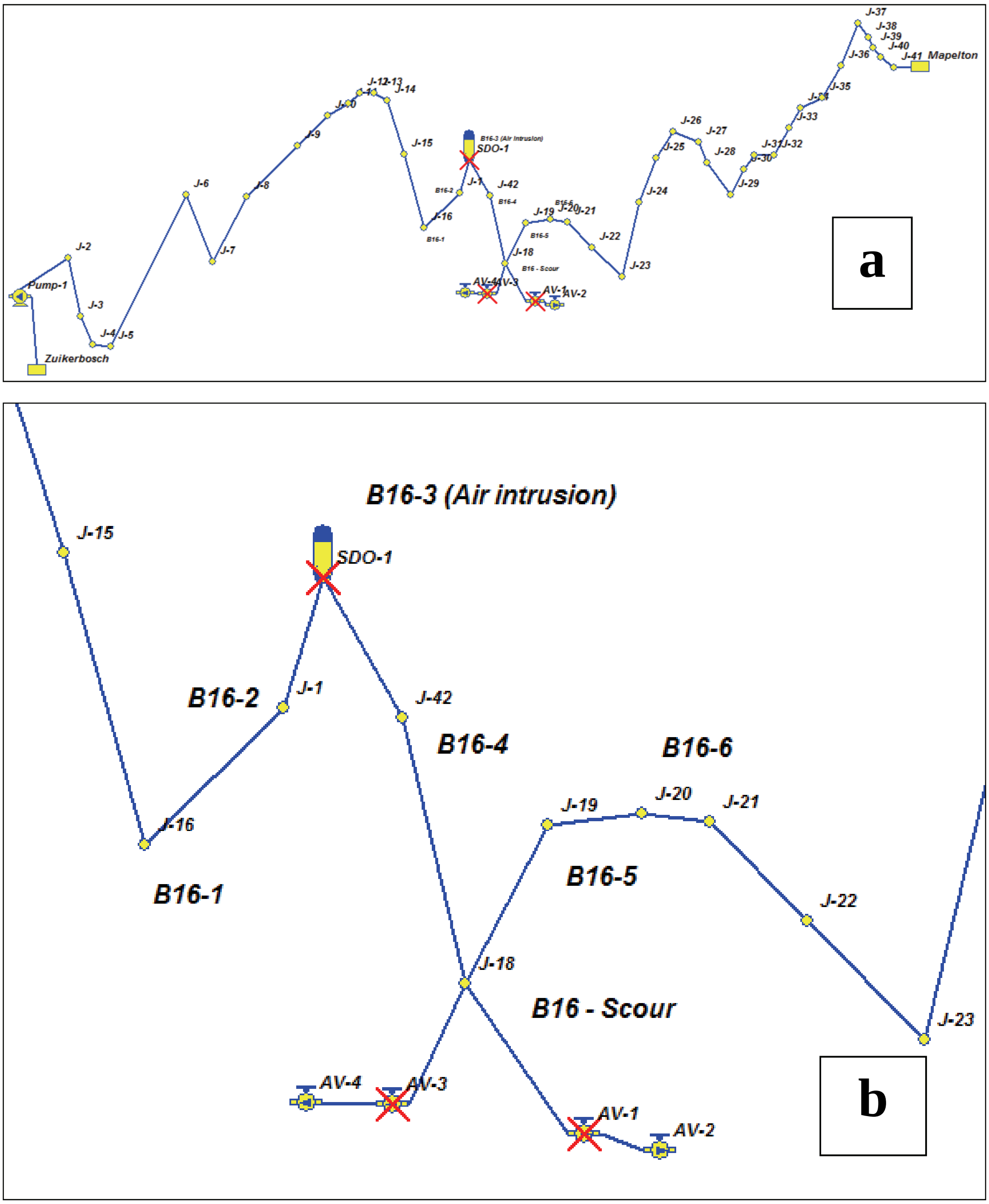

Figure 4-39: Schematic layout (a) of the surge model for B16 and detail of the pressure recording positions (b)

Table 4-16: Details of the surge profile for B16

Node	Chainage (m)	Elevation (m)	Pipe segment length (m)
J-1	0,00	1485,81	
J-2	400,00	1487,85	400,00
J-3	1150,00	1479,05	750,00
J-4	2561,65	1495,90	1411,65
J-5	4000,00	1512,25	1438,35
J-6	6575,00	1499,85	2575,00
J-7	8300,00	1520,30	1725,00
J-8	10500,00	1536,30	2200,00
J-9	12000,00	1514,60	1500,00
J-10	13300,00	1527,65	1300,00
J-11	14600,00	1494,95	1300,00
J-12	15500,00	1507,70	900,00
J-13	16770,00	1490,80	1270,00
J-14	20100,00	1530,40	3330,00
J-15	22000,00	1506,75	1900,00
J-16	23750,00	1520,50	1750,00
J-17	24581,10	1518,60	831,10
	Location where the air was introduced.		
J-18	26956,68	1538,75	2375,58
	Location where the negative wave was generated.		
J-19	27827,81	1545,20	871,13
J-20	28630,12	1552,50	802,31
J-21	29250,00	1550,24	619,88
Mapleton	29545,39	1548,18	295,39

4.4.2 Leakage influence on pressure waves in B16

The theoretical assessment of the B16 pipeline with SURGE 2000, for different sizes of leaks concluded that:

- It is difficult to detect a small leak (less than 10 % of the flow in the pipeline) but larger leaks have a noticeable influence on the head time graphs which can be used to determine the location of the leak.

Since no physical leak tests were conducted on the B16 pipeline, the theoretical assessment could not be compared with physical recorded data.

4.4.3 Air bubble influence on pressure waves in B16 Pipeline

Field tests were undertaken on 11 and 12 June 2009 to review the influence of air on the propagation of the induced pressure waves in the pipeline. **Table 4-17** shows the positions on the pipeline where pressure recordings were undertaken during these tests.

Table 4-17: Details of the pressure recording positions on the B16 Pipeline

Pressure gauging point	Chainage (m) #	Elevation (m)
B16-1*	11 950	1514,00
B16-2*	12 600	1523,90
B16-3##	13 300	1527,65
B16-4**	13 900	1508,65
Scour (to generate transient waves)	14 448	1494,80
B16-5*	15 500	1507,70
B16-6*	15 775	1506,10

Notes:

***Chainage increases towards Mapleton (direction of flow)***

******* ***Pressures were recorded at these points***

******** ***Discharge associated with the creation of the negative pressure wave, was recorded***

***Location where air was introduced***

Three inverse transient events were generated by opening a valve at the Scour point B16-4. Details of the 3 events are reflected in **Table 4-18.**

Table 4-18: Summary of the three events conducted on 12 June 2009

<table>
<tr><th>Event</th><th>Date</th><th>Status of the alteration</th></tr>
<tr><td>A</td><td rowspan="3">12 June 2010</td><td>Normal operation discharging about 800 ML/day through the B16 pipeline.</td></tr>
<tr><td>B</td><td rowspan="2">17,4 kg air introduced at node B16-3</td></tr>
<tr><td>C</td></tr>
</table>

Figure 4-40 and **Figure 4-41** show respectively the equipment that was installed to release water from the B16 pipeline (a 450 mm fast acting butterfly valve) and water spray as water was expelled from the B16 pipeline during one of the tests. The discharge rate through this valve reached 870 l/s.

Figure 4-40: Equipment installed to be able to release flow from the B16 pipeline to generate a negative pressure wave

Figure 4-41: Flow released from the B16 pipeline to generate the negative pressure wave (inverse transient)

4.4.4 Review of the recorded data

Hobo and Dataq recorders were used to record the pressure variations at a frequency of 1 and 10 Hz respectively at B16-1; B16-2; B16-4; B16-5 and B16-6. **Table 4-17** above indicates details of these gauging positions, whist **Table 4-19** indicates details of the equipment which was installed. **Figure** 4-42 shows a typical installation of the recording equipment.

Table 4-19: Details of the recording equipment which was used for the pressure recordings on the B16 Pipeline

Location	B16-1	B16-2	B16-3	B16-4	B16-5	B16-6
Logger 1 (fast)	Graphtec 1	Graphtec 2	Location where air was introduced	HOBO *	DATAQ	DATAQ Ch 1
Logger ID	1	2		951316	48AC594F	489B4101
Transducer 1	25 BarG	25BarG		16BarG	16 Bar A	10 Bar G
Transducer ID	Y096798	Z113991		51	A031787	PT27
Frequency (Hz)	10	10		1	10	5
Logger 2 (slow) *	Hobo	Hobo		Graphtec	Hobo	DATAQ Ch2
Logger ID	784503	1025537		2	784504	489B4101
Transducer 2	16BarA	16BarA		16 BarG	10 Bar A	PT26
Transducer ID	Y038236	A031788		52	A031785	10 BarG
Frequency (Hz)	1	1		10	1	5

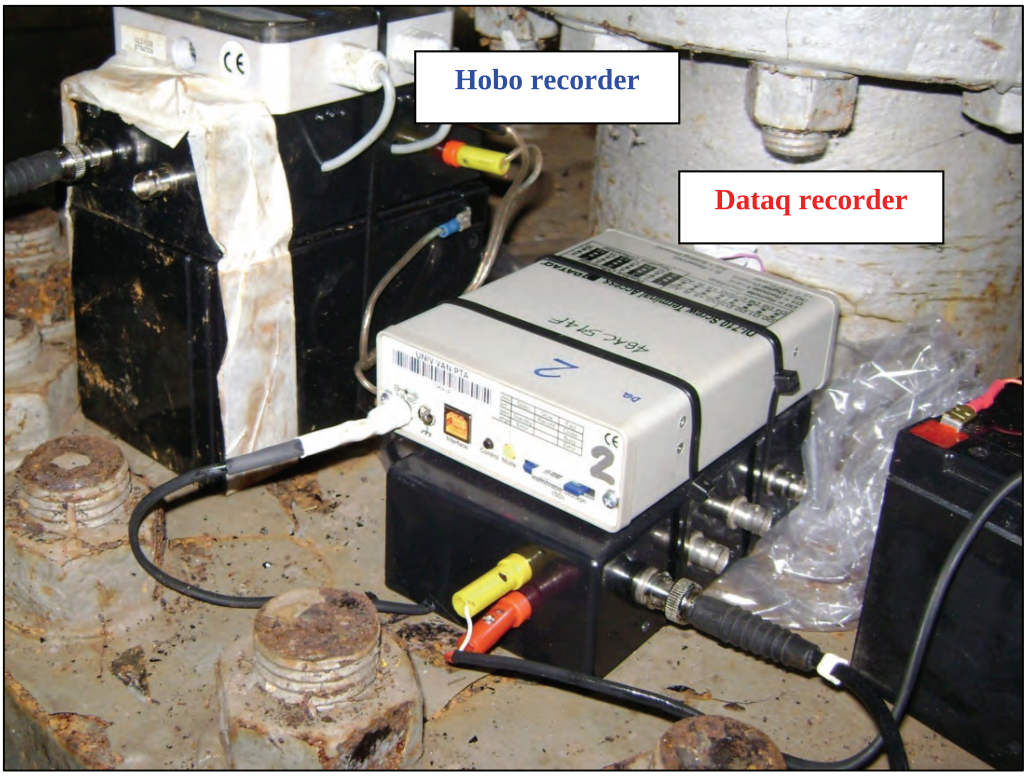

Figure 4-42: Typical installation of the data recorders

The results were reviewed and are graphically presented in **Figure 4-43** to **Figure 4-45** where the relative pressure heads for the three events are plotted.

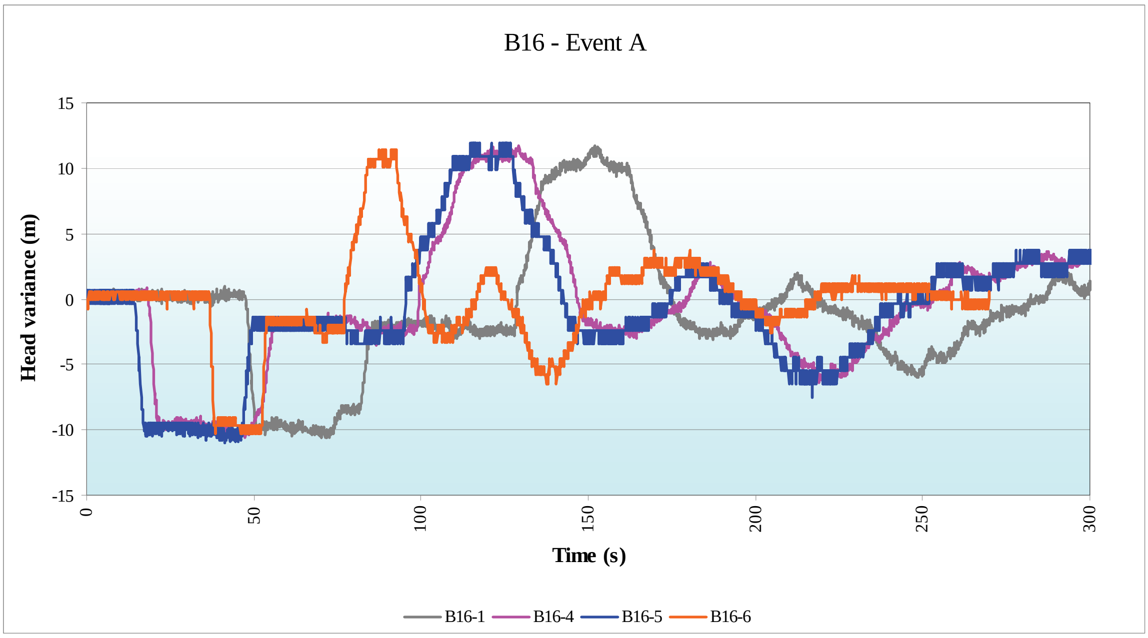

Figure 4-43: Relative pressure fluctuation at the different nodes – Event A (B16)

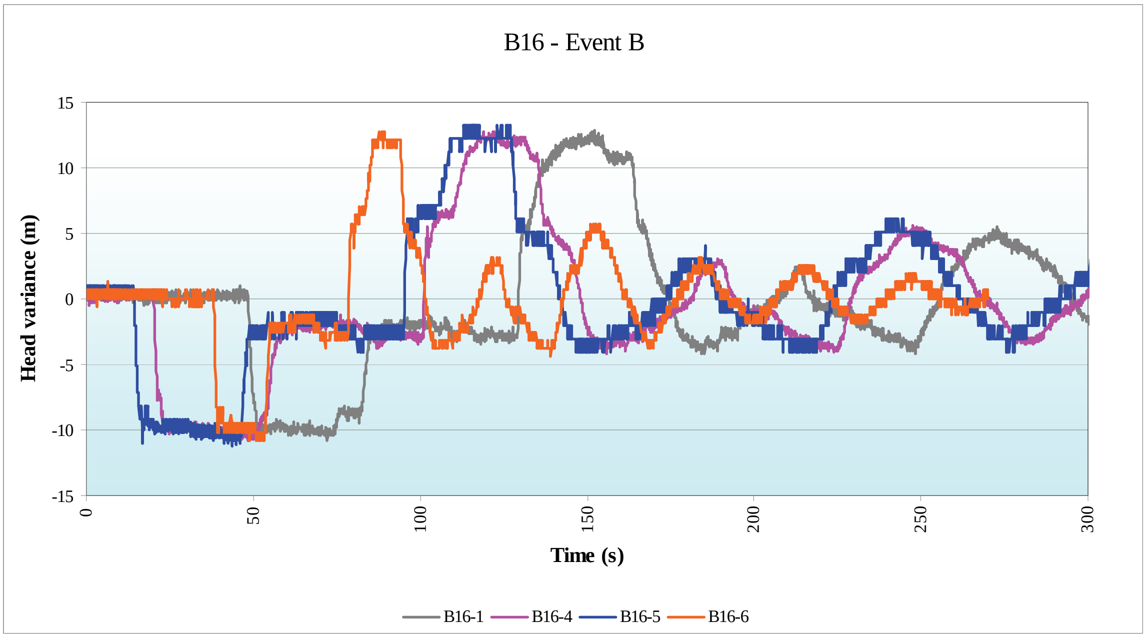

Figure 4-44: Relative pressure fluctuation at the different nodes – Event B (B16)

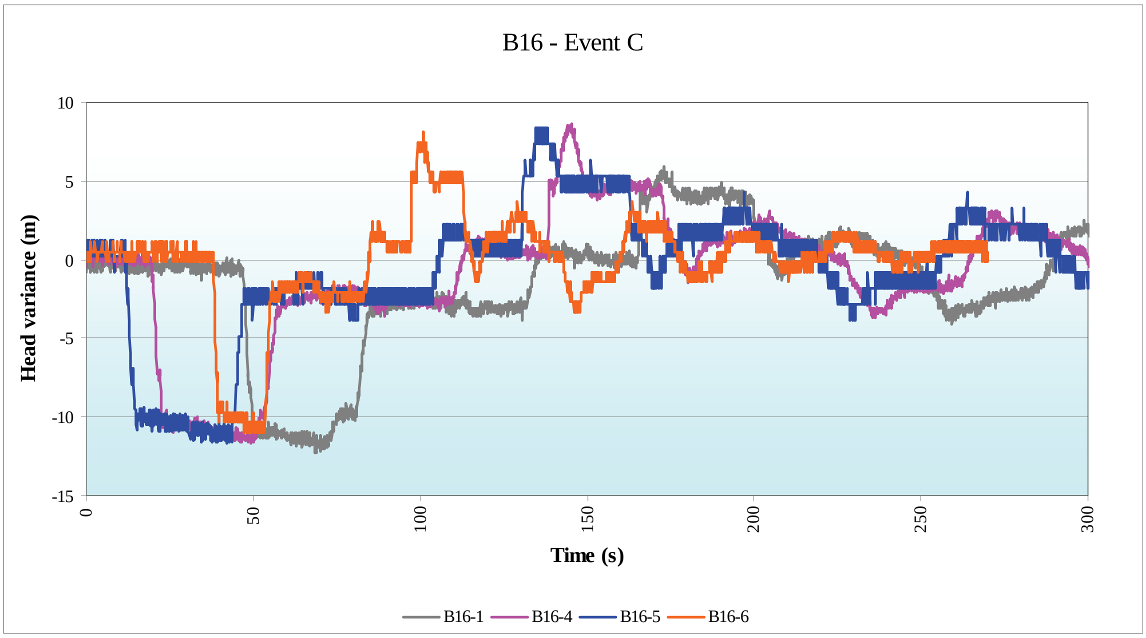

Figure 4-45: Relative pressure fluctuation at the different nodes – Event C (B16)

Since the opening and closing of the butterfly valve was done manually, the pressure fluctuations (induced inverse transients) are different. Furthermore, the relative **short distances between the portions of the recordings on the B16 pipeline**, forced that the research team investigate the **first downward leg** of the recorded pressures at the different recording positions. **Figure 4-46** to **Figure 4-48** indicate the first downward pressure leg for the three events which were created.

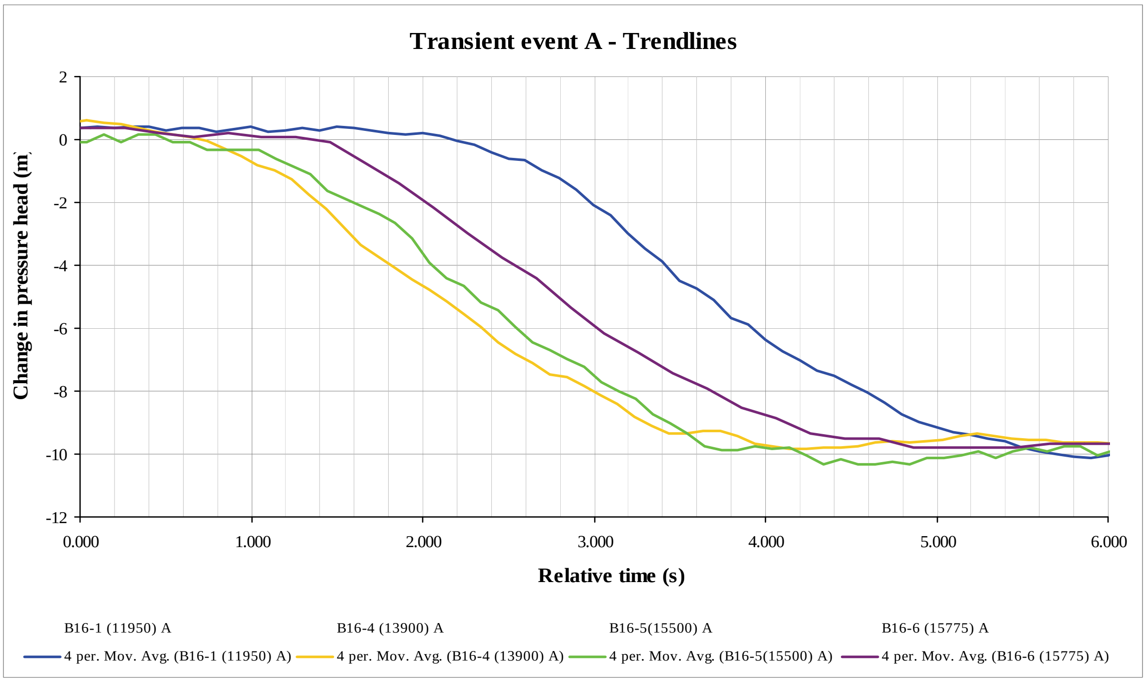

Figure 4-46: Recorded downward leg of the pressure head variance from the steady state head – Event A

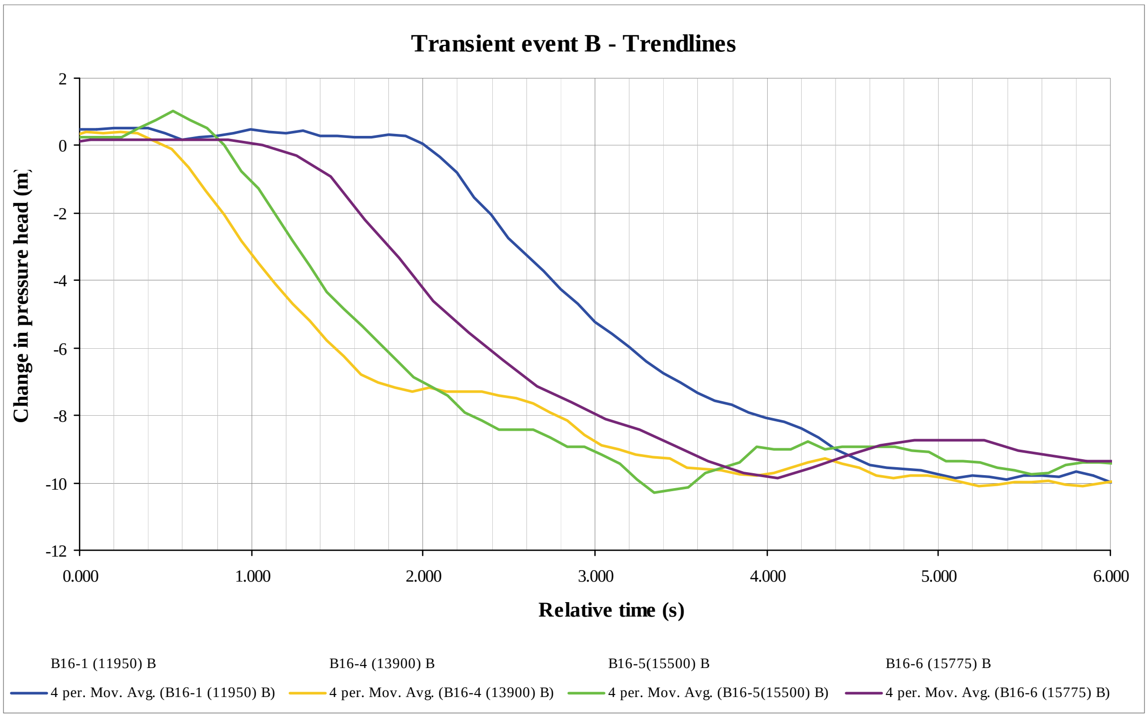

Figure 4-47: Recorded downward leg of the smoothed pressure head variance from the steady state head – Event B

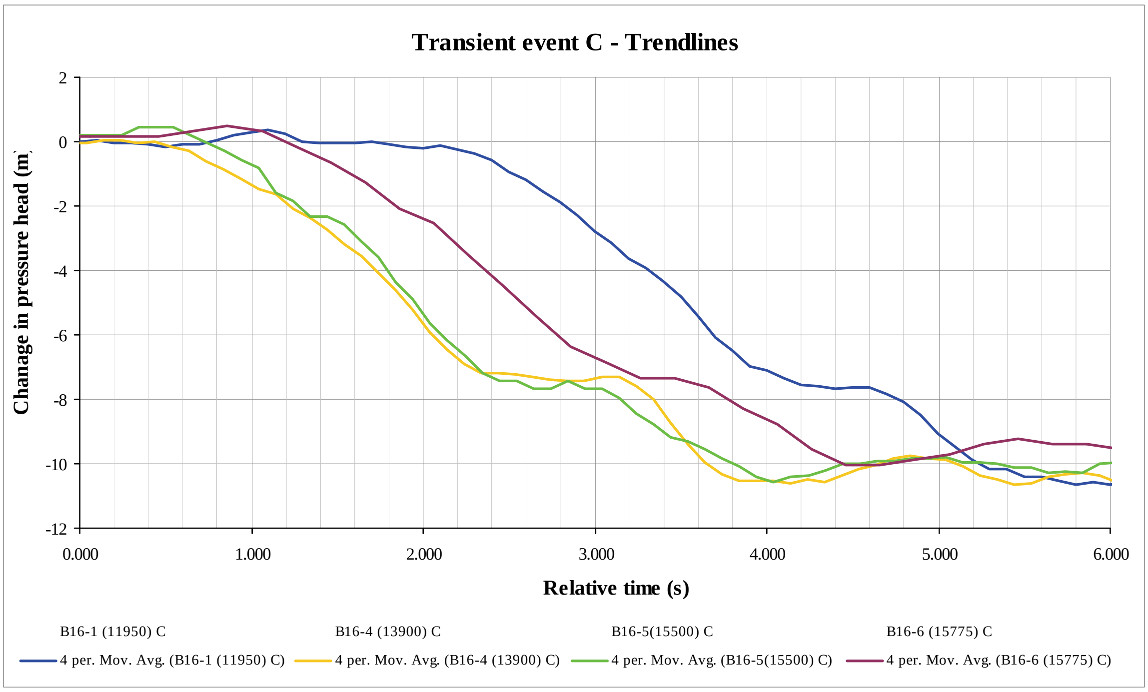

Figure 4-48: Recorded downward leg of the smoothed pressure head variance from the steady state head – Event C

By inspection it is clear that the influence of the induced air bubble at B16-3 is visible in the recorded pressures at nodes B16-4 and B16-5 for Events B and C.

It can also be observed that in the case of Event C, the induced negative head is influenced by the way in which the scour valve was opened (stepped manner).

Figure 4-49 and **Figure 4-50** represent the pressure variances for events B and C respectively on a common time scale relative to the opening time of the valve (in vertical dotted lines referenced as "start") and the time when the reflected or rebounded wave from position B16-3 where the air bubble was located, is observed at the node (in vertical dotted lines referenced as "rebound").

The notation used in **Figure 4-49** and **Figure 4-50** are as follows for the dotted vertical lines on the figures:

X B16 B Start, CC

Where:

X reflects the event (A, B or C);

B reflects the position of the recording (1, 2, 4, 5 or 6)

CC reflect the time lapse in seconds since the event was initiated at node B16-4

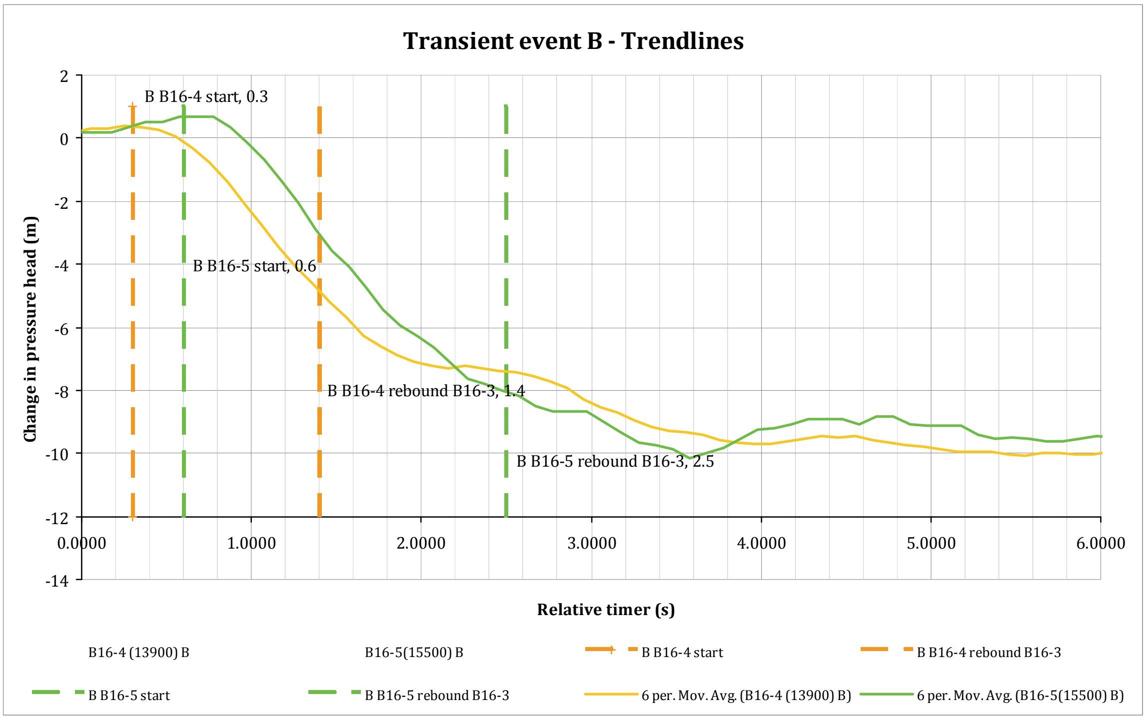

Figure 4-49: Indication of the observed time when the influence of the rebounding wave is noticed – Event B

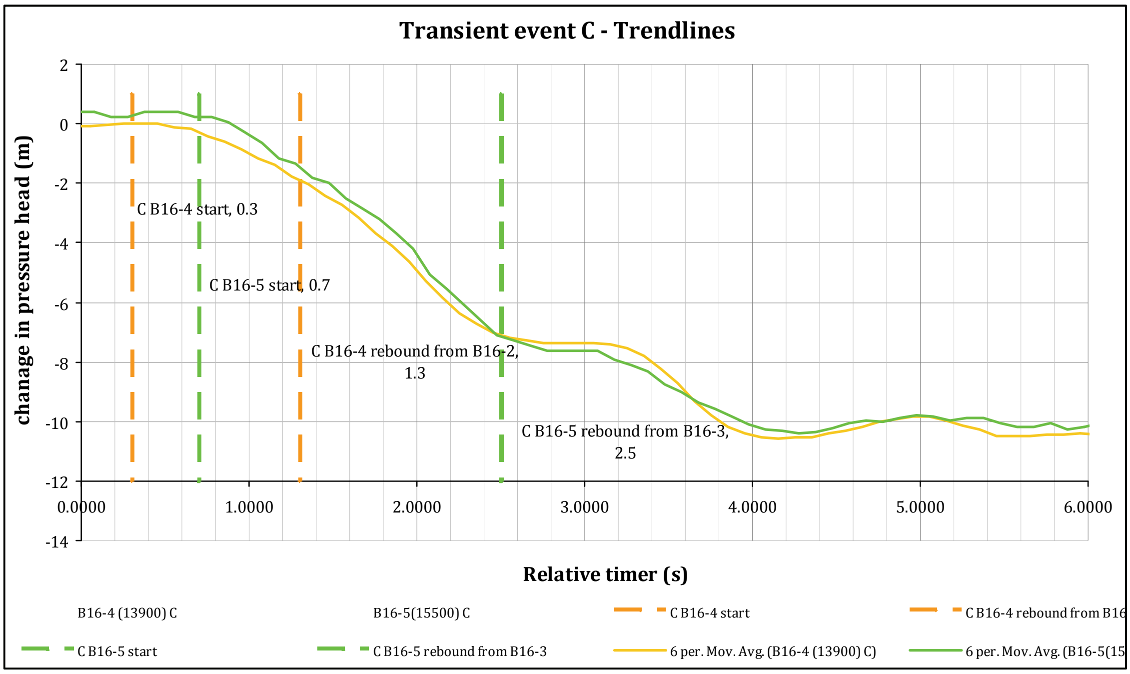

Figure 4-50: Indication of the observed time when the influence of the rebounding wave is noticed – Event C

Verification of the "origin" of the reflection wave and hence the **location of the deficiency** in the pipeline could be reviewed by considering the wave propagation and then compare it to the recorded data. **Figure 4-51** and **Figure 4-52** indicate the calculated expected relative time for the wave front to be noticed at node B16-4 and B16-5 for a wave celerity speed of 1250 m/s.

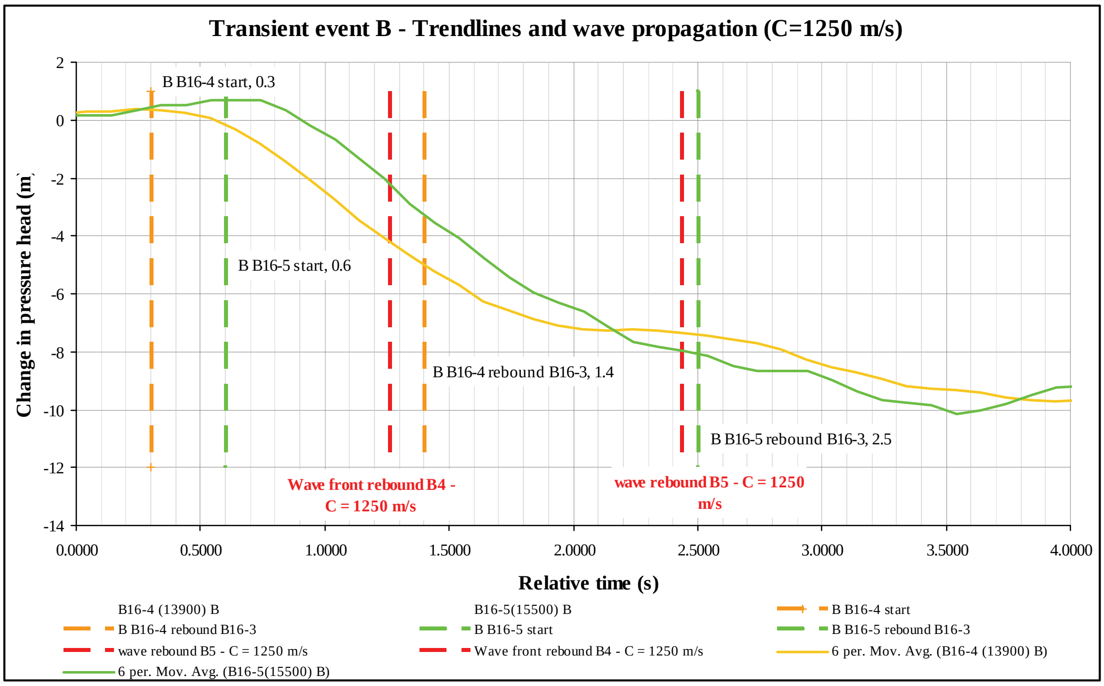

Figure 4-51: Calculated expected time for the reflecting wave to be observed at the observation points – Event B

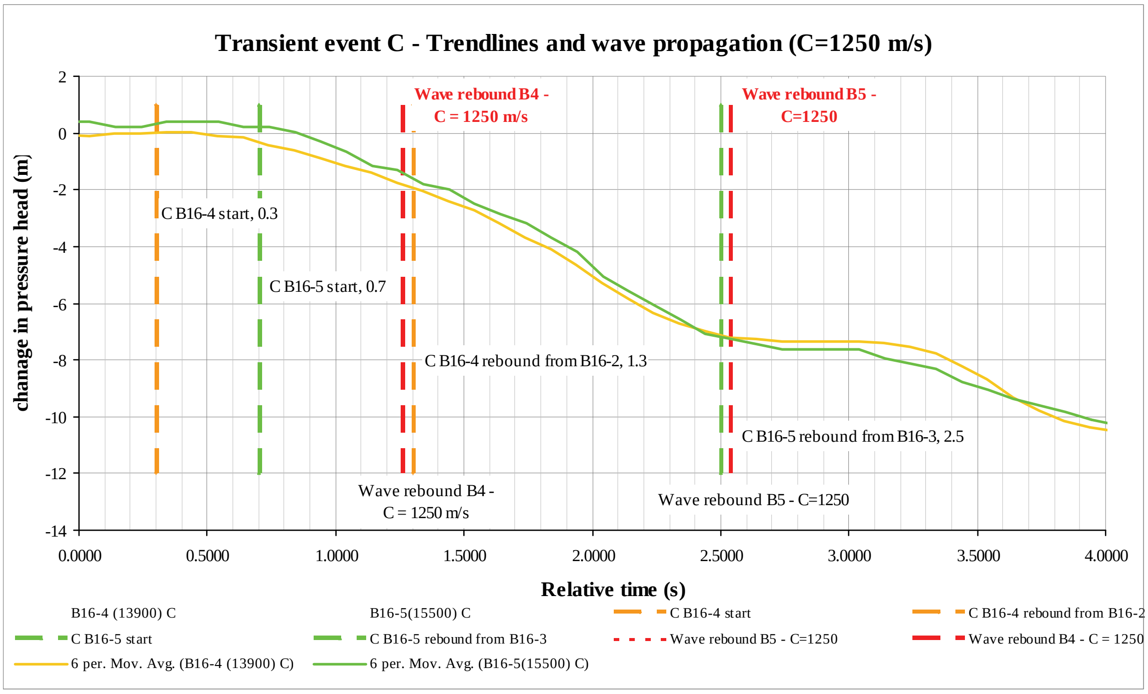

Figure 4-52: Calculated expected time for the reflecting wave to be observed at the observation points – Event C

The accuracy to determine the position of the deficiency is dependent on the frequency of the recording and hence for this experimental work, the accuracy of the position of the deficiency could be determined by (1/10*1250) = 125 m. **This emphasise the importance of the frequency at which the data needs to be recorded.**

It can be concluded, from the investigation conducted on the B16 Pipeline, that it is possible to use **inverse transients to reflect which sections of a pipeline have not been effectively de-aerated**.

4.4.4 Theoretical analyses of the influence of air on the wave propagation in the B16 pipeline

Table 4-20 reflects the analyses that were performed to evaluate the influence of an air bubble on the movement of the pressure wave.

Figure 4-53 shows the schematic layout of the surge model used to model the influence of an air bubble on the wave propagation.

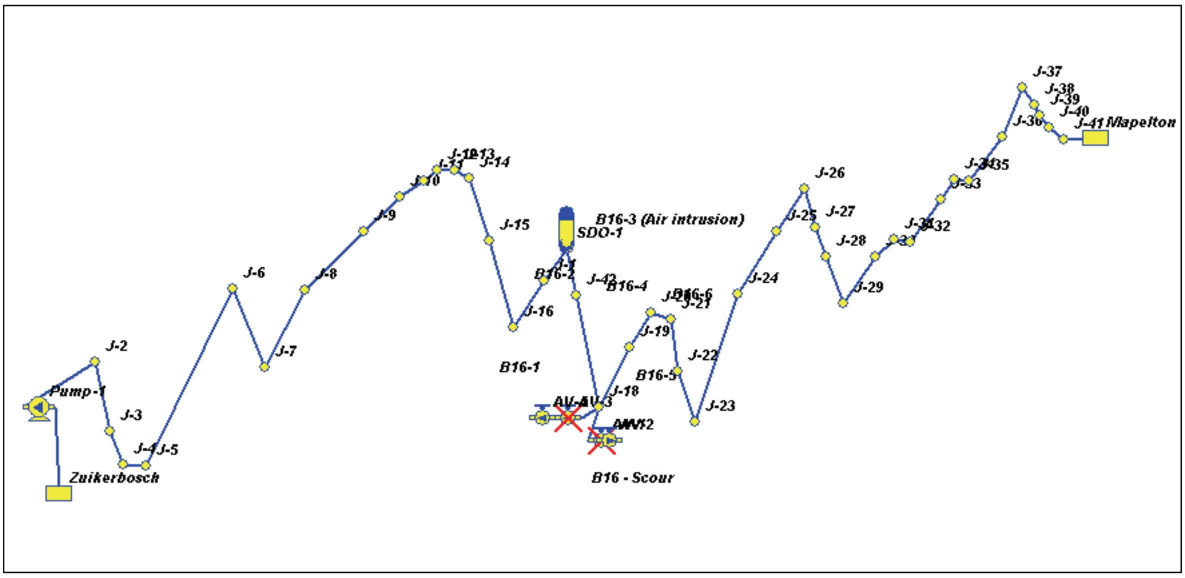

Figure 4-53: Schematic layout of the B16 pipeline modelled with SURGE 2000

Table 4-20: Surge analysis to reflect the influence of an air bubble on the pressure wave propagation

Analysis	Flow rate (m^3/s)	Air bubble		Induced negative wave	
		Node	Volume air (m^3)	Node	Induced flow (l/s)
B16 C Add L Air	3,523	B16-3	1,5	J-18	350

Figure 4-54 indicates the difference in the pressure time relationship at node J-42 (B16-4) when the B16 Pipeline is analysed with and without an air bubble at B16-3.

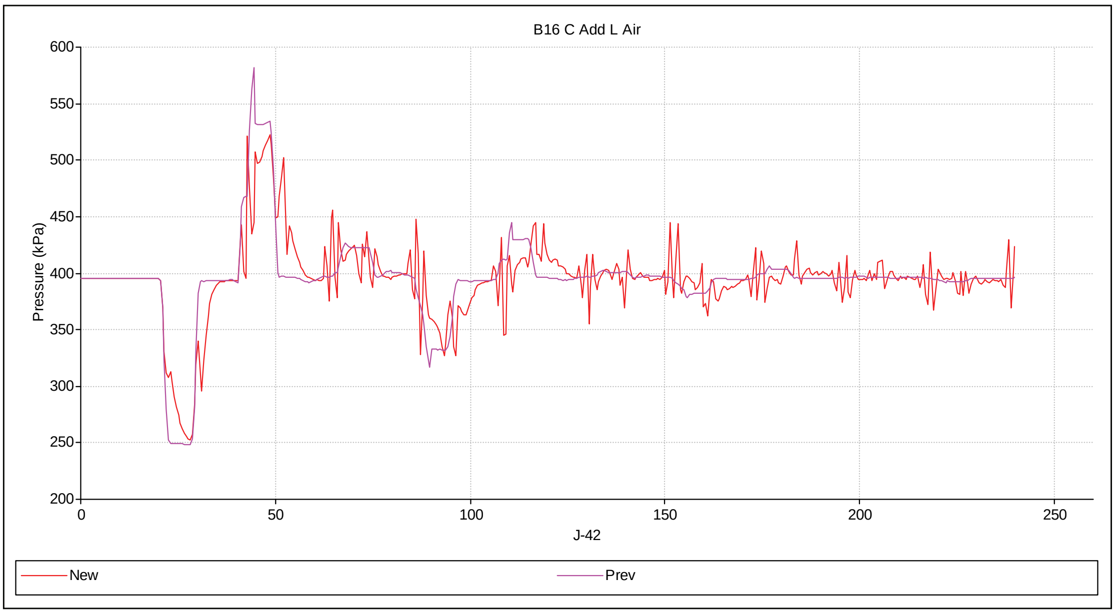

Figure 4-54: Pressure variation at B16-4 when the B16 Pipeline is analysed without (Prev) and with (New) an air bubble at node B16-3

Figure 4-55 indicates the calculated pressure variance at nodes B16-4 and B16-5 when the B16 Pipeline is analysed with an air bubble located at node B16-3.

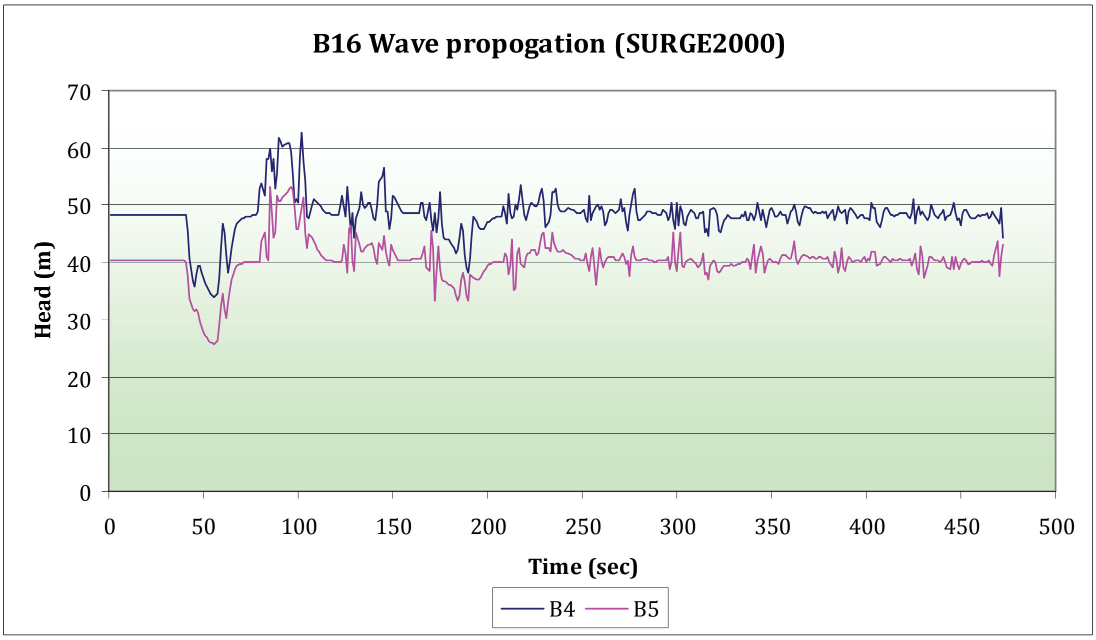

Figure 4-55: Calculated pressure variance at nodes B16-4 and B16-5 when the B16 Pipeline is analysed with an air bubble located at node B16-3

Figure 4-56 and **Figure 4-57** reflect the pressure variance on the downward leg of the head-time graph at nodes B16-4 and B16-5 when the system is assessed with and without an air pocket at node B16-3.

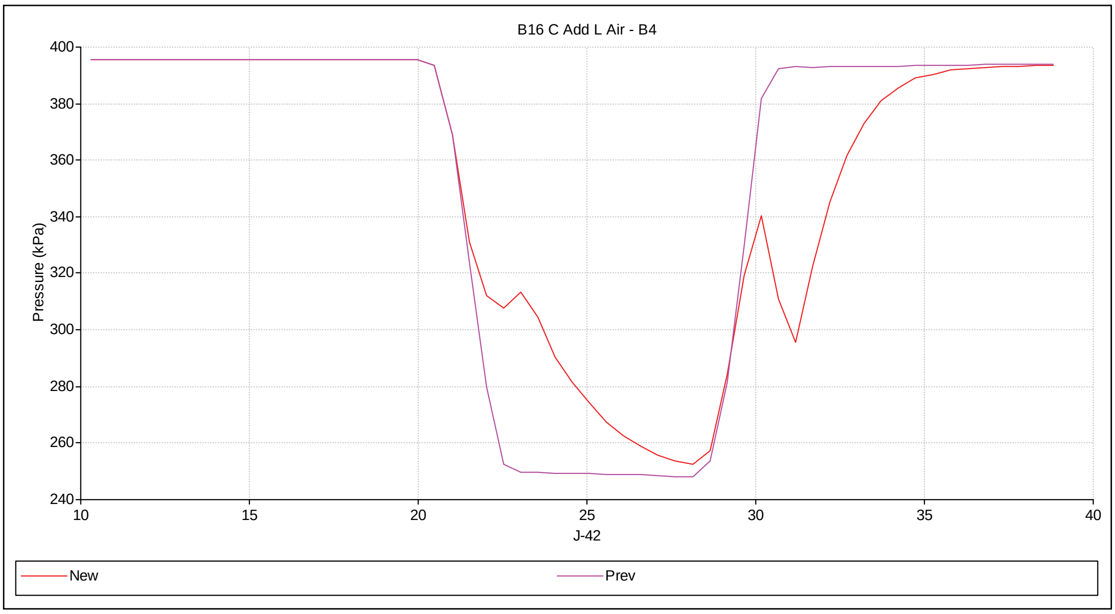

Figure 4-56: Pressure head time relationship for the B16 pipeline without (Prev) and with air (new) at B16-4

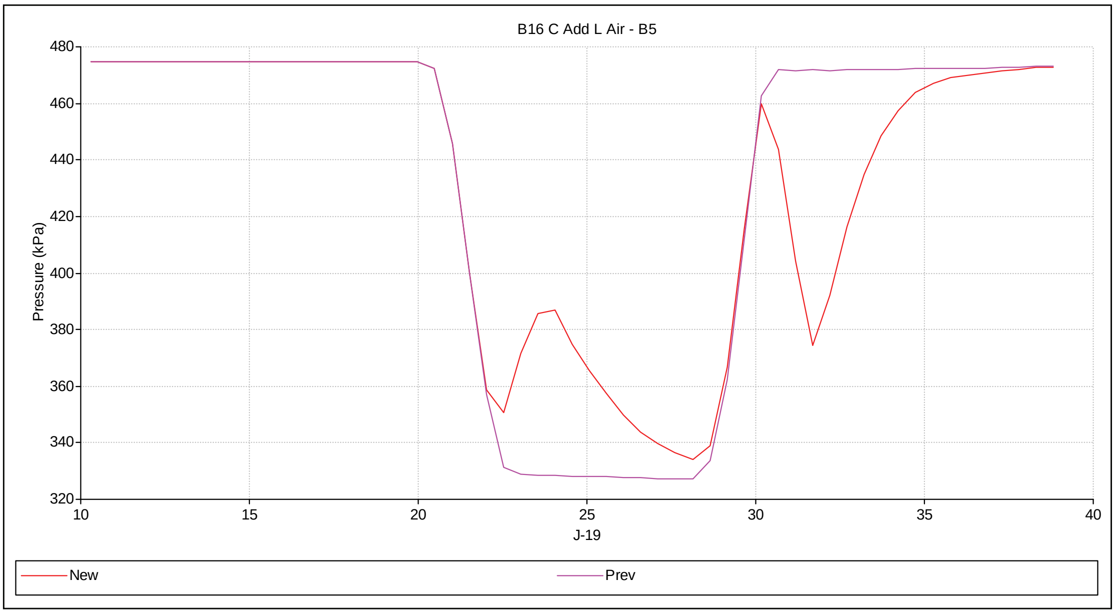

Figure 4-57: Pressure head time relationship for the B16 pipeline without (Prev) and with air (new) at B16-5

These results show a similar trend as the observed data recordings during the field tests (**Figure 4-46** and **Figure 4-47**).

Based on the theory of wave propagation **Figure 4-58** was compiled based on the calculated results from the SURGE2000 model, showing the expected time for a reflecting or rebounding wave from B16-3 to reach B16-4 and B16-5. This result is almost identical to what has been observed (**Figure** 4-52), creating confidence that the air bubble at B16-3 could be traced by assessing the head time variance and identifying the instability that is generated at the node where air is captured.

The data files are included electronically on the accompanying CD and the documents available on the accompanying CD is reflected in **Appendix 4D**.

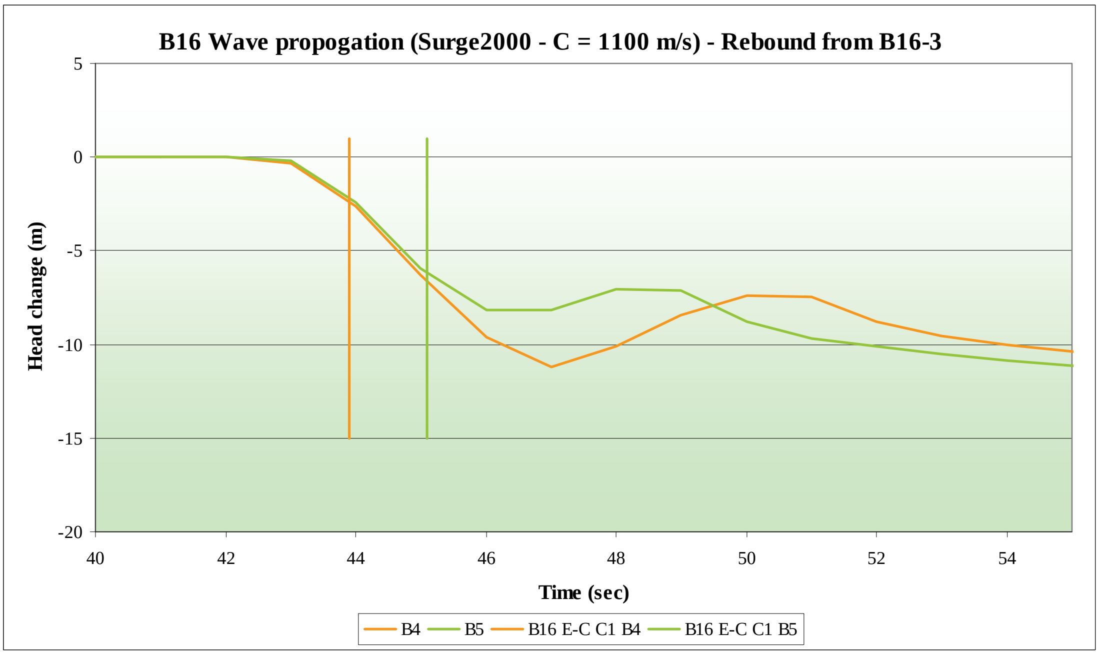

Figure 4-58: Calculated pressure variance of the B16 pipeline and the expected time for the rebound wave to reach the observation locations B16-4 and B16-5 for Event C

Figure 4-58 reflects a change in slope of the calculated head time relationship at nodes B16-4 and B16-5.

4.5 Conclusion

The fieldwork and the simulated results support the following conclusions with regard to the use of inverse transient to determine the location of deficiencies in pipelines.

It can thus be concluded that the procedure to generate inverse transients could be used to:

- Establish the presence of un-aerated section of a pipeline;

- Locate leaks in a pipeline (larger than 1% of the flow in the pipeline);

The accuracy to define the position of the deficiency is dependent on the recording frequency at which the data is recorded, but should preferably be more that 50 Hz.

5 Using the Inverse Transient Technique to determine the operational status of pipelines

5.1 Introduction

Inverse transients have been suggested by researchers (Chapter 2) to be used as a non-destructive and non-interruptive procedure to determine the presence of deficiencies in pipeline systems. These would typically be used to determine the presence and location of leaks and air pockets as well as the location where an unknown valve (or unwanted object) restricts the flow.

Leaks in water distributions systems are a common problem while the ineffective de-aeration of larger diameter transfer systems reduces the hydraulic capacity of these systems. In the following paragraphs some details are provided to assist in the implementation of this technique.

The application of inverse transients could provide valuable insight and definition of the characteristic change and presence of deficiencies in the systems. This requires that the initial dynamic characteristics of systems should be obtained during the installation of the system, providing a footprint of the initial dynamic behaviour against which future recorded data can be compared.

5.2 Accurate system description

It is paramount that an accurate description of the system be obtained whenever inverse transients are considered for evaluating any system. The following details of the system are required:

- System layout with dimensional details and location of all the components;
- Diameter, Classes, Material and wall thickness of all the pipes in the system;
- Establishing the hydraulic capacity (roughness), wave propagation characteristics and positions where pressure and flow recordings could be conducted.
- Establishing the accuracy to which the deficiency needs to be defined to be able to establish the rate at which the data should be recorded (10 m);

- Compiling a theoretical model of the system and conduct dynamic analyses to establish the background fingerprint of the ideal operating system. This should be compared with the initial recorded dynamics if it is available; and

- Determine the locations where the inverse transient will be generated and the positions where the pressure and flow recordings will be undertaken. At least three recording positions should be used between the point where the pressure wave is generated and the expected positions where the deficiencies are expected.

5.3 Data Recording and frequency

The objective to locate the deficiency as accurate as possible, requires the following steps:

- Determine an average expected wave celerity (say 800 m/s);

- Define the accuracy required to identify the deficiency (say 10 m);

- Calculate the minimum frequency at which the data need to be recorded (10/800 = 0,0125 s which require a recording rate of 80 Hz;

- Select the data recording equipment capable to record long data sets in such a format that it can be viewed and abstracted to a spread sheet environment that does not exceed the capacity of the spread sheet programme due to a limited number of lines (rows); and

- Identify locations where the data will be recorded. At least three recording positions should be installed between the location where the pressure wave is generated and the location where the deficiencies are expected.

5.4 Interpretation of the results

The interpretation of the results are complicated by the fact that any pressure wave will be reflected from all loss components (valves, cross connections, bends, pumps, diameter changes and locations where the wave celerity changes. This requires a systematic review of the wave patterns and calculation of the possible origin of the reflection wave.

Experience and time will improve the interpretation of the results to be able to define the type, size and location of the deficiencies.

The need to use wave pattern recognition software or to develop fuzzy logic assessment procedures might be a way to simplify the identification of the location of deficiencies.

The challenges should motivate further assessment to fully implement the technique and motivate the requirement in a new system so as to obtain the background fingerprint of wave propagation in the system. This could then be used with later assessments to compare and accurately pinpoint the deficiencies.

6 Conclusion and Recommendations

The literature study confirms the possible use of the method of inverse transients to determine the presence and location of air pockets and leaks in pipelines. The contribution by Vitkovsky et al. (2000) and other researchers reflected in Chapter 2 (Literature Study) provided further reference to the use, capabilities and application of this technique.

The results obtained in the theoretical assessment and physical assessment reflected how the pressure time relationships should be evaluated and highlights the importance to assess the influence of the reflection wave from the deficiency. All loss elements in any water distribution system where the technique of inverse transients are implemented will also generate reflection waves. These multiple number of reflection waves, some of which might have been changed due to the layout of the system (superimposed waves), will influence the pressure-time relationship at the pressure recording positions.

The steps for the implementation of inverse transients can be summarised as follows:

- Obtain and verify all the data required to compile a theoretical assessment of the system;
- Determine how much detail must be included for accurate computation;
- Identify the practical difficulties of the implementation and possible success of this methodology for the system to be reviewed;
- Theoretically analyse the system as the base case to obtain details of the wave dynamics from which the favourable position where the pressure recordings should be undertaken could be identified;
- Select the appropriate pressure and flow recording equipment and the apparatus required to induce a transient in the system;
- Define an outline of a set of rules to define the sampling rate, the sample size and the location of the measurements sites;
- Install and verify the operation of all the recording equipment;

- Initiate a safe (non-destructive) transient event;

- Measure the transient pressures at the measurement sites;

- Assess the recorded data and determine if the inverse transients which were introduced provided sufficient pressure variance in the system (If not the field recordings might have to be repeated);

- Reproduce an accurate model of the variable input used in the physical setup;

- Identify the possible locations of the deficiencies in the system by comparing the simulated and field recordings;

- Introduce these deficiencies in the theoretical dynamic simulation model and compare the results with the recorded results;

- Compile a report on the possible location, nature and extent of the discrepancies; and

- Conduct a physical field inspection to verify deficiencies.

The hypothesis presented for this project report was that: Inverse transients can be used as a non-destructive, non-intrusive and un-intermittent test to determine the presence and location of air pockets and leaks in pipelines.

The key results obtained from this study during the field tests and theoretical evaluation indicated that:

- Inverse transient procedure is non-destructive, non-intrusive and does not require the service to be interrupted;
- The results provided detectable proof of the presence and location of air pockets and significant leaks;
- Leakage rates of 10% of the flow rate in the system will be identifiable;
- Air pockets with a volumetric size of 10% of the value of the flow rate will be identifiable; and
- Available equipment and knowhow of inverse transients, make the use of inverse transient a cost effective procedure to quantify the status and locate deficiencies in a system.

Based on the field work it seems as if the precise location and size of the leaks are more challenging and complex to identify than that of air pockets in the pipeline due to the difference of the specific characteristics of the reflection waves from leaks and air bubbles.

In the case of an air pocket the reflection wave will result is:

- Increase in the pressures in the direction the reflection wave is traveling (**Figure 3-8);**

- The discharge at the point where the transient is created will increase for a short period of time (**Figure 3-11**) when the return wave reaches the location where the transient was generated; and

- Beyond the air pocket or leak (moving away from the position where the transient was created) the transferring pressure wave will decrease and the variation in the pressure fluctuation will be dampened (**Figure** 3-7). The location of the deficiency would not be defined on the transferring pressure wave.

It is recommended that:

- All new pipeline installations should be tested to provide a baseline (fingerprint) of the systems behaviour which would later be used in comparison assessments;

- Further field investigations and modelling of different pipe systems be undertaken to provide more results and understanding of the interpretation of the results; and

- Typical pressure graphs be produce based on further field work, reflecting the wave propagation and pressure variance resulting from leaks and air pockets.

7 References

1. Bergant, A., Tijsseling, A., Vitkovsky, J.P., Covas, D., Simpson, A. & Lambert, M. (2003a) *Further investigation of parameters affecting water hammer wave attenuation, shape and timing. Part 1: mathematical tools.* Proceedings of the 11th International Meeting of the IAHR Work Group on the Behaviour of Hydraulic Machinery under Steady Oscillatory Conditions, Stuttgart, Germany.

2. Bergant, A., Tijsseling, A., Vitkovsky, J.P., Covas, D., Simpson, A. & Lambert, M. (2003b) *Further investigation of parameters affecting water hammer wave attenuation, shape and timing. Part 2: case studies.* Proceedings of the 11th International Meeting of the IAHR Work Group on the Behaviour of Hydraulic Machinery under Steady Oscillatory Conditions, Stuttgart, Germany.

3. Bollaert, E. and Schleiss, A. 2001. *Air Bubble Effects on Transient Water Pressures in Rock Fissures due to High Velocity Jet Impact*. Laboratory of Hydraulic Constructions, LCH, Swiss Federal Institute of Technology Lausanne. http://lchww.epfl.ch

4. Brown, K. (2007). *Modelling leakage in water distribution systems*. MSc. Thesis. The Florida State University.

5. Brunone, B, Ferrante, M, and Ubertini, L (2000) *Leak analyses in pipes using Transients.* www.hunter.cuny.edu/rome-nyc/Brunone.doc – Viewed on 20 August 2009.

6. Brunone, B, Ferrante, M (2002) *Pipe system diagnostics and leak detection by unsteady-state tests*, Elsevier Science Ltd.

7. Chadwick, A., Morfett, J. & Borthwick, M. (2004) *Hydraulics in Civil and Environmental Engineering.* Spon Press, London.

8. Covas, D., & Ramos, H. (1999). *Leakage Detection in Single Pipelines Using Pressure Wave Behaviour.* Water Industry Systems: modelling and optimization applications. Volume One. Edited By Savic, D.A., & Walters, G.A.. Research Studies Press LTD, Baldock, Hertfordshire, England.

9. Covas, D., and Ramos, H. (2001). *Hydraulic transients used for leakage detection in water distribution systems.* Proceedings of the 4th International Conference on Water Pipeline Systems, BHR Group. Cranfield, U.K., pp 227-242.

10. Daugherty, R.L., Franzini, J.B. & Finnemore, J.E. (1989). *Fluid Mechanics with Engineering Applications.* McGraw Hill, Singapore.

11. Eiswirth, M., Heske, C., Burn, L.S. & DeSilva, D. (2001). *New methods for water pipeline assessment.* IWA 2. World Water Congress. Berlin, Germany.

12. Ivetic, M. and Savic, D.A. 2002. *Practical Implications of Using Induced Transients for Leak Detection.* 3rd World Water Forum, Kyoto, Session "Integrated River Basin Environment Assessment".

13. Jönsson, L. 2001. *Experimental studies of leak detection using hydraulic transients*. Dep. Water Resources Engineering, University of Lund, Sweden.

14. Kapelan, Z.S. Savic, D.A. and Walters, G.A. 2003. A hybrid inverse transient model for leakage detection and roughness calibration in pipe networks, *Journal of Hydraulic Research,* Vol. 41, No 5, pp 481-492.

15. Ken-Han Wang, Qiang Shen and Boaxu Zhang. 2002. *Modeling propagation of pressure surges with the formation of an air pocket in pipelines.* Science Direct.

16. Kirkland, C. 2002. *Controlling and understanding the effects of air in pipelines*. Amiad Australia (Pty) Ltd. http://www.wioa.org.au/conf_papers.htm.

17. Liggett, J.A., & Chen, L-C. (1994). Inverse Transient Analysis in Pipe Networks. *Journal of Hydraulic Engineering*, Vol 120, No 8, pp 934-955

18. Portable Type Ultrasonic Flowmeter (Portaflow X) Instruction Manual (2001). Fuji Electric Instruments Co., Ltd.

19. Pudar, R.S. and Liggett, J.A. 1992. Leaks in pipe networks. *Journal of Hydraulic Engineering*, ASCE, Vol 118, No 7, pp 1031-1046.

20. Stathis, J. & Loganathan, G.V. (1999) *Analysis of Pressure-Dependent Leakage in Water Distribution Systems.* Preparing for the 21st Century: Water Resources Planning and Management Conference 1999 Proceedings.

21. Stryker, J. 2003. *Water Hammer and Air in Pipes*. http://www.irrigationtutorials.com.

22. Surge 2008 Users Guide, Appendix 1:Water Hammer Analysis – Essential and Easy (and Efficient)

23. Van Vuuren, S.J. 1990. *Theoretical overview of surge analysis*. Department of Civil Engineering, University of Pretoria, South Africa.

24. Van Vuuren, S.J., Van Dijk, M. & Steenkamp, J.N. (2004a). *Air in large diameter pipes.* Water Research Commission. WRC Report No. 1177/1/04. Pretoria

25. Van Vuuren, S.J., Van Dijk, M. & Steenkamp, J.N. (2004b). *Guidelines For Effective De-Aeration.* Water Research Commission. WRC Report No. 1177/2/04. Pretoria

26. Vent-O-Mat Help file (2008). Version 3.0.0. SINOTECH CC

27. Vitkosvky, J.P., Simpson, A.R., & Lambert, M.F. (2000). 'Leak Detection and Calibration Using Transients and Genetic Algorithms.' *Journal of Water Resources Planning and Management*, Vol 126, No 4, pp 262-265.

28. Wang, X-J., Lambert, M.F., Simpson, A.R., Liggett, J.A., & Vitkovsky, J.P. (2002). 'Leak Detection in Pipelines using Damping of Fluid Transients.' *Journal of Hydraulic Engineering*, Vol 128, No 7, pp 697-711.

29. Wylie, E.B. & Streeter, V.L. (1978) *Fluid Transients*. McGraw Hill, New York.